

# **Ruthenium tris(bipyridine) derivatives – Photoactive units in supramolecular donor-acceptor systems**



## **Dissertation**

zur Erlangung des Grades eines  
Doktors der Naturwissenschaften  
(Dr. rer. nat.)

der Naturwissenschaftlichen Fakultät IV  
– Chemie und Pharmazie –  
der Universität Regensburg

vorgelegt von  
**Michael Kercher**  
aus Bremen  
**2002**

Promotionsgesuch eingereicht am: 19.07.2002

Tag der mündlichen Prüfung: 05.09.2002

Die Arbeit wurde angeleitet von: Prof. Dr. B. König

Prüfungsausschuß:

Prüfungsvorsitz: Prof. Dr. O. Reiser

1. Prüfer: Prof. Dr. B. König

2. Prüfer: Prof. Dr. L. De Cola

3. Prüfer: Prof. Dr. N. Korber

Teilergebnisse aus dieser Arbeit wurden mit Genehmigung der Naturwissenschaftlichen Fakultät, vertreten durch den Betreuer der Arbeit, in folgenden Beiträgen vorab veröffentlicht:

#### **Publikationen:**

M. Kercher, B. König, *Molecules* **2001**, m205.

M. Kercher, L. De Cola, H. Zieg, B. König, *J. Am. Chem. Soc.* accepted

H. F. M. Nelissen, M. Kercher, L. De Cola, M. C. Feiters, R. J. M. Nolte, *Chem. Eur. J.* accepted

#### **Tagungsbeiträge:**

König, B., Kercher, M., Pelka, M., De Cola, L.: Photoinduced electron transfer between donor-acceptor moieties arranged by coordination compounds. ESF-Meeting on Chemistry and Physics of Multifunctional Materials (Taming the Properties of Molecules), Sant Feliu de Guixols, Spain, 8. - 12. September 1999. (Poster Contribution)

Kercher, M., König, B., De Cola, L.: Scandium Mediated Supramolecular Assembly for Photoinduced Electron Transfer. Volkswagen-Workshop, Wildbad Kreuth, Germany, 3. - 5. May 2000. (Poster Contribution)

Kercher, M., König, B., De Cola, L.: Photoinduced Electron Transfer (PET) in Non-Covalently Linked Moieties. CW-Meeting, Structure and Reactivity, Lunteren, The Netherlands, 6. - 7. February 2001. (Lecture)

Nelissen, H. F. M., Kercher, M., De Cola, L., Feiters, M. C., Nolte, R. J. M.: Switch-on Luminescence Detection of Steroids by Tris(bipyridyl)ruthenium(II) Complexes with Multiple Cyclodextrin Binding Sites. CW-Meeting, Structure and Reactivity, Lunteren, The Netherlands, 6. - 7. February 2001. (Poster Contribution)

Kercher, M., De Cola, L.: Photoinduced Electron Transfer in Non-covalently linked systems. 4-Center-Meeting, Taormina, Italy, 19. - 21. April 2001. (Lecture)

Kercher, M., König, B., De Cola, L.: Non-covalently linked Donor-Acceptor Systems. Graduate College Sensory Photoreceptors - Summermeeting, Nové Hradý, Czech Republic, 20. – 24. July 2001. (Lecture)

Kercher, M., König, B., De Cola, L.: Photoinduced Electron Transfer in a Scandium (III) mediated Supramolecular Assembly; a Modular Approach. Graduate College Sensory Photoreceptors - Summermeeting, Nové Hradý, Czech Republic, 20. – 24. July 2001. (Poster Contribution)

Kercher, M., Nelissen, H. F. M., De Cola, L., Feiters, M. C., Nolte, R. J. M.: Photoinduced Electron Transfer in a non-covalently linked Ruthenium(trisbipyridine)-Cyclodextrin-Viologen-System. Graduate College Sensory Photoreceptors, Summermeeting - Nové Hradý, Czech Republic, 20. – 24. July 2001. (Poster Contribution)

Kercher, M., König, B., De Cola, L.: Photoinduced Transfer Processes in Coordination Compounds. ESF-Meeting on Chemistry and Physics of Multifunctional Materials (Chemical Building Blocks for New Materials), Acquafredda di Maratea, Italy, 22. - 27. September 2001. (Poster Contribution)

Kercher, M., König, B., De Cola, L.: Photoinduced Transfer Processes in Coordination Compounds. HRSMC Symposium, Amsterdam The Netherlands, 30. October 2001. (Poster Contribution)

Kercher, M., Nelissen, H. F. M., De Cola, L., Feiters, M. C., Nolte, R. J. M.: Cooperative Binding of Bis-Alkyl-Viologens to Ruthenium(trisbipyridine) bearing Cyclodextrins - Photoinduced Electron Transfer. CW-Meeting, Structure and Reactivity, Lunteren, The Netherlands, 4. - 5. February 2002 (Poster Contribution)

Kercher, M.: Photoinduced Electron Transfer between Metal Coordinated Cyclodextrin Assemblies and Viologens. International Conference on Coordination Chemistry (ICCC35), Heidelberg, Germany, 20. - 26. July 2002 (Lecture)

Die vorliegende Arbeit wurde finanziert durch:

Volkswagen Stiftung

Graduierten-Kolleg der Universität Regensburg ‘Sensory photoreceptors in natural and artificial systems’

European Commission – Marie Curie fellowship HPMT-CT-2001-00311



It was the best of times, it was the worst of times,  
it was the age of wisdom, it was the age of foolishness,  
it was the epoch of belief, it was the epoch of incredulity,  
it was the season of Light, it was the season of Darkness,  
it was the spring of hope, it was the winter of despair,  
we had everything before us, we had nothing before us,  
we were all going direct to Heaven, we were all going direct the other way.

(Charles Dickens)





<b>Table of Contents</b>	<b>Page</b>
<b>1 EFFICIENCY OF ELECTRON TRANSFER PROCESSES IN NON-COVALENTLY ASSEMBLED DONOR – ACCEPTOR SYSTEMS.....</b>	<b>1</b>
1.1 HYDROGEN BONDS.....	2
1.1.1 Carboxylic Acid Dimers .....	2
1.1.2 Peptide Based Motifs.....	4
1.1.3 Watson-Crick base pairs.....	5
1.1.4 Diimide Motif.....	6
1.1.5 “Hamilton” Receptors.....	7
1.1.6 Proton Coupled Electron Transfer / Salt Bridges .....	8
1.2 HYDROPHOBIC INTERACTIONS .....	9
1.2.1 Cyclodextrins .....	9
1.2.2 Calixarenes.....	10
1.2.3 Carcerands .....	11
1.3 COORDINATIVE BONDS .....	11
1.4 $\pi$ -STACKING .....	13
1.5 ELECTROSTATIC INTERACTIONS.....	13
1.6 INTERLOCKED MOLECULES (CATENANES) .....	14
1.7 CONCLUSION .....	14
1.8 REFERENCES.....	16
<b>2 PHOTOINDUCED ENERGY- AND ELECTRON TRANSFER PROCESSES WITHIN DYNAMIC SELF-ASSEMBLED DONOR-ACCEPTOR ARRAYS.....</b>	<b>23</b>
2.1 INTRODUCTION.....	24
2.2 EXPERIMENTAL .....	25
2.2.1 Spectroscopy.....	25
2.2.2 Materials .....	25
2.2.3 Synthesis.....	26
2.3 RESULTS AND DISCUSSION .....	29
2.3.1 Design of a dynamic self-assembled donor - acceptor pair.....	29
2.3.2 Synthesis of the photoactive components.....	31
2.3.3 Formation of the assemblies .....	34
2.3.4 Photophysical properties of 5 and its scandium assembly.....	38
2.3.5 Self-assembly of energy donor-acceptor dyads. Intramolecular Energy Transfer .....	39
2.3.6 Self-assembly of electron donor-acceptor dyads. Intramolecular Electron Transfer .....	48

2.4	CONCLUSION .....	51
2.5	REFERENCES .....	52
<b>3</b>	<b>PHOTOINDUCED ELECTRON TRANSFER BETWEEN METAL COORDINATED CYCLODEXTRIN ASSEMBLIES AND VIOLOGENS .....</b>	<b>57</b>
3.1	INTRODUCTION .....	58
3.2	RESULTS AND DISCUSSION .....	60
3.2.1	<i>Synthesis</i> .....	60
3.2.2	<i>Photophysical Properties</i> .....	61
3.2.3	<i>Photoinduced electron transfer processes</i> .....	63
3.3	CONCLUSION .....	69
3.4	EXPERIMENTAL .....	69
3.4.1	<i>General</i> .....	69
3.4.2	<i>Microcalorimetric Titrations</i> .....	70
3.4.3	<i>Time-resolved photophysics</i> .....	71
3.4.4	<i>Synthesis</i> .....	71
3.5	REFERENCES .....	74
<b>4</b>	<b>ENERGY TRANSFER BETWEEN <math>\text{Ru}(\text{BPY})_3^{2+}</math> AND DO3A COMPLEXED LANTHANIDES .....</b>	<b>79</b>
4.1	INTRODUCTION .....	80
4.2	SYNTHESIS .....	83
4.3	PHOTOPHYSICS .....	87
4.4	CONCLUSION .....	95
4.5	EXPERIMENTAL .....	95
4.5.1	<i>Photophysical measurements</i> .....	95
4.5.2	<i>Synthesis</i> .....	96
4.6	REFERENCES .....	101
<b>5</b>	<b>ZUSAMMENFASSUNG .....</b>	<b>105</b>
<b>6</b>	<b>SUMMARY .....</b>	<b>107</b>
<b>7</b>	<b>DANKSAGUNG / ACKNOWLEDGEMENT .....</b>	<b>109</b>

## **1 Efficiency of electron transfer processes in non-covalently assembled donor – acceptor systems**

Electron transfer reactions in chemistry have caught the attention of a wide audience in the scientific community.<sup>[1]</sup> The photoinduced electron transfer field has been developed to better understand photosynthesis and to mimic it. Uncountable acceptor and donor dyads and triads have been synthesized as model systems, using covalent linkages between the redox moieties.<sup>[2-7]</sup> This allows to control the distance and the relative orientation between the active components reasonably well. From these studies, it was possible to gain insight into the understanding of intramolecular photophysical processes. Marcus theory has been used to describe electron transfer processes within covalently linked donor-acceptor systems.<sup>[8]</sup>

Since the development of supramolecular chemistry,<sup>[9,10]</sup> several groups started to employ non-covalently linked molecules in all areas of chemistry. In the field of photoinduced electron- and energy transfer,<sup>[11]</sup> this development led to highly sophisticated systems. The synthetic effort can be reduced drastically since only modules are prepared, which are self-assembled to extended non-covalently linked redox active aggregates.

In this review the aggregates are distinguished by the type of non-covalent interactions used for assembly, such as hydrogen bonds, electrostatic interaction, aromatic  $\pi$ -stacking, hydrophobic interactions and coordinate metal-ligand bonds. In the following chapters the work on the different binding motifs will be reviewed and discussed. A full coverage of all work in the field is far beyond the scope of this review and I apologize to all authors, whose important work is not included in detail. The aim is rather to present a selection of typical and well investigated examples from all different types of assemblies and compare their intra-assembly electron transfer efficiencies.

## 1.1 Hydrogen bonds

This is by far the class of aggregates with the highest number of examples.<sup>[12]</sup> Hydrogen bonds can be formed by many organic functional groups and a further division is therefore necessary.

### 1.1.1 Carboxylic Acid Dimers

Carboxylic acids tend to form dimers in unpolar organic solvents. In 1992 the first example of a redox donor acceptor dyad using this motif for assembly was introduced by Nocera and co-workers.<sup>[13]</sup> He studied the photoinduced electron transfer process between a zinc porphyrin, bearing a carboxylic acid function and 3,4-dimethyl-benzoic acid in dichloromethane. The determined association constant was  $552\text{ M}^{-1}$  in chloroform. For that reason the concentration for aggregate formation had to be quite high which is not convenient for photophysical investigations. Nevertheless, Nocera was able to determine the rate of the forward- and the back electron transfer to be  $3.0 \cdot 10^{10}\text{ s}^{-1}$  and  $6.2 \cdot 10^9\text{ s}^{-1}$ , respectively. A direct comparison with a covalently linked system of same distance between the two centers was not given.

A nice comparison between a hydrogen,  $\sigma$ - and  $\pi$  bonds has been published by Williams et al.<sup>[14]</sup> Again porphyrins were used as photoactive units (see Figure 1). Upon photoexcitation of the zinc porphyrin, an electron from the zinc porphyrin is transferred to the Fe(III) moiety, reducing it to Fe(II). Finally charge recombination takes place to get the system back to its starting state.

The hydrogen-bonded linkage was compared with two covalent links of two fused cyclopentanes and two fused cyclopentens (figure 2). The labile hydrogen bonded system associates with a constant of  $440\text{ M}^{-1}$  and shows the shortest distance between the two metals through bonds, but the longest distance through space. This is due to the intrinsic geometry of the carboxylic acids. The angle between the porphyrins in the  $\sigma$ -bond-bridged cyclopentanes is about 124 degrees, leading to the smaller through space distance of the three systems.

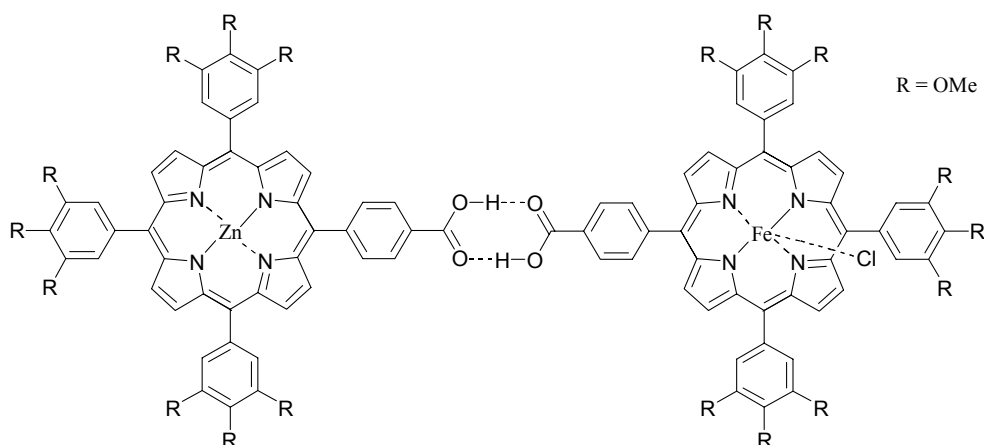


Figure 1. Hydrogen bound electron transfer model compounds used by Williams et al.

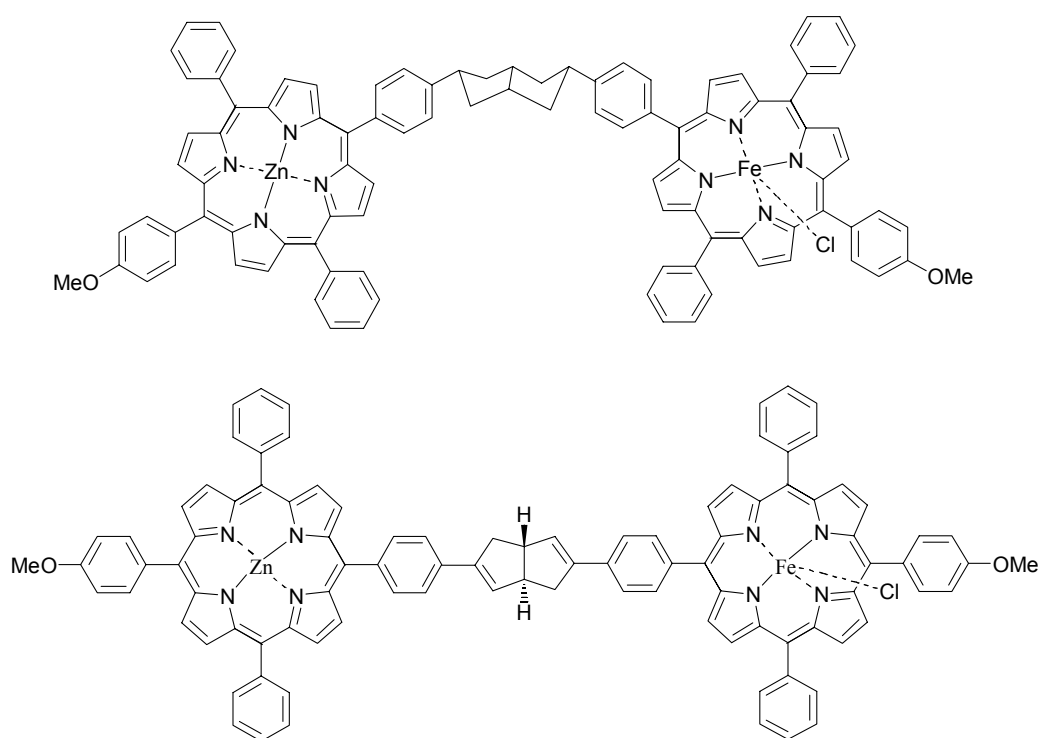


Figure 2. Reference systems for photoinduced electron transfer studies by Williams et al.

The rate constants for the electron transfer process exhibit an almost equal value for H-bonded (figure 1) and  $\pi$  bonded porphyrins (figure 2 bottom) ( $8.1 \times 10^9 \text{ s}^{-1}$  and  $8.8 \times 10^9 \text{ s}^{-1}$ , respectively). With a  $\sigma$ - bond- bridge (figure 2 top), the observed electron transfer rate is  $4.3 \times 10^9 \text{ s}^{-1}$ . This is somewhat surprising, since the estimated driving force for the electron transfer is 0.17 eV less exoergic for the non-covalently linked units. This

implies that the electronic coupling across an H-bond is superior then the one across two C-C single bonds. Furthermore the difference between the  $\sigma$ - and  $\pi$ - bridging ligand suggests that the electron transfer occurs through bond.

These results suggest that electron transfer in proteins might occur under participation of H-bonds between residues of amino acids like Asn, Gln, Arg, Asp, and Glu.

### 1.1.2 Peptide Based Motifs

The first example in this field was published in 1993 by Tamiaki et al.<sup>[15]</sup> A peptide chain forming a  $\beta$ -turn linking a porphyrin with a quinone was used to study the photoinduced electron transfer from the porpphyrin to the quinone. The rate which has been determined to  $2.1 \cdot 10^8 \text{ s}^{-1}$  lead the authors to the conclusion that a transfer through the hydrogen bond is slightly favored over the one through the  $\sigma$ - bonds.

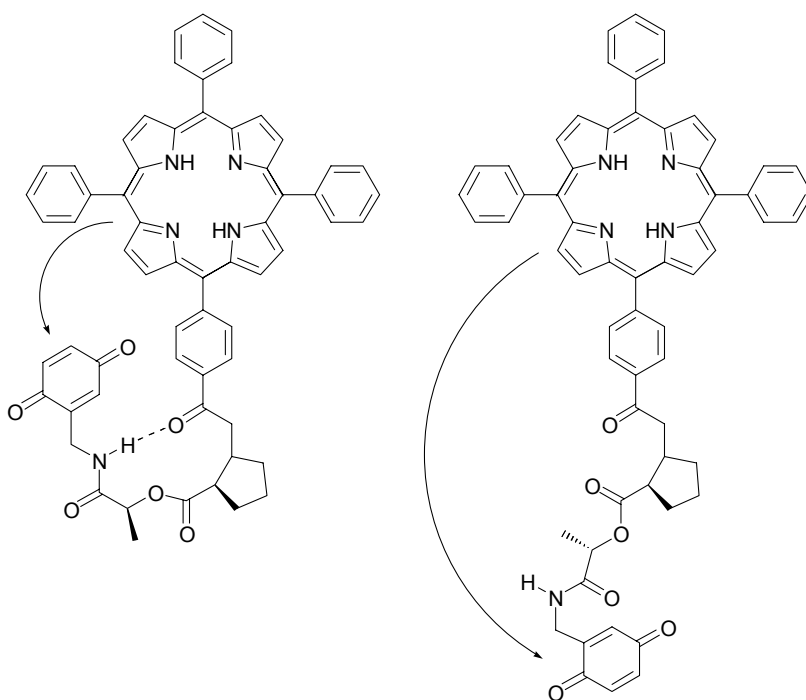


Figure 3. Peptide type donor-acceptor dyad, mimicking  $\beta$ -turn in apolar (left) and polar solvent (right).

A clearer proof for the effectiveness of  $\beta$ -turns as mediators of electron transfer was provided by Williamson and Bowler.<sup>[16]</sup> The porphyrin-quinone dyad (figure 3) exhibits

fast electron transfer ( $1.1 \times 10^9 \text{ s}^{-1}$ ) in  $\text{CH}_2\text{Cl}_2$  (left structure). In this medium the hydrogen bond of the  $\beta$ -turn is formed and effective. In polar solvent like DMSO, the  $\beta$ -turn is not formed and the system is deactivated by normal fluorescence of the porphyrin (right structure). That suggests that the electron transfer is either suppressed or very slow compared with the intrinsic luminescence lifetime of the porphyrin, because of the increased distance of the two redox partners.

### 1.1.3 Watson-Crick base pairs

The nucleobases adenine (A), cytosine (C), guanine (G), and thymine (T) are forming the alphabet of life and are the most prominent example of the selective complementary hydrogen bonding. Complementary pairs are formed between A/T and C/G, to give 2 and 3 hydrogen bond respectively. The easy synthetic accessibility make the nucleobases perfect tools in hydrogen-bond mediated electron transfer studies.

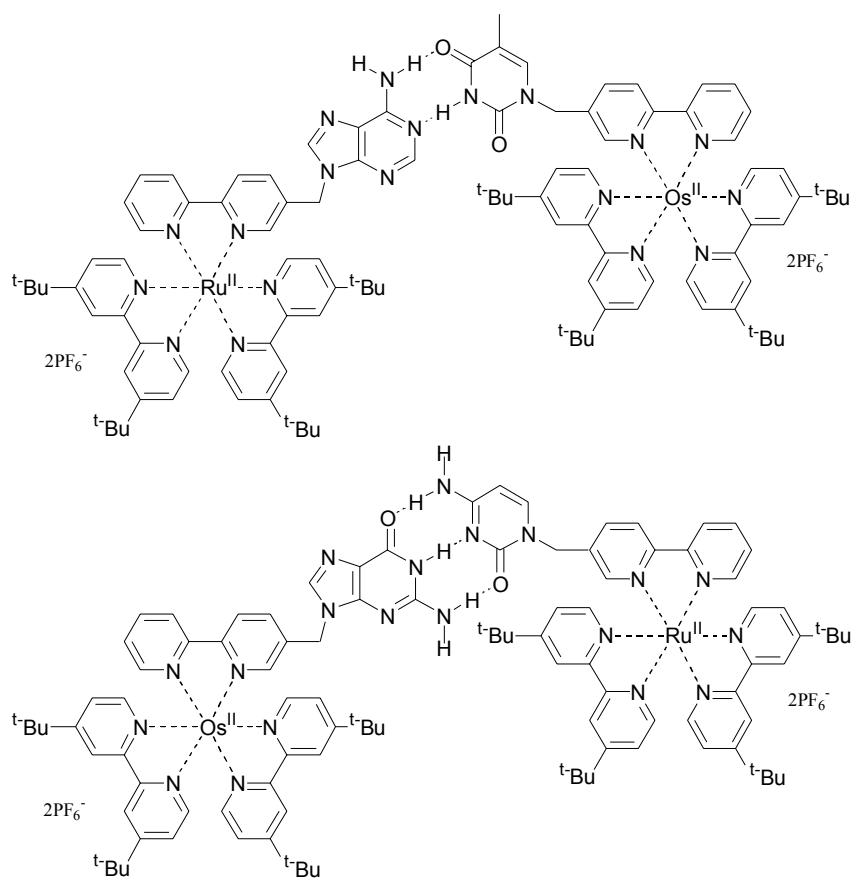


Figure 4. (a) A/T<sup>[25]</sup> and (b) C/G<sup>[26]</sup> bound dyads of Ru(bpy)<sub>3</sub> and Os(bpy)<sub>3</sub>

Numerous examples have been published, using porphyrins as photoactive component.<sup>[17-24]</sup>

The same kind of effort was directed to ruthenium polypyridyl and osmium polypyridyl-complexes, with base pairs as coupling motif.<sup>[27]</sup>

In the two systems displayed in figure 4, an energy transfer from the excited Ru(II) to Os(II) can be observed and monitored by the emission of the osmium polypyridyl complex. The single components retain their basic spectroscopical and electrochemical properties. This is not surprising since the CH<sub>2</sub>-spacer is electronically insulating the metal complex from the bridging nucleobases.

#### 1.1.4 Diimide Motif

Modification of the periphery of chromophores with 2,6 diacylaminopyridine- or 2,6 diaminopyridine- units can lead to the formation of a triple hydrogen bond with imides.

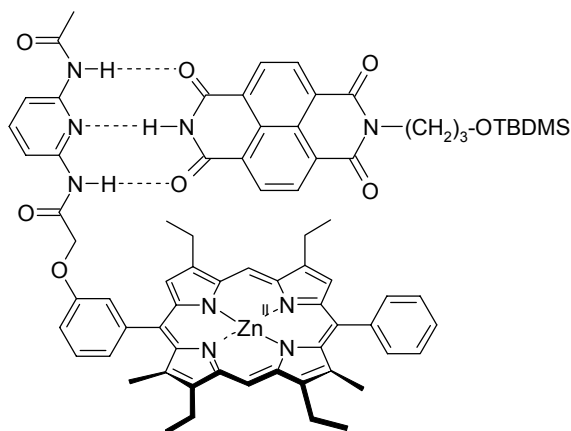


Figure 5. Triple hydrogen bond holding together a porphyrin and a naphthalene tetracarboxamide.<sup>[28]</sup>

The binding constant between both moieties in figure 5 is with  $1.6 \cdot 10^4 \text{ M}^{-1}$  in CDCl<sub>3</sub> and even  $1.3 \cdot 10^5 \text{ M}^{-1}$  in C<sub>6</sub>D<sub>6</sub> surprisingly high. The electron transfer rate for this system was not determined. However, the fast decay of the absorption band of the reduced acceptor (tetracarboxamide) is suggesting a  $k$  in the order of  $10^{10} \text{ s}^{-1}$ . Most likely  $\pi$ -stacking between the porphyrin and the naphthalene unit is contributing to the



association constant. A similar system with side-on orientation possesses binding constants, 2 orders of magnitude smaller.<sup>[29]</sup> Sessler et al. applied the same principle to a chlorine based dyad, determining a rate constant for electron transfer in dichloromethane of  $3.1 \times 10^9 \text{ s}^{-1}$ .<sup>[30]</sup>

### 1.1.5 “Hamilton” Receptors

Increasing the number of hydrogen bonds naturally increases the binding strength between the single components. By doubling the motif of the previous section, Hamilton et al. developed a receptor for barbiturates, forming 6 hydrogen bonds simultaneously.<sup>[31]</sup>

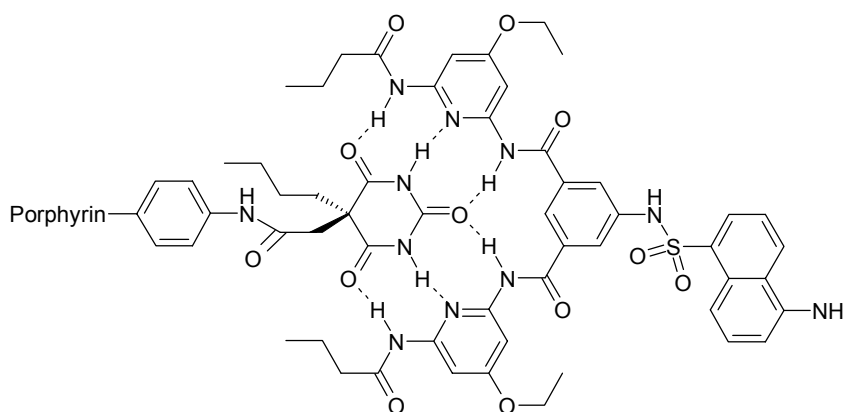


Figure 6. Hamilton receptor bound barbiturate

In the depicted assembly (figure 6),<sup>[32]</sup> an association constant of  $10^6 \text{ M}^{-1}$  in  $\text{CH}_2\text{Cl}_2$  allows to work in diluted conditions, which are desirable for accurate photophysical experiments. At a concentration of  $2 \times 10^{-5} \text{ M}$ , the barbiturate bearing porphyrin is accepting energy from the dansyl group, quenching the dansyl luminescence with an energy transfer rate of  $k_{\text{en}} = 2.4 \times 10^9 \text{ s}^{-1}$ .

Other studies using the same binding motif but focussing on ruthenium trisbipyridines as photoactive units were done by Isied and co-worker.<sup>[33-35]</sup> The main advantage of the Hamilton-receptor / barbiturate system is clearly the high association constant, which allows high dilution. Nevertheless, the work is still limited to unpolar solvents.

### 1.1.6 Proton Coupled Electron Transfer / Salt Bridges

This motif has initially been developed to mimic electron transfer in proteins. An amidinium-carboxylate salt bridge models the interaction between arginine and aspartate in proteins. The interesting property of these hydrogen bonds is that they are directional. That means an internal electrostatic field is created. An electron passing through a salt bridge will experience that field. This will have a direct influence on the rate of electron transfer. Nocera et al. addressed this problem in the system, sketched in figure 7.<sup>[36,37]</sup> Of course it must be kept in mind that reversing the bridge actually means changing the substitution of the donor and the acceptor and therefore changing the electrochemistry. This has a direct influence on the driving force ( $\Delta G$ ) of the electron transfer process.

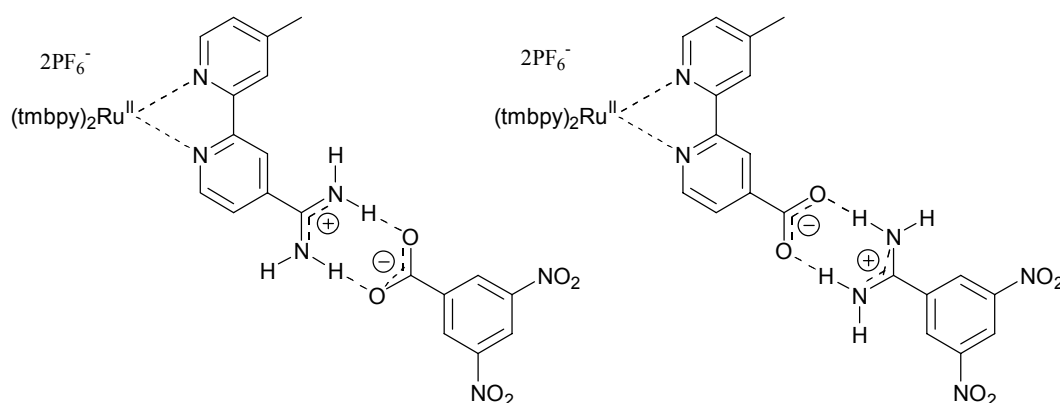


Figure 7. Salt bridges between  $(\text{tmbpy})_2\text{Ru}(\text{dmbpy})$  and dinitrobenzene.

In the left assembly of figure 7, the electron has to travel against the field created by the permanent dipole, whereas in the right case the electric dipole moment is in favor of the electron transfer. Nocera et al. calculated for both cases a proton coupled electron transfer rate of  $k_{\text{pcet}} = 8.4 \cdot 10^6 \text{ s}^{-1}$  (figure 7 left) and  $810 \cdot 10^6 \text{ s}^{-1}$  (figure 7 right), respectively.<sup>[37]</sup>

If the assembly is formed using two carboxylic acids (compare chapter 1.1.1),  $k_{\text{pcet}}$  was determined to  $43 \cdot 10^6 \text{ s}^{-1}$ . That clearly shows how salt bridges are able to enhance or slow the rate of electron transfer, depending on their direction. This principle might lead to the development of molecular diodes, in the framework of research on nanotechnology through the bottom up approach.

## 1.2 Hydrophobic Interactions

This motif of non-covalent interactions is based on cavities with different environment than the surrounding solvent.<sup>[38]</sup> Subsequently, inclusion compounds are formed. Within the hydrophobic interactions, three different approaches can be distinguished.

### 1.2.1 Cyclodextrins

Cyclodextrins are cyclic  $\alpha$ -1,4 glycosidic linked  $\alpha$ -D-glucopyranose entities. Most common are the  $\alpha$ -,  $\beta$ -, and  $\gamma$ - cyclodextrins, possessing 6, 7, and 8 sugar units. They all form hydrophobic cavities and are soluble in polar solvents. Aromatic and aliphatic guests can bind into the cavities of cyclodextrins with reasonably high association constants.<sup>[39]</sup> Cyclodextrins themselves are photoinactive but their chemistry is well explored and they can be appended via their primary or secondary sites with different chromophores to interesting photosensitive components. Weidner and Pikramenou observed a photoinduced electron transfer in a ruthenium bis terpyridin, bearing one permethylated  $\beta$ -cyclodextrin upon addition of quinons which penetrated the hydrophobic cavity.<sup>[40,41]</sup> In further investigations of the same parent system, addition of biphenylterpyridyl-terpyridyl osmium, lead to a dyad (figure 8) in which a very fast photoinduced electron transfer between the two metal centers could be observed.<sup>[42]</sup>

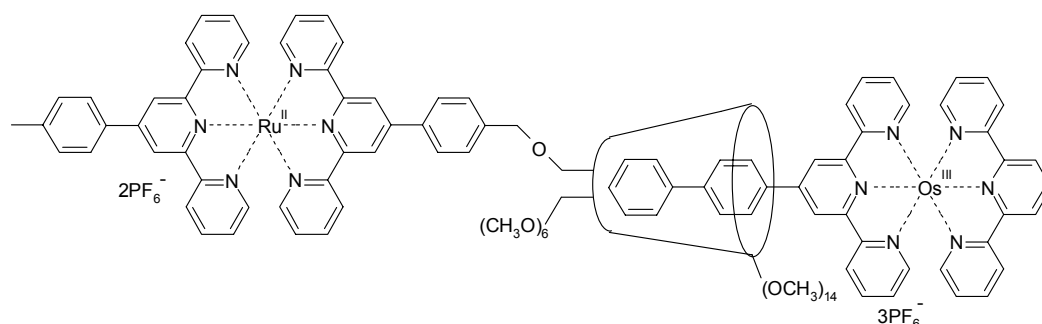


Figure 8. Ru(tpy)<sub>2</sub> – Os(tpy)<sub>2</sub> dyad, assembled by hydrophobic interaction through a  $\beta$ -cyclodextrin

The measured rate for the electron transfer between Ru(II) and Os(III) is  $9.5 \cdot 10^9 \text{ s}^{-1}$ . In a covalent system with a distance of 13 Å between both metal centers, the rate of electron transfer was determined to  $5.5 \cdot 10^9 \text{ s}^{-1}$ .<sup>[43]</sup>

More sophisticated studies have been published recently. Nolte et al. report a ruthenium tris bipyridine with six cyclodextrins that can bind bisalkylviologens.<sup>[44]</sup> The bound viologens quench the ruthenium luminescence via electron transfer. The binding of guests has been determined to  $2.8 \times 10^5 \text{ M}^{-1}$ . The luminescence can be restored by the competitive binding of guests with higher association constants such as bile acids.<sup>[45]</sup>

Besides ruthenium and osmium polypyridyls, also rhenium complexes have been investigated as electron acceptors, bearing cyclodextrins, which can host a donor.<sup>[46]</sup> Studies with cyclodextrin appended porphyrins have also been published. In an example of Ogoshi et al., a bis-plane-capped porphyrin is responding via electron transfer on the binding of quinones into the hydrophobic cavity of the cyclodextrins.<sup>[47]</sup>

### 1.2.2 Calixarenes

Just like cyclodextrins, calixarenes are forming hydrophilic cavities and are therefore able to bind guests. In this field as well, transition metal polypyridine complexes, such as ruthenium- and rhenium- bipyridyls, have received attention.<sup>[48-50]</sup> The main difference to the cyclodextrins is here that mostly a quencher (quinone) is part of the calixarene (figure 9) and suppresses the luminescence of the photoactive moiety by electron transfer.

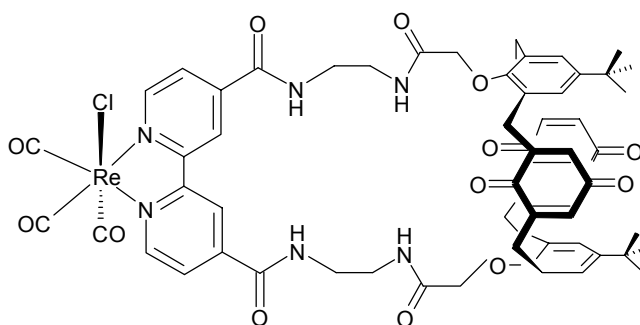


Figure 9. Quinone containing calixarene - rhenium complex

Binding of a suitable guest is blocking the quenching mechanism and restoring the luminescence. Through this concept, the published examples are designed as ‘switch-on’ sensors. This idea is basically the opposite approach of what we encountered so far. In the previous examples, the discussed systems are held together by a non-covalently

interaction. It is nevertheless also quite common, to build covalently linked system which photoinduced electron transfer can be suppressed by non-covalently binding of a guest.

### 1.2.3 Carcerands

Carcerands and Hemicarcerands are cage-type entities, which can host various small guests. The luminescence of encapsulated 2,3-butanedione can be quenched by external electron donors, such as diphenylamine ( $k_q = 3.5 \cdot 10^4 \text{ s}^{-1}$ ), benzidine ( $k_q = 4.2 \cdot 10^5 \text{ s}^{-1}$ ), or tetramethylphenylendiamin ( $k_q = 4.0 \cdot 10^8 \text{ s}^{-1}$ ).<sup>[51]</sup> These values are smaller than the quenching constants for free 2,3-butanedione in bimolecular processes. Also other examples are present in the literature.<sup>[52,53]</sup> They all have in common the reverse principle what we have seen so far. Hydrophobic interactions are used to separate donor and acceptor to slow down the diffusion controlled intrinsic rate constant of photoinduced electron transfer.

## 1.3 Coordinative bonds

Even though this motif of non-covalent interaction is having several advantages over some of the other discussed motifs, surprisingly few examples have been published. Of particular interest are coordinative bonds involving kinetically labile metal centers.

Early examples often involve metal containing porphyrins, in which pyridins are bound via coordinative bonds to the metal.<sup>[54-56]</sup>

In an approach by Fabbrizzi et al. a metal coordination is used in a more interesting way. A zinc(II) ion is used as template and docking site for a donor or acceptor (figure 10).<sup>[57,58]</sup>

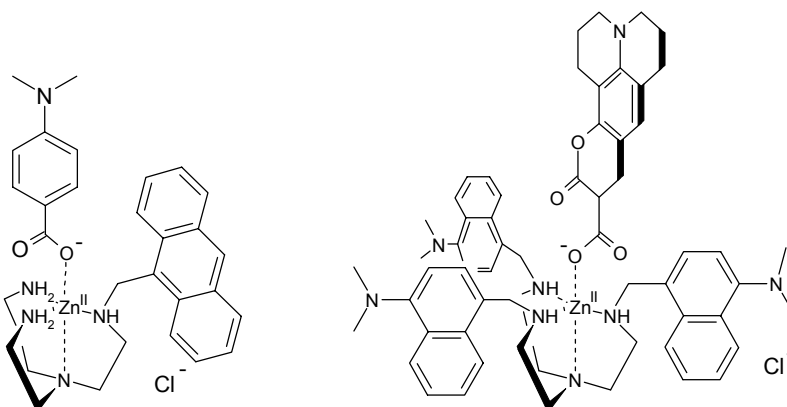


Figure 10. Supramolecular dyads, assembled by innocent metal ions, via coordinative bonds.

The depicted tetraamines (Figure 10) are shaped upon complexation of zinc, leaving one coordination site for donor- or acceptor molecules, containing a carboxylic function. Very high association constants could be achieved, because of the ionic interaction. For the anthracene containing moiety (Figure 10 left)<sup>[57]</sup> a  $K_{11}$  of  $280,000 \text{ M}^{-1}$  and for the other (Figure 10 right)<sup>[58]</sup> an even stronger binding of  $K_{11} = 1,000,000 \text{ M}^{-1}$  in ethanolic solution was determined. In both cases, the luminescence of the tetraamine appended chromophore was quenched upon complexation of a *N,N*-dimethylaniline-derivative or coumarine-343, respectively. In the coumarine case, the rate of energy transfer could be calculated to exceed  $3.5 \cdot 10^9 \text{ s}^{-1}$ . The advantages offered by the coordinative assembly are related to their dynamic nature. The dyads could be reversibly assembled and disassembled by small pH-changes.

Another interesting examples derives from the groups of König and Desvergne, in which a deprotonated riboflavin coordinates to a zinc-cyclen.<sup>[59]</sup> The cyclen bears a phenothiazine that is donating an electron upon light excitation of the flavin. The association constant between both moieties is about  $800,000 \text{ M}^{-1}$ . The coordinative bonds are strong enough to work in highly polar and even protic solvents, as in the last example.

## 1.4 $\pi$ -stacking

This motif of non-covalent linkage is found quite often in combination with hydrogen bonding. A lot of work has been dedicated to systems in which a quinone is ‘stacked’ over the plane of a porphyrin<sup>[60,61]</sup> or a hydroquinone,<sup>[62]</sup> while assisted by hydrogen bonds. Pure  $\pi$ -stacking is observed in molecular clips<sup>[63,64]</sup> and - tweezers<sup>[65-67]</sup> but best to my knowledge, has not been applied in supramolecular donor acceptor systems.

## 1.5 Electrostatic interactions

Electrostatic interactions has recently attracted a lot of attention in rotaxanes, which have been developed as molecular machines.<sup>[68]</sup>

Stoddart and Balzani have published an entire series of papers on what they call ‘Molecular Meccano’. The following examples are taken from this series. Pseudorotaxanes can be dethreaded via photoinduced electron transfer.<sup>[69,70]</sup>

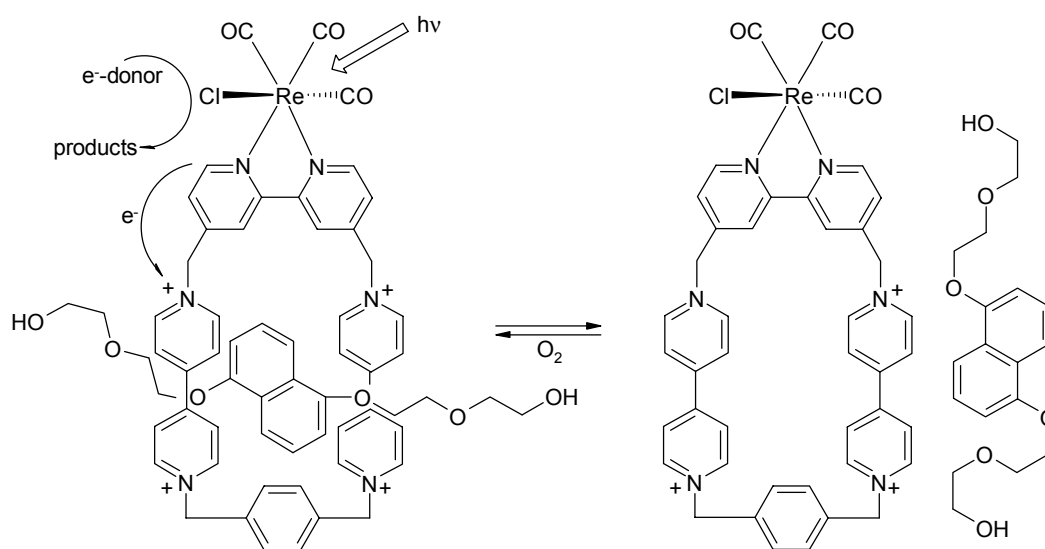


Figure 11. Photoinduced dethreading process of an electrostatically - stacked pseudorotaxane<sup>[69]</sup>

Excitation of the rhenium complex into the MLCT band will create Re(II) and a bipyridine anion. The excess electron from the bipyridine will be further transported to

the viologen-frame, reducing it to the neutral species. This process is so fast and so efficient that the transition metal complex is not luminescent in solution at room temperature.<sup>[71]</sup> This is an indication for an ultrafast process, probably on the picosecond time domain. Usually the back electron transfer from the reduced viologen to the metal, is also very fast and the dethreading of the axle, which involves the motion of a fairly big molecule cannot compete with the transfer of an electron. Nevertheless in presence of sufficient amounts of a sacrificial electron donor (oxalate,  $c=10^{-2}$  M), the metal can be reduced again to Re(I). The back electron transfer is prevented and the molecular motion favored. The disassembled species can be monitored by the luminescence of the free naphthalene axle.

The described principle was taken even further in the design of a molecular-level abacus,<sup>[72]</sup> in which the axle possesses a ruthenium trisbipyridine as a stopper, and two different viologens as docking stations for a cyclophane-ring. On light induced stimuli, the ring can be shifted between both 'stations'.

Here we see a similar approach as already described in chapter 1.2.2.

## 1.6 Interlocked molecules (Catenanes)

Sauvage and Balzani showed that photoinduction can be used as a trigger for the shutteling process in an unsymmetrical copper catenane.<sup>[73]</sup> In the described system, a 2,9-diphenyl-1,10-phenanthroline-PEG ring is interlocked with a phenanthroline-terpyridine-ring. A copper(I) is templated between the two phenanthroline units. Upon excitation, a metal to ligand charge transfer is forming copper(II), which prefers a trigonal bipyrimidal coordination. Therefore the ring with the terpyridine will shuttle around, supplying the copper with the proper coordination sphere.

## 1.7 Conclusion

Non-covalent interactions are able to compete with covalent bond in many ways. High association constants, as demonstrated in chapter 1.1 and 1.3, of up to  $10^6$  M<sup>-1</sup> can be realized with hydrogen bonds and coordinative interactions. In these strongly bound



systems, a steady architecture can be achieved by self-assembly. The stability can be controlled by parameters like pH and solvent polarity.

Interlocked molecules and electrostatic interactions, as non-covalent link between donor and acceptor, have been studied intensively in the last decade because they are offering a direct access into nanoscience. In these applications, a fast electron transfer rate is not desired, because the necessary molecular motion has to compete with it. Direct comparison between the motif on electrostatic interaction and interlock has, best to my knowledge, not been investigated yet.

The rate of photoinduced electron transfer in non-covalently linked systems can, in carefully chosen examples, indeed compete with the rates for covalent links. This statement is valid for the most common motifs. Excellent examples of the competitiveness have been discussed in chapter 1.1.1,<sup>[14]</sup> for hydrogen bonds, and in chapter 1.2.1,<sup>[42]</sup> for hydrophobic interactions. It was shown that the rate of electron transfer in hydrogen bound donor and acceptor is with  $8.1 \cdot 10^9 \text{ s}^{-1}$  about 90% as efficient as the covalent linkage including  $\pi$ -bonds. For cyclodextrin bound donor-acceptor systems, the rate constant could be determined to  $9.5 \cdot 10^9 \text{ s}^{-1}$  for the illustrated example. This is within the available data in good agreement with covalently,  $\sigma$ -bound, similar system.

Within the coordinative bonds, the small number of published examples makes a comparison with covalently linked systems quite difficult. Very few authors have provided the rates of electron- and energy transfer, and in those cases,<sup>[58]</sup> no covalently linked model systems for comparison were available. It remains a challenge to set a first milestone.

## 1.8 References

- [1] V. Balzani, Ed., *Electron Transfer in Chemistry*; Wiley-VCH: Weinheim, **2001**.
- [2] M. N. Paddon-Row, *Stimulating Concepts in Chemistry*; F. Vögtle, J. F. Stoddart, M. Shibasaki, Eds.; Wiley-VCH: Weinheim, **2000**; pp 267 - 291.
- [3] D. M. Guldi, *Chem. Soc. Rev.* **2002**, *31*, 22 – 36.
- [4] N. Armaroli, *Chem. Soc. Rev.* **2001**, *30*, 113 - 124.
- [5] A. P. de Silva, D. B. Fox, A. J. M. Huxley, T. S. Moody, *Coord. Chem. Rev.* **2000**, *205*, 41 – 57.
- [6] F. Barigelletti, L. Flamigni, *Chem. Soc. Rev.* **2000**, *29*, 1 - 12.
- [7] F. Diederich, M Gomez-Lopez, *Chem. Soc. Rev.* **1999**, *28*, 263 – 277.
- [8] R. A. Marcus, *Angew. Chem.* **1993**, *105*, 1161 – 1172; *Angew. Chem. Int. Ed. Engl.* **1993**, *32*, 1111 - 1121.
- [9] J.-M. Lehn, *Supramolecular Chemistry*; Wiley-VCH: Weinheim, 1995.
- [10] J.-M. Lehn, *Angew. Chem.* **1988**, *100*, 91 – 116; *Angew. Chem. Int Ed. Engl.* **1988**, *27*, 89 – 112.
- [11] M. D. Ward, *Chem. Soc. Rev.* **1997**, *26*, 365 - 375.
- [12] C. J. Chang, J. D. K. Brown, M. C. Y. Chang, E. A. Baker, D. G. Nocera; in *Electron Transfer in Chemistry*; V. Balzani, Ed.; Wiley-VCH: Weinheim, 2001; Vol. 3, 409 - 461.
- [13] C. Turró, C. K. Chang, G. E. Leroi, R. I. Cukier, D. G. Nocera, *J. Am. Chem. Soc.* **1992**, *114*, 4013 – 4015.
- [14] P. J. F. de Rege, S. A. Williams, M. J. Therien, *Science* **1995**, *269*, 1409 – 1413.
- [15] H. Tamiaki, K. Maruyama, *Chem. Lett.* **1993**, 1499 – 1502.

- [16] D. A. Williamson, B. E. Bowler, *J. Am. Chem. Soc.*, **1998**, *120*, 10902 – 10911.
- [17] A. Harriman, D. J. Magda, J. L. Sessler, *Chem. Commun.* **1991**, 345 – 346.
- [18] A. Harriman, D. J. Magda, J. L. Sessler, *J. Phys. Chem.* **1991**, 1530 – 1532.
- [19] A. Harriman, Y. Kubo, J. L. Sessler, *J. Am. Chem. Soc.* **1992**, *114*, 388 – 390.
- [20] J. L. Sessler, B. Wang, A. Harriman, *J. Am. Chem. Soc.* **1993**, *115*, 10418 – 10419.
- [21] J. L. Sessler, B. Wang, A. Harriman, *J. Am. Chem. Soc.* **1995**, *117*, 704 – 714.
- [22] T. Arimura, C. T. Brown, S. L. Springs, J. L. Sessler, *Chem. Commun.* **1996**, 2293 – 2294.
- [23] M. Sirish, B. G. Maiya, *J. Porphyrins Phthalocyanins* **1998**, *2*, 327 – 335.
- [24] A. Berg, Z. Shuali, M. Asano-Someda, H. Levanon, M. Fuhs, K. Möbius, R. Wang, C. Brown, J. L. Sessler, *J. Am. Chem. Soc.* **1999**, *121*, 7433 – 7534.
- [25] C. M. White, M. F. Gonzales, D. A. Bardwell, L. H. Rees, J. C. Jeffery, M. D. Ward, N. Armaroli, G. Calogero, F. Barigilletti, *J. Chem. Soc., Dalton Trans.* **1997**, 727 – 735.
- [26] N. Armaroli, F. Barigilletti, G. Calogero, L. Flamigni, C. M. White, M. D. Ward, *Chem. Commun.* **1997**, 2181 – 2182.
- [27] M. D. Ward, F. Barigilletti, *Coord. Chem. Rev.* **2001**, *216*, 127 – 154.
- [28] A. Osaka, E. Shiratori, R. Yoneshima, T. Okada, S. Taniguchi, N. Mataga, *Chem. Lett.* **1995**, 913 – 914.
- [29] A. Osaka, R. Yoneshima, H. Shiratori, T. Okada, S. Taniguchi, N. Mataga, *Chem. Commun.* **1998**, 1567 – 1568.
- [30] J. L. Sessler, C. T. Brown, D. O'Connor, S. L. Springs, R. Wang, M. Sathisatham, T. Hirose, *J. Org. Chem.* **1998**, *63*, 7370 – 7374.

- [31] S. K. Chang, A. D. Hamilton, *J. Am. Chem. Soc.* **1988**, *110*, 1318- 1319.
- [32] P. Tecilla, R. P. Dixon, G. Slobodkin, D. S. Alavi, D. H. Waldeck, A. D. Hamilton, *J. Am. Chem. Soc.* **1990**, *112*, 9408 – 9410.
- [33] T. Chin, Z. Gao, I. Lelouche, Y.-g. shin, A. Purandare, S. Knapp, S. S. Isied, *J. Am. Chem. Soc.* **1997**, *119*, 12849 – 12858.
- [34] A. S. Salameh, T. Ghaddar, S. S. Isied, *J. Phys. Org. Chem.* **1999**, 247 – 254.
- [35] T. Ghaddar, E. W. Castner, S. S. Isied, *J. Am. Chem. Soc.* **2000**, *122*, 1233 – 1234.
- [36] J. A. Roberts, J. P. Kirby, D. G. Nocera, *J. Am. Chem. Soc.* **1995**, *117*, 8051 – 8052.
- [37] J. P. Kirby, J. A. Roberts, D. G. Nocera, *J. Am. Chem. Soc.* **1997**, *119*, 9230 – 9236.
- [38] L. Fabbrizzi, M. Licchelli, A. Taglietti in *Electron Transfer in Chemistry*; V. Balzani, Ed.; Wiley-VCH: Weinheim, 2001; Vol. 3, 462 - 500.
- [39] M. V. Rekharsky, Y. Inoue, *Chem. Rev.* **1998**, *98*, 1875 – 1917.
- [40] S. Weidner, Z. Pikramenou, *Chem. Commun.* **1998**, 1473 – 1474.
- [41] J. M. Haider, Z. Pikramenou, *Eur. J. Inorg. Chem.* (2001) 189 - 194.
- [42] J. M. Haider, M. Chavarot, S. Weidner, I. Sadler, R. M. Williams, L. De Cola, Z. Pikramenou, *Inorg. Chem.* **2001**, *40*, 3912 – 3921.
- [43] B. Gholamkhass, K. Nozaki, T. Ohno, *J. Phys. Chem. B* **1997**, *101*, 9010 - 9021.
- [44] H. F. M. Nelissen, A. F. J. Schut, F. Venema, M. C. Feiters, R. J. M. Nolte, *Chem. Commun.* **2000**, 577 – 578.
- [45] B. Nelissen, PhD-Thesis, Nijmegen, **2002**.
- [46] A. Nakamura, S. Okutsu, Y. Oda, A. Ueno, F. Toda, *Tetrahedron Lett.* **1994**, *35*, 7241 – 7244.

- [47] Y. Kuroda, M. Ito, T. Sera, H. Ogoshi, *J. Am. Chem. Soc.* **1993**, *115*, 7003 – 7004.
- [48] M. Hissler, A. Harriman, P. Jost, G. Wimpff, R. Ziesel, *Angew. Chem.* **1998**, *110*, 3439 – 3443; *Angew. Chem. Int. Ed. Engl.* **1998**, *37*, 3249 – 3252.
- [49] A. Harriman, M. Hissler, P. Jost, G. Wimpff, R. Ziesel, *J. Am. Chem. Soc.* **1999**, *121*, 14 – 27.
- [50] P. D. Beer, V. Timoshenko, M. Maestri, P. Passaniti, V. Balzani, *Chem. Commun.* **1999**, 1755 – 1756.
- [51] A. J. Parola, F. Pina, E. Ferreira, M. Maestri, V. Balzani, *J. Am. Chem. Soc.* **1996**, *118*, 11610 – 11616.
- [52] A. Farran, K. Deshayes, C. Matthews, I. Balanescu, *J. Am. Chem. Soc.* **1995**, *117*, 9614 – 9615.
- [53] A. Farran, K. Deshayes, *J. Phys. Chem.* **1996**, *100*, 3305 – 3307.
- [54] C. A. Hunter, J. K. M. Sanders, G. S. Beddard, S. Evans, *J. Chem. Soc., Chem. Commun.* **1989**, 1765 – 1766.
- [55] H. Imahori, E. Yoshizawa, K. Yamada, K. Hagiwara, T. Koda, Y. Sakata, *J. Chem. Soc., Chem. Commun.* **1995**, 1133 – 1134.
- [56] C. A. Hunter, R. K. Hyde, *Angew. Chem.* **1996**, *108*, 2064 – 2067; *Angew. Chem. Int. Ed. Engl.* **1996**, *35*, 1936 – 1939.
- [57] G. De Santis, L. Fabbrizzi, M. Licchelli, A. Poggi, A. Taglietti, *Angew. Chem.* **1996**, *108*, 224 – 226; *Angew. Chem. Int. Ed. Engl.* **1996**, *35*, 202 – 204.
- [58] M. Di Casa, L. Fabbrizzi, M. Licchelli, A. Poggi, A. Russo, A. Taglietti, *Chem. Commun.* **2001**, 825 – 826.
- [59] B. König, M. Pelka, H. Zieg, T. Ritter, H. Bouas-Laurent, R. Bonneau, J. P. Desvergne, *J. Am. Chem. Soc.* **1999**, *121*, 1681 – 1687.

- [60] Y. Aoyama, M. Asakawa, Y. Matsui, H. Ogoshi, *J. Am. Chem. Soc.* **1991**, *113*, 6233 – 6240.
- [61] T. Hayashi, T. Miyahara, S. Kumazaki, H. Ogoshi, K. Yoshihara, *Angew. Chem.* **1996**, *108*, 2096 – 2100; *Angew. Chem. Int. Ed. Engl.* **1996**, *35*, 1964 – 1966.
- [62] F. D'Souza, *J. Am. Chem. Soc.* **1996**, *118*, 923 – 924.
- [63] F.-G. Klärner, J. Panitzky, D. Bläser, R. Boese, *Tetrahedron* **2001**, *57*, 3573 – 3687.
- [64] J. N. H. Reek, A. E. Rowan, M. J. Crossley, R. J. M. Nolte, *J. Org. Chem.* **1999**, *64*, 6653 – 6663.
- [65] R. Ruloff, U. P. Seebach, A. E. Merbach, F.-G. Klärner, *J. Phys. Org. Chem.* **2002**, *15*, 189 – 196.
- [66] F.-G. Klärner, U. Burkert, M. Kamieth, R. Boese, *J. Phys. Org. Chem.* **2000**, *13*, 604 – 611.
- [67] F.-G. Klärner, U. Burkert, M. Kamieth, R. Boese, J. Benet-Buchholz, *Chem. Eur. J.* **1999**, *5*, 1700 – 1707.
- [68] V. Balzani, A. Credi, F. M. Raymo, J. F. Stoddart, *Angew. Chem.* **2000**, *112*, 3484-3530; *Angew. Chem. Int. Ed. Engl.* **2000**, *39*, 3349 – 3391.
- [69] P. R. Ashton, V. Balzani, O. Kocian, L. Prodi, N. Spencer, J. F. Stoddart, *J. Am. Chem. Soc.* **1998**, *120*, 11190 – 11191.
- [70] P. R. Ashton, R. Ballardini, V. Balzani, E. C. Constable, A. Credi, O. Kocian, S. J. Langford, J. A. Preece, L. Prodi, E. R. Schofield, N. Spencer, J. F. Stoddart, S. Wenger, *Chem. Eur. J.* **1998**, *4*, 2413 – 2422.
- [71] P. R. Ashton, V. Balzani, A. Credi, O. Kocian, D. Passini, L. Prodi, N. Spencer, J. F. Stoddart, M. S. Tolley, M. Venturi, A. J. P. White, D. J. Williams, *Chem. Eur. J.* **1998**, *4*, 690 – 607.

- [72] P. R. Ashton, R. Ballardini, V. Balzani, A. Credi, K. R. Dress, E. Ishow, C. J. Cleverlaan, O. Kocian, J. A. Preece, N. Spencer, J. F. Stoddart, M. Venturi, S. Wenger, *Chem. Eur. J.* **2000**, *6*, 3558 – 3574.
- [73] A. Livoreil, J.-P. Sauvage, N. Amaroli, V. Balzani, L. Flamigni, B. Ventura, *J. Am. Chem. Soc.* **1997**, *119*, 12114 – 12124.





## 2 Photoinduced Energy- and Electron Transfer Processes within Dynamic Self-assembled Donor-Acceptor Arrays<sup>†</sup>

Abstract:

The synthesis and the photophysical properties of a series of non-covalently assembled donor-acceptor systems, dyads, is reported. The presented approach uses an “innocent” coordination compound, a scandium(III) acetyl acetonate derivative, as core and promotor of the dyad formation. Intercomponent photoinduced energy and/or electron transfer processes within the dynamic assembly, which yields to a statistical library of donor-acceptor systems, is reported. The assemblies for energy transfer processes are constituted by an energy donor, Ru(bpy)<sub>3</sub><sup>2+</sup>-based component (bpy = 2,2'-bipyridine), and by an energy acceptor moiety, anthracene-based unit, both substituted with a chelating ligand, acetyl acetone, that via coordination with a scandium ion will assure the formation of the dyad. If N,N,N',N'-tetramethyl-2,5-diaminobenzyl substituted acetyl acetonate ligands are used in the place of 9-acyl-anthracene, intramolecular photoinduced electron transfer from the amino derivative (electron donor) to the Ru(bpy)<sub>3</sub><sup>2+</sup>-unit was detected upon self assembly, mediated by the scandium complex. The photophysical processes can be studied on the lifetime of the kinetically labile complexes.

---

<sup>†</sup> The results of this chapter are accepted for publication:

M. Kercher, B. König, H. Zieg, L. De Cola, *J. Am. Chem. Soc.*

## 2.1 INTRODUCTION

Distance, relative orientation and the molecular structure that separates a donor group from an acceptor moiety largely influence the feasibility of intramolecular electron and energy transfer processes.<sup>[1-4]</sup> To study the effect of these parameters, most of the effort has been devoted to the synthesis of covalently linked systems.<sup>[5-8]</sup> Self-assembly is a feature of modern chemistry,<sup>[9-13]</sup> which has been applied recently to arrange donor-acceptor dyads. In particular hydrogen bonding, salt bridges and hydrophobic interactions have been investigated.<sup>[14-26]</sup> Surprisingly few examples that employ kinetically labile coordination compounds for assemble the donor-acceptor units have been published.<sup>[27-32]</sup> The non-covalent approach offers some advantages: i) the synthetic effort is reduced since only substructures are prepared and self-assembled to obtain more complex architectures. The modular strategy allows the synthesis of different aggregates from only a few building blocks. ii) the electronic interaction can be strongly modulated by solvent, temperature and concentration of the components; iii) electron- and energy transfer process can be studied over reversible bonds, longer distance, and new information are obtained on the electronic coupling via different linkage. However several disadvantages must also be considered in this approach. The low association constants often prevent photophysical studies for which high dilution conditions are required. Also in many cases (hydrogen bonds) the use of protic solvent is prevented.

We report here the synthesis and photophysical studies of a variety of photoactive components, and their assembly. In particular the photoinduced processes in donor-acceptor dyads, obtained by the assembly of such components via an “innocent” metal ion, scandium(III), will be discussed. The high association constants, the possibility to work in many solvents, and finally the accessibility to many different components, to construct our dyads, are the most interesting features of our supramolecular structures. In these dynamic assemblies the scandium is only a structural motif, that hold together an energy donor or electron acceptor, such as bis(2,2'-bipyridine)[4-{butane-1,3-dione-1-yl}-4'-methyl-2,2'-bipyridine]ruthenium-(II)-bis(hexafluorophosphate), and an energy

acceptor, 9-anthroylacetone, or an electron donor, 3-[2,5-(*N,N,N',N'*-tetramethyldiamino)benzyl]-2,4-pentadione (see scheme 1).

## 2.2 EXPERIMENTAL

### 2.2.1 Spectroscopy

The UV-Vis absorption spectra were recorded on a Hewlett-Packard diode array 84533 spectrophotometer. Recording of the emission spectra was done with a SPEX 1681 Fluorolog spectrofluorimeter. Lifetimes were determined using a Coherent Infinity Nd:YAG-XPO laser (1 ns pulses FWHM) and a Hamamatsu C5680-21 streak camera equipped with a Hamamatsu M5677 Low-Speed Single-Sweep Unit. Transient absorption spectroscopy was performed by irradiation of the sample with a Coherent Infinity Nd:YAG-XPO laser (1 ns pulses FWHM). The sample was probed by a low-pressure, high-power EG&G FX-504 Xe lamp. The passed light was dispersed by an Acton SpectraPro-150s imaging spectrograph equipped with 150 or 600 g mm<sup>-1</sup> grating and tunable slit (1-500 μm) resulting in a 6 or 1.2 nm maximum resolution, respectively. The data was collected with a system containing a gated intensified CCD detector (Princeton Instruments ICCD-576G/RB-EM) and an EG&G Princeton Applied Research Model 9650 digital delay generator. *I* and *I*<sub>0</sub> are measured simultaneously using a double 8 kernel 200μm optical fiber with this OMA-4 setup. WINSPEC (V 1.6.1, Princeton Instruments) used under Windows, programmed and accessed the setup.

### 2.2.2 Materials

4,4'-Dimethyl-2,2'-bipyridine (**1**),<sup>[33]</sup> 4'-methyl-2,2'-bipyridine-4-carboxylic acid (**2**),<sup>[34]</sup> 4'-methyl-2,2'-bipyridine-4-methylester (**3**),<sup>[35]</sup> rutheniumbisbipyridine dichloride,<sup>[36]</sup> 4-bromomethylene-4'-methyl-2,2'-bipyridine (**6**),<sup>[37]</sup> 2,5-(*N,N,N',N'*-tetramethyldiamino)benzaldehyde (**10**),<sup>[38]</sup> and Sc(acac)<sub>3</sub><sup>[39,40]</sup> were synthesized according to established methods. All solvents employed for photophysical measurements were of

spectroscopical grade and purchased from Aldrich. The benzonitrile used for the dynamic exchange of ligands was of HPLC grade and purchased from Aldrich.

### 2.2.3 Synthesis

**4-(1,3-butyldione)-4'-methyl-2,2'-bipyridine (4):** N-Isopropylidencyclohexylamine (247 mg, 1.7 mmol) was deprotonated in THF (20ml) with 1.7 mmol LDA at 0 °C over a period of 30 min and slowly added to 365 mg (1.6mmol) of 3, stirred for 4 h at that temperature and additional 16 h at room temperature. After neutralization with 1N HCl, the solution was diluted with CH<sub>2</sub>Cl<sub>2</sub> and extracted several times with saturated aqueous NH<sub>4</sub>Cl and water. The organic layer was evaporated to dryness and the crude product was purified by column chromatography (silica, CH<sub>2</sub>Cl<sub>2</sub>/CH<sub>3</sub>OH/NH<sub>4</sub>OH 200:10:1) to yield 220 mg (54%). <sup>1</sup>H-NMR (300 MHz, CDCl<sub>3</sub>) δ 2.27 (s, 3H), 2.45 (s, 3H), 6.39 (s, 1H), 7.17 (m, 1H), 7.75 (m, 1H), 8.26 (s, 1H), 8.56 (m, 1H), 8.74 (s, 1H), 8.78 (m, 1H), 15.76 (b, 1H) - <sup>13</sup>C-NMR (75 MHz, CDCl<sub>3</sub>, apt) δ 21.41 (-), 26.95 (-), 98.34 (-), 117.94 (-), 120.50 (-), 122.30 (-), 125.38 (-), 142.88 (+), 148.54 (+), 149.28 (-), 150.20 (-), 155.32 (+), 157.36 (+), 178.87 (+), 197.26 (+); IR (KBr) ν 2922, 1611, 1593, 1545, 1364, 1259, 1079, 831, 780, 841, 668, 514 cm<sup>-1</sup>; MS (FAB) m/z 255.11 (100) [M+H<sup>+</sup>], 154.01 (77); 136.03 (62)

**Bis(2,2'-bipyridine)-[4-(1,3-butyldione)-4'-methyl-2,2'-bipyridine]ruthenium-(II)-bis-(hexafluorophosphate) (5):** Bis(2,2'-bipyridine)dichloro-ruthenium (II) dihydrate (390 mg, 0.75 mmol) was refluxed with 189 mg (0.74 mmol) 4-(1,3-butyldione)-4'-methyl-2,2'-bipyridine in 20 ml ethanol/water (3:1) for 4h. The solvent was removed in vacuo and the residue dissolved in 10 ml water. The remaining starting material was removed by multiple extraction with CH<sub>2</sub>Cl<sub>2</sub> until the organic layer stayed clear. The crude product was precipitated as hexafluorophosphate from water to yield 520 mg (73%). <sup>1</sup>H-NMR (300 MHz, CD<sub>3</sub>CN) δ 2.31 (s), 2.59 (s), 6.67 (s), 7.32 (m) 7.39 (m), 7.44 (m), 7.59 (m), 7.75 (m), 7.89 (m) 8.09 (m), 8.55 (m), 8.80 (m), 15.76 (b) MS (ESI)

m/z 813.13 (30) [ $M^{2+}PF_6$ ], 334.08 (100) [ $M^{2+}$ ];  $C_{35}H_{30}N_6O_2Ru$  calc. 668.147, found 668.16

**3-(4-Methylen-4'-methyl-2,2'-bipyridyl)-2,4-pentadione (7):** Sodium acetyl acetate (180 mg, 1.5 mmol) and 4-bromomethylen-4'-methyl-2,2'-bipyridine (6) (320 mg, 1.2 mmol) were refluxed in THF (30 ml) for 6 h. The reaction mixture was stirred overnight at room temperature and evaporated to dryness. The residue was taken up in  $CH_2Cl_2$  and washed with diluted acetic acid. Evaporation to dryness and chromatography ( $SiO_2/CH_2Cl_2-CH_3OH-NH_3$  (25% in water), 100:5:0.5 (v/v),  $R_f = 0.3$ ) yielded 180 mg (54%) of **7** as a yellow oil;  $^1H$ -NMR (400 MHz,  $CDCl_3$ )  $\delta$  2.09 (s, 6H pentadion- $CH_3$ , enol-form), 2.18 (s, 6H pentadion- $CH_3$ , keto-form), 2.44 (s, 6H, bipyridine- $CH_3$ , keto- and enol-form), 3.22 (d,  $3J = 7.4$  Hz, 2H, bipyridine- $CH_2$ , keto-form), 3.75 (d, 2H, bipyridine- $CH_2$ , enol-form), 4.13 (d,  $3J = 7.4$  Hz, 1H, pentadion-CH, keto-form), 7.11 (m, 4H, bipyridine-H, keto- and enol-form), 8.24 (m, 4H, bipyridine-H, keto- and enol-form), 8.55 (m, 4H, bipyridine-H, keto- and enol-form), 16.89 (s, 1H, enol-OH);  $^{13}C$ -NMR (100 MHz,  $CDCl_3$ )  $\delta$  21.13 (+), 23.35 (+), 29.69 (+), 32.70 (-), 33.27 (-), 68.62 (+), 106.74 ( $C_{quat}$ ), 120.49 (+), 120.97 (+), 121.98 (+), 122.03 (+), 122.28 (+), 124.06 (+), 124.80 (+), 124.84 (+), 148.16 ( $C_{quat}$ ), 148.92 (+), 148.95 (+), 149.39 (+), 149.51 (+), 150.04 ( $C_{quat}$ ), 155.61 ( $C_{quat}$ ), 156.51 ( $C_{quat}$ ), 192.01 ( $C_{quat}$ ), 202.55 ( $C_{quat}$ ); IR (film)  $\nu$  3054, 3007, 2923, 1727, 1595, 1428, 824  $cm^{-1}$ ; MS (70 eV, EI) m/z 282 (22)[ $M^+$ ], 267 (20) [ $M^+-CH_3$ ], 239 (100) [ $M^+-C(O)CH_3$ ], 43 (20) [ $C(O)CH_3^+$ ].

**Bis(2,2'-bipyridine)[3-(4-Methylen-4'-methyl-2,2'-bipyridyl)-2,4-pentadion]-ruthenium-(II)bis(hexafluorophosphate) (8):** Bis(2,2'-bipyridine)dichloro-ruthenium (II) dihydrate (310 mg, 0.6 mmol) and 3-(4-methylen-4'-methyl-2,2'-bipyridyl)-2,4-pentadione (180 mg, 0.64 mmol) were refluxed in ethanol/water (3:1, 20 ml). The dark red solution was evaporated to dryness and the residue was purified by multiple gel permeation chromatography steps (Sephadex LH 20,  $CH_3OH$ ), yielding 360 mg (73%) of **8** (chloride salt) as a dark red solid, mp 248 °C. Counter ions were exchanged in water by treatment with aqueous  $KPF_6$  to give **8** ( $PF_6$  salt) as an orange residue, mp 172

°C; TLC (SiO<sub>2</sub>, CH<sub>3</sub>OH-aqueous NH<sub>4</sub>Cl-CH<sub>3</sub>NO<sub>2</sub>, 7:2:1,  $R_f$  = 0.54); <sup>1</sup>H-NMR (400 MHz, CD<sub>3</sub>CN) δ 2.10 (s), 2.13 (s), 2.51 (m), 2.89 (m), 3.00 (m), 7.22 (m), 7.37 (m), 7.52 (m), 7.69 (m), 8.03 (m), 8.34 (m), 8.46 (m); IR (KBr) ν 2958, 1605, 1483, 1466, 1427, 841, 556 cm<sup>-1</sup>; MS (ESI) m/z 695 (28) [M<sup>+</sup>], 261 (100)

**3-[2,5-(N,N,N',N'-Tetramethylamino)benzylidene]-2,4-pentandione (11):** 500 mg (2.6 mmol) 2,5-(N,N,N',N'-Tetramethylamino)benzaldehyde (**10**) and 0.24 ml (2.4 mmol) acetylacetone were combined with 2-3 drops of piperidine in 25 ml dry chloroform and refluxed for 5 h. The mixture was evaporated to dryness. Column chromatography (silica, PE/EE 7:3). yielded 400 mg (61%) **11** ( $R_f$  = 0.22) of a dark-red oil. - IR (KBr): ν = 2980 cm<sup>-1</sup>, 2941, 2865, 2829, 2789, 1686, 1658, 1505, 1242, 945. - <sup>1</sup>H NMR (400 MHz, CDCl<sub>3</sub>): δ = 2.21 (s, 3H, pentandione-CH<sub>3</sub>), 2.41 (s, 3H, pentandione-CH<sub>3</sub>), 2.65 (s, 6H, dimethylamino-CH<sub>3</sub>), 2.83 (s, 6H, dimethylamino-CH<sub>3</sub>), 6.61 (d, 4J = 2.9 Hz, 1H, phenyl-H), 6.76 (dd, 3J = 8.8 Hz, 4J = 2.9 Hz, 1H, phenyl-H), 7.00 (d, 3J = 8.8 Hz, 1H, phenyl-H), 7.87 (s, 1H, benzylidene-H). - <sup>13</sup>C NMR (100 MHz, CDCl<sub>3</sub>): δ = 26.73 (+), 31.24 (+), 40.87 (+), 45.24 (+), 114.20 (+), 116.06 (+), 119.40 (+), 127.76 (C<sub>quat</sub>), 139.74 (C<sub>quat</sub>), 141.24 (C<sub>quat</sub>), 144.34 (C<sub>quat</sub>), 146.48 (C<sub>quat</sub>), 197.17 (C<sub>quat</sub>), 204.52 (C<sub>quat</sub>). - MS (70 eV), m/z (%): 274 (100) [M<sup>+</sup>], 231 (36) [M<sup>+</sup> - CH<sub>3</sub>CO], 188 (22) [M<sup>+</sup> - 2 CH<sub>3</sub>CO].

**3-[2,5-(N,N,N',N'-Tetramethylamino)benzyl]-2,4-pentandione (12):** A solution of 180 mg (0.65 mmol) 3-[2,5-(N,N,N',N'-tetramethylamino)benzylidene]-2,4-pentandione (**11**) and 10 mg palladium/carbon (10%) in 50 ml methanol was hydrogenated at 5\*10<sup>6</sup> Pa hydrogen pressure for 1 h at room temperature. After filtration on celite, the methanol was removed in vacuo and the product was purified via column chromatography (silica, PE/EE 7:3). Yield: 140 mg (78%) **12** ( $R_f$  = 0.44) of a slightly yellow solid, Mp. 56 °C. - IR (KBr): ν = 2978 cm<sup>-1</sup>, 2937, 2822, 2781, 1612, 1511, 1191, 947, 811. - <sup>1</sup>H NMR (400 MHz, CDCl<sub>3</sub>): δ = 1.98 (s, 6H, pentandione-CH<sub>3</sub>, enol-form), 2.06 (s, 6H, pentandione-CH<sub>3</sub>, keto-form), 2.50 (s, 6H, dimethylamino-CH<sub>3</sub>,

keto-form), 2.56 (s, 6H, dimethylamino-CH<sub>3</sub>, enol-form), 2.77 (s, 6H, dimethylamino-CH<sub>3</sub>, enol-form), 2.79 (s, 6H, dimethylamino-CH<sub>3</sub>, keto-form), 3.09 (m, 2H, benzyl-CH<sub>2</sub>, keto-form), 3.61 (s, 2H, benzyl-CH<sub>2</sub>, enol-form) 4.07 (bs, 1H, pentandione-CH, keto-form), 6.34 (d, 3J = 3.0 Hz, 1H, phenyl-H, enol-form), 6.41 (d, 3J = 3.0 Hz, 1H, phenyl-H, keto-form), 6.53 (m, 2H, phenyl-H, keto- and enol-form), 6.99 (d, 3J = 2.7 Hz, 1H, phenyl-H, keto-form), 7.01 (d, 3J = 2.7 Hz, 1H, phenyl-H, enol-form). - <sup>13</sup>C NMR (100 MHz, CDCl<sub>3</sub>): δ = 23.05 (+), 27.74 (-), 29.39 (+), 30.91 (-), 40.88 (+), 40.98 (+), 45.37 (+), 45.59 (+), 68.88 (+), 109.18 (C<sub>quat</sub>), 111.28 (+), 112.06 (+), 112.58 (+), 114.88 (+), 120.39 (+), 121.37 (+), 134.79 (C<sub>quat</sub>), 135.52 (C<sub>quat</sub>), 142.82 (C<sub>quat</sub>), 147.60 (C<sub>quat</sub>), 167.69 (C<sub>quat</sub>), 191.85 (C<sub>quat</sub>), 204.35 (C<sub>quat</sub>). - MS (70 eV), m/z (%): 276 (100) [M<sup>+</sup>], 233 (16) [M<sup>+</sup> - CH<sub>3</sub>CO]. - C<sub>16</sub>H<sub>24</sub>N<sub>2</sub>O<sub>2</sub>: calc. C 69.53 H 8.75 N 10.14; found C 69.46 H 8.82 N 10.10.

**General method for the assembly of scandium complexes:** Up to 10 mg scandium-tris-acetylacetonate was dissolved with desired equivalents of ligands in 1 ml of benzonitrile. The solution was degassed and a static vacuum of 10<sup>-3</sup> Pa was applied. The reaction flask was left at room temperature, while the solvent and all volatile compounds were collected in a liquid nitrogen cooled flask. After complete evaporation of the solvent, the residue was redissolved and taken to dryness in the same manner twice, to ensure a complete exchange of ligands.

## 2.3 RESULTS AND DISCUSSION

### 2.3.1 Design of a dynamic self-assembled donor - acceptor pair

Acetyl acetonates (acac) are good ligands to complex trivalent metals ions, leading in the case of scandium(III) ions to thermodynamically stable (but kinetically labile) coordination compounds. The association constant in water for the formation of the

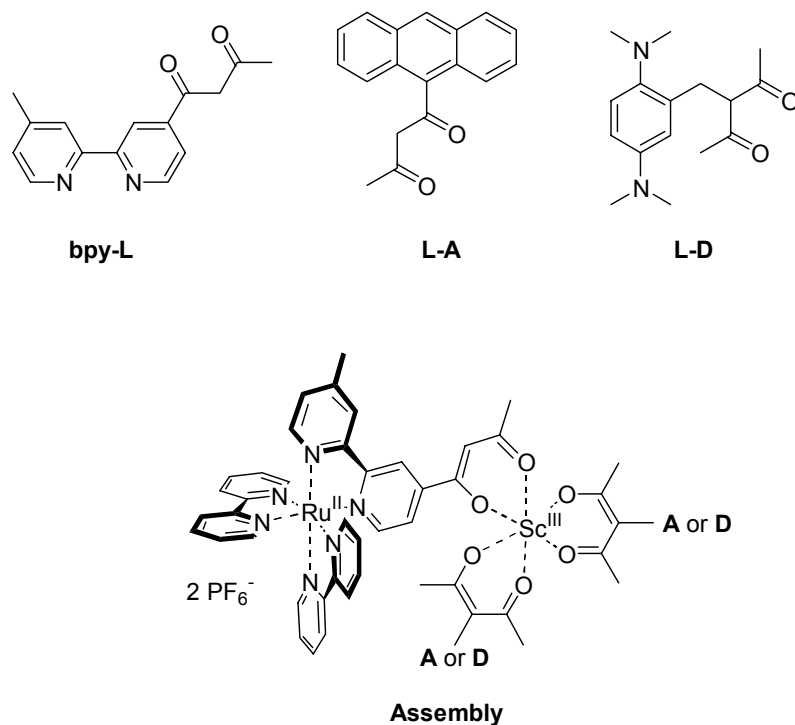
hexacoordinated complex is  $K_{\beta} > 10^{15} \text{ M}^{-1}$ .<sup>[40]</sup> We can therefore expect that with such high  $K_{\beta}$  complete association even at high dilution, necessary for photophysical investigations, occurs. The absorption spectra of  $\text{Sc}^{\text{(III)}}(\text{acac})_3$  shows no bands at energy below  $33500 \text{ cm}^{-1}$ . This enables us to build up species containing energy or electron donor and acceptor units that can be selectively excited in the visible region. Scandium(III) complexes cannot be oxidized and with a redox potential of  $\text{Sc}^{3+/2+}$   $E = -2.47 \text{ V vs Fc/Fc}^+$ , the complex will behave as an innocent spectator in electron transfer processes between suitable donor and acceptor ligands coordinated to it.

$\text{Sc}^{\text{(III)}}(\text{acac})_3$  complexes are kinetically labile. The average lifetime of the complex is about 5 ms, before an acetylacetonate is exchanged.<sup>[41]</sup> Therefore, using a statistical approach such complexes can be dynamically assembled from a reservoir of available ligands. Depending on the choice of substituted acac ligands an entire dynamic library of complexes can be created, from which some are able to constitute the correct building blocks for intramolecular energy or electron transfer processes. For our studies we have chosen 2 different substituents on the acac ligand, 3-[2,5-(*N,N,N',N'*-tetramethyldiamino)benzyl]-2,4-pentadione as electron donor, **L-D**, and an acac ligand containing an anthracene unit, 9-anthroylacetone, **L-A**, as energy acceptor (see scheme 1). The photosensitizer that behaves as electron acceptor or energy donor is a ruthenium complex,  $[\text{Ru}(\text{bpy-L})(\text{bpy})_2]^{2+}$  (**bpy-L** = 1-(4'-methyl-[2,2'-bipyridinyl-4-yl])butan-1,3-dione and bpy is 2,2'-bipyridine). The choice of these components is dictated by their well known spectroscopic and electrochemical properties.

In particular the ruthenium complex has (i) an absorption in the visible where the other components do not absorb, allowing a selective excitation, (ii) the lowest excited state is luminescent, and with lifetime of the order of hundreds of ns in acetonitrile.<sup>[42]</sup> This will allows us to observe even rather slow processes occurring in the excited states, but also to treat the dynamic assemblies as discrete (static) molecular species in the excited state, therefore excluding chemistry in this time domain. Furthermore because of the relatively easy substitution of the bipyridine ligands, it was possible to introduce the same type of chelating ligand, acac, on the Ru-based compound. We have therefore prepared and studied the  $\text{Ru}(\text{bpy})_2(\text{bpy-L})^{2+}$  complex, **5**, that is able by self-assembly to coordinate a substituted scandium complex (containing the photoactive acac ligand, **L-D** or **L-A**) to



form a suitable dyad for photoinduced energy or electron transfer processes (see scheme 1).



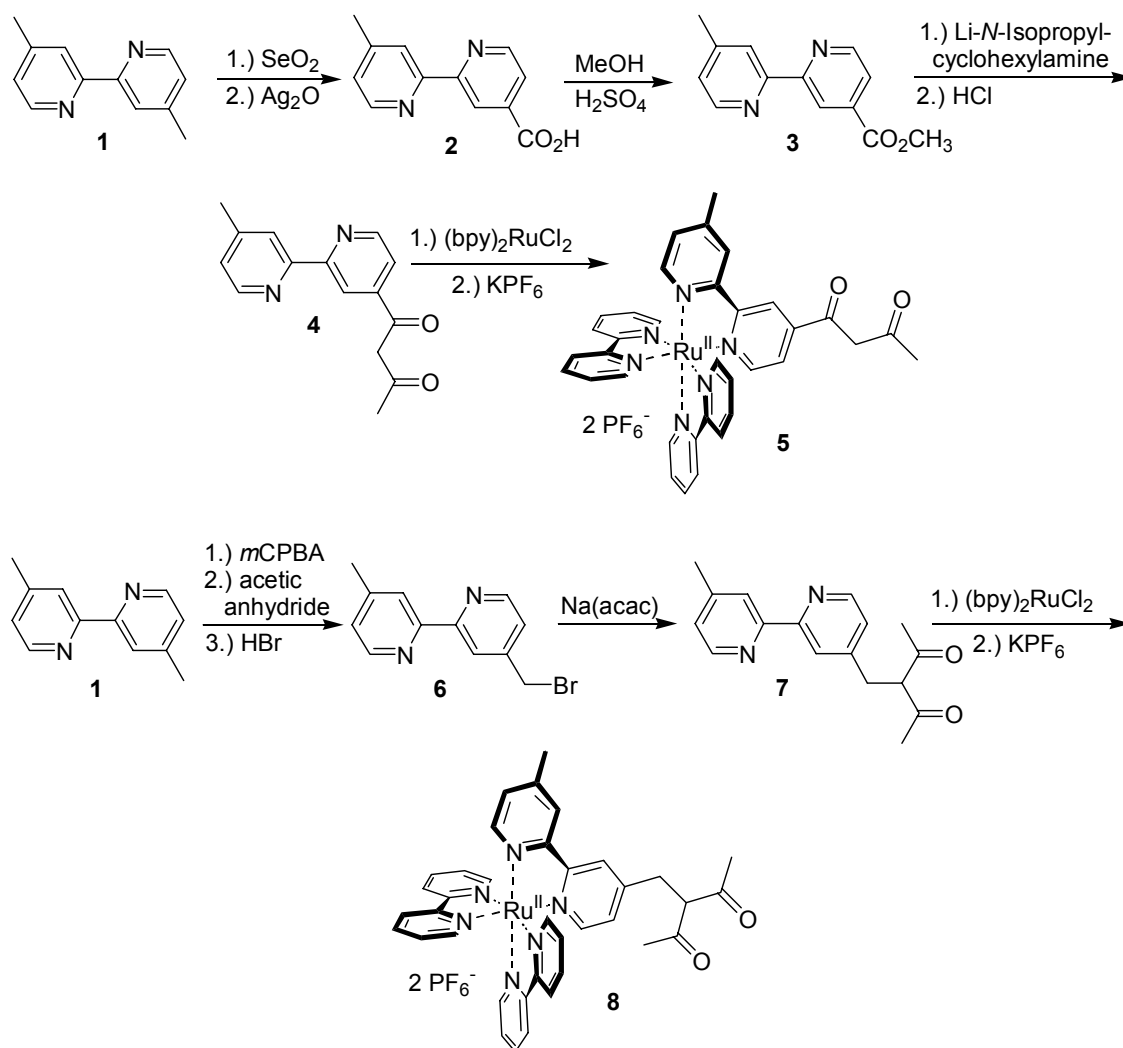
**Scheme 1.** Formulae of the components **bpy-L**, **L-A**, and **L-D**, and a schematic representation of self-assembled dyads via the coordination to the scandium (III) ion.

### 2.3.2 Synthesis of the photoactive components

Ruthenium trisbipyridine complexes have been widely used to study photoinduced electron- and energy- transfer processes for their unique photophysical and redox properties.<sup>[42-44]</sup> The chemistry of bipyridines is very well explored and ensures the availability of suitable functionalized compounds.<sup>[45,46]</sup> The synthesis of a ruthenium complex with a acac binding site for scandium (III) ions is shown in scheme 2. 4,4'-Dimethyl-2,2'-bipyridine (**1**)<sup>[33]</sup> was oxidized according to a two-step procedure, reported by McCafferty et al. with SeO<sub>2</sub> and Ag<sub>2</sub>O.<sup>[34]</sup> The free carboxylic acid **2** was

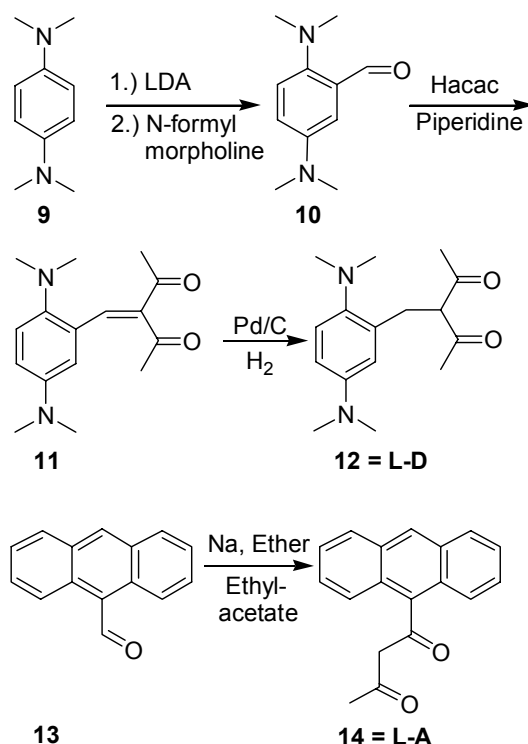
converted into the methyl ester **3**<sup>[35]</sup> and compound **bpy-L** (**4**) could be obtained upon addition of lithium-*N*-isopropyliden-cyclohexylamin and acidic workup in 54% yield. The ruthenium complex **5** was formed upon reaction of ruthenium-bis-2,2'-bipyridine dichloride with **bpy-L** in a mixture of water and ethanol. The product has been obtained as PF<sub>6</sub><sup>-</sup> salt in 73 % yield.

To achieve a different connectivity between acac and bipyridine 4-bromomethylene-4'-methyl-2,2'-bipyridine (**6**)<sup>[37]</sup> was reacted with sodium acac to give **7** in 54% yield. Although the compound is a suitable ligand to give scandium acac complexes as confirmed by mass spectrometry, it could not be used to study photoinduced energy- and electron transfer processes. Upon formation of the corresponding ruthenium complex **8** the ligand shows significant photolability with consequent decomposition.



**Scheme 2.** Synthesis of ruthenium tris bipyridine functionalized acac ligands,  $\text{Ru}(\text{bpy})_2(\text{bpy-L})$

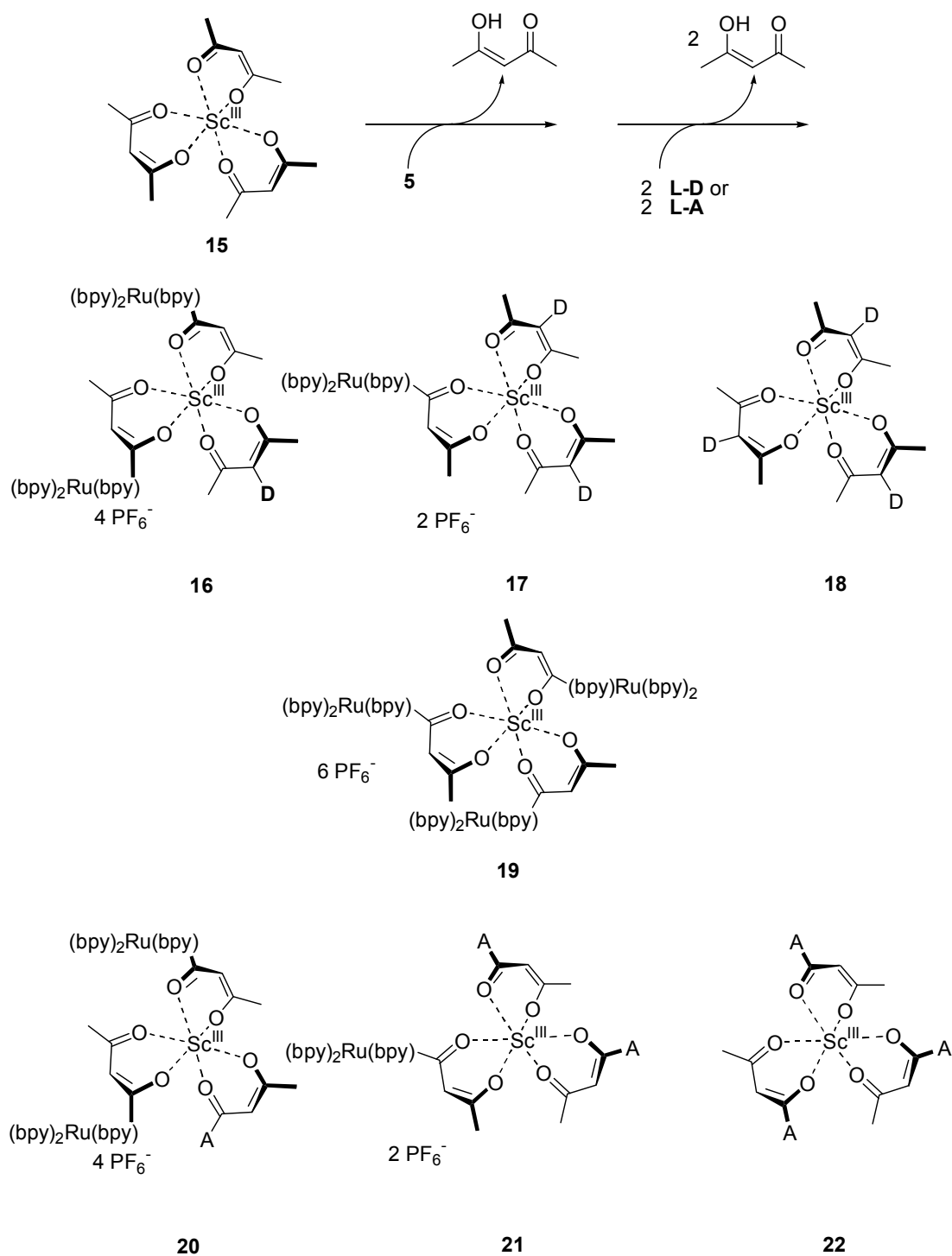
For the synthesis of an acac ligand containing an electron donor group, **L-D**, commercially available tetramethyl-phenyldiamine was formylated<sup>[38]</sup> followed by a condensation reaction with acetyl acetone, to give the benzylideneacetylacetone in 61% yield. Hydrogenation of the double bond led in 78% yield to the desired  $\beta$ -diketone **12 (L-D)**. The anthracene-acac conjugate **14 (L-A)** was obtained following a procedure reported by Evans et al.<sup>[47]</sup> by reacting 9-acetylanthracene with ethylacetate in presence of sodium (scheme 3).



**Scheme 3.** Synthesis of anthracene and tetramethyl phenylenediamine functionalized acac ligands

### 2.3.3 Formation of the assemblies

For the preparation of the dyads assembled via a scandium(III)(acac)<sub>3</sub> complex a mixture of the parent scandium(III) trisacetylacetonate, **15**,<sup>[39,40]</sup> ruthenium complex **5** and compounds **L-D** or **L-A** were mixed in the appropriate stoichiometry in benzonitrile and a pressure of 10<sup>-3</sup> Pa was applied (see scheme 4). Benzonitrile is a high boiling solvent in which the PF<sub>6</sub> salt of the ruthenium complex is showing good solubility. Applying high vacuum to the mixture, the solvent and the unsubstituted acetylacetonate, the only volatile compounds, are slowly evaporated, driving the equilibrium towards the formation of the scandium complexes with substituted acac ligands. This procedure yields a statistical library of different scandium compounds, assemblies **16**, **17**, **18**, and **19** are obtained when **L-A** is employed, while assemblies **19**, **20**, **21** and **22** are produced if **L-D** is one of the reagents, as shown in scheme 4.

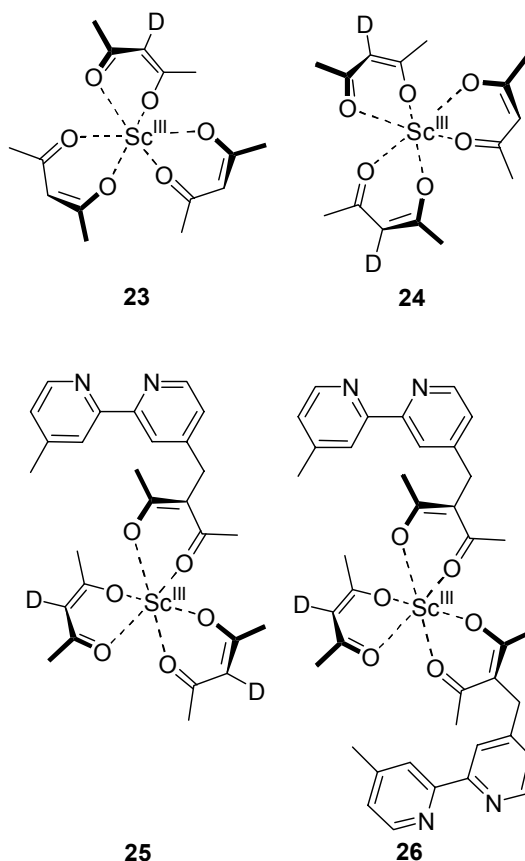


**Scheme 4.** Preparation of substituted scandium(III)(acac)<sub>3</sub> complexes by dynamic ligand exchange

The ligand exchange can be monitored by NMR. The disappearance of the resonance of the characteristic proton at carbon 3 of 2,4-pentadione clearly indicates the exchange of unsubstituted acac ligands. A complete assignment of resonances is not possible due to the complexity of the mixture.

Assuming simple statistics with equal binding strength for all  $\beta$ -diketones the relative abundance of different substitution patterns can be calculated. All complexes were prepared in a stoichiometry of 1:2 of the ruthenium complex **5** to **L-D** or **L-A**, respectively. The theoretical relative abundance of the scandium complexes predict the least favourable complex bearing three ruthenium acac ligands (**19**) to be obtained in less than 4%. From this assembly only a luminescence contribution to the background of the emission spectra of the mixture is expected. Complexes bearing photoactive units and quenchers form the majority of all coordination complexes, 66%, and will give detectable indication of electron or energy transfer process. Assemblies not bearing any ruthenium complexes (**18** and **22**), present in 30%, will not contribute to absorption in the visible, where the excitation is going to be performed, or luminescence in the 550 – 800 nm region, where the ruthenium emission is monitored. Their absorption in the visible ( $\lambda > 450$  nm) where the ruthenium complex present its metal-to-ligand-charge-transfer (MLCT) bands is negligible. In the case of the anthracene-substituted acac ligands, the scandium complex **22** bearing three of these ligands is not soluble in benzonitrile and has been isolated from the mixture. Here we can assume to have a mixture of three different complexes in which at least one ruthenium-substituted acac ligand is present. Obviously no complete quenching of the luminescence of the ruthenium-acac compounds can be expected by formation of mixed scandium complexes. The abundance of complexes in the equilibrium having donor and acceptor ligand, such as **16/17** and **20/21**, is much less than 100%. In addition, a small amount of non-coordinated ruthenium ligands **5** may contribute to an unquenched background signal.

Mass spectrometry was used to monitor complex formation and distribution of ligands. In the EI mass spectra of the equilibrium mixture of  $\text{Sc}(\text{acac})_3$  (**15**) with two equivalents of **12**, molecular ions of the complexes **15** ( $m/z = 342$ ; 20%), **23** ( $m/z = 518$ ; 12%), **24** ( $m/z = 694$ ; 6%), and **18** ( $m/z = 870$ ; 4%), shown in schemes **4** and **5**, were detected.



**Scheme 5.** Scandium(III) complexes detected by mass spectrometry.

This supports the assumption that all coordination compounds are present in the equilibrium. The different sensitivity of detection for each compound in EI-MS does not allow any quantitative conclusions. With ionisation methods such as FAB or ESI, which allow a much better quantitative analysis, no scandium containing complexes could be detected.<sup>[48]</sup>

Addition of one equivalent of 3-(4-methylen-4'-methyl-2,2'-bipyridyl)-2,4-pentadione **7** to the mixture of complexes **15**, **18**, **23**, and **24** lead to detectable signals of the newly formed complexes **25** ( $m/z = 876$ ; 22%) and **26** ( $m/z = 882$ ; 8%) in the EI mass spectrum. This confirms the dynamic character of the mixture of coordination compounds. The given percentages for the molecules do not represent absolute abundance in solution. They only indicate the abundance of the detected fragments in the mass spectra.

More evidence for the formation of scandium complexes with mixed acac ligands and the dynamic character of the library will be provided in the photophysical section.

### 2.3.4 Photophysical properties of **5** and its scandium assembly

Table 1. Photophysical data in acetonitrile

	Abs <sub>max</sub> / nm	Em <sub>max</sub> / nm	$\Phi_{\text{aerated}}$	$\tau_{\text{aerated}}$ / ns	$\tau_{\text{deaerated}}$ / ns
<b>Ru(bpy)<sub>3</sub></b>	455	614	0.016	160	890
<b>5</b>	458	624	0.011	150	525

The absorption and emission spectra of ruthenium complex **5** and of the reference compound  $\text{Ru(bpy)}_3^{2+}$  in acetonitrile solution are reported in Figure 1. Some photophysical data are summarized in table 1. The spectra show the characteristic <sup>1</sup>MLCT bands in the visible region that in complex **5** are slightly red shifted compared to the absorption of the parent compound. This can be explained considering that the lowest excited state involves the transition  $\text{Ru} \rightarrow \text{bpy-L}$  since the acetylacetonate is a weak electron-withdrawing group. The direct substitution of the bpy with the acac moiety provides a good electronic coupling between the bpy and the acac group.<sup>[42]</sup> The UV region of the spectrum is dominated by the intense absorption bands of the bipyridine ligands (300 nm), and by comparison with the  $\text{Sc(acac)}_3$  compound, the weak transition centered on the acac ligands (210 nm) can also be assigned. As already mentioned the scandium complex does not contribute to the absorption spectrum in the visible region.

The room temperature emission spectrum in aerated acetonitrile solution (Fig. 1 inset) shows a maximum at 624 nm also slightly red shifted compared with the reference complex, and in agreement with the assignment of a <sup>3</sup>MLCT as the lowest excited state



involving a transition from the Ru to the **L** ligand. The excited state lifetime and the emission quantum yield are reported in Table 1.

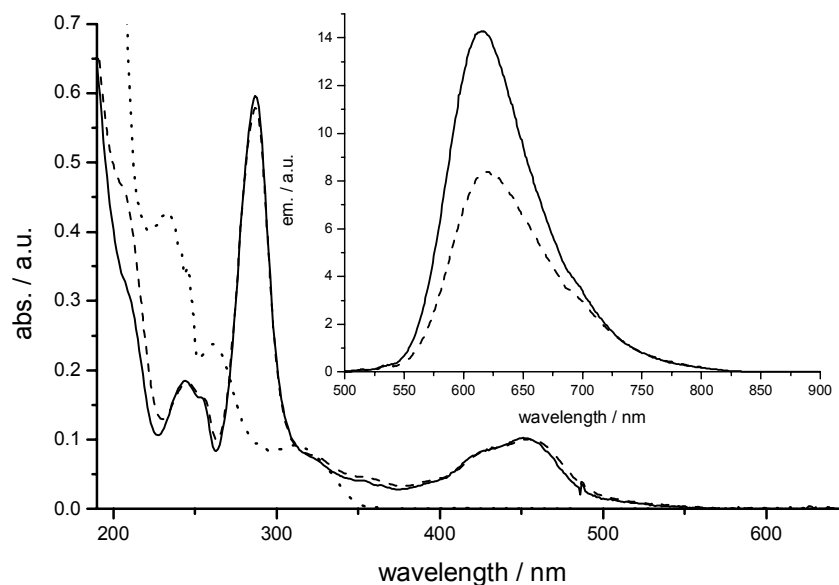


**Figure 1.** UV-Vis absorption spectra and inset room temperature emission spectra of Ru(bpy)<sub>3</sub><sup>2+</sup> (full line), **5** (dashed line)  $C \approx 10^{-5}$  M, and Sc(acac)<sub>3</sub> (dotted line)  $C \approx 10^{-3}$  M in acetonitrile solutions.

Complexation of **5** to scandium(III) ions does not change the photophysical properties significantly.

### 2.3.5 Self-assembly of energy donor-acceptor dyads. Intramolecular Energy Transfer

Upon appropriate choice of components it is possible to build up, using the scandium as “assembler”, an energy donor-acceptor dyad. We have chosen an energy donor such as a ruthenium unit, **5**, and as energy acceptor an anthracene derivative, **L-A**. The two components have been previously investigated in covalently linked systems<sup>[49-51]</sup> and the

energy transfer processes from the excited ruthenium unit to the triplet excited state of the anthracene have been shown by emission quenching<sup>[50]</sup> and time resolved spectroscopy.<sup>[49]</sup>

We expect on the basis of the energetics (see scheme 6) a triplet-triplet energy transfer from the ruthenium moiety to the 9-acyl-anthracene, since we are exciting in the <sup>1</sup>MLCT band of the transition metal complex. At such energy in fact, population of the singlet excited state of the anthracene moiety cannot occur.

In the assembly process a statistic distribution of species is possible and an interesting library of compounds is obtained. The only assemblies that will give a photoinduced energy transfer process are those containing both, one or two units of **5** and one or two units of **L-A** (complex **20** and **21**, scheme 4). For our investigation they will behave identically and no attempts were made to separate them. On the other hand the formation of the assemblies containing only anthracene and/or ruthenium complex, even though will make the measurements more complicated, will not influence the final results, aiming to the investigation of the energy transfer process and determination of its rate.

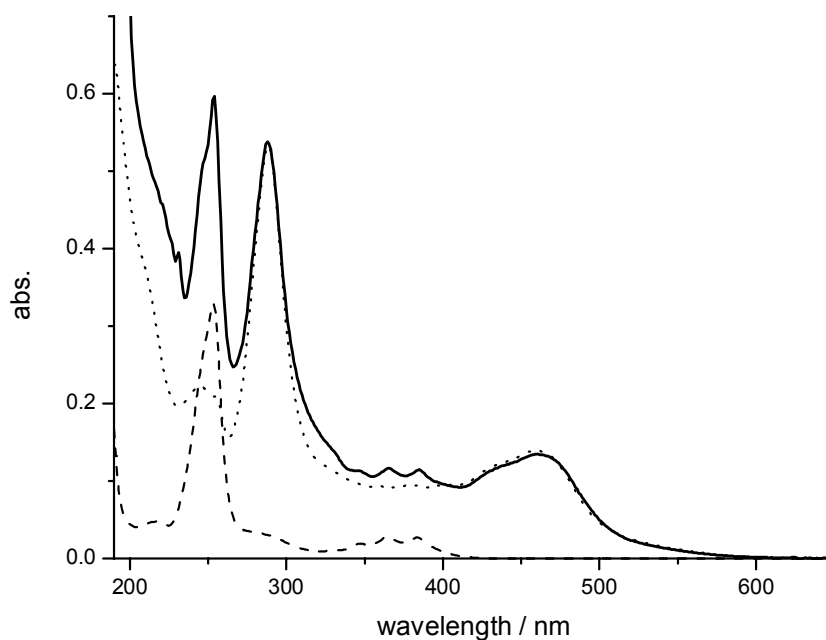


**Figure 2.** UV-Vis absorption spectra of **5** (dotted line), **LA** (dashed line), and the assembly of both (Ru-Sc-LA) (full line) in deaerated acetonitrile solution.  $C \approx 10^{-5} \text{M}$ .

The absorption spectra of the separate components and of the assemblies are shown in figure 2. In the assembly the visible region is dominated by the already mentioned MLCT bands of the ruthenium units, and the close UV region by the characteristic absorption bands of the anthracene moiety that also shows an intense band at 253 nm. Since  $\text{Ru}(\text{bpy})_3^{2+}$  is a known sensitizer for singlet oxygen and anthracene is known to form endoperoxides with singlet oxygen,<sup>[52]</sup> all experiments were carried out in oxygen free acetonitrile solutions.

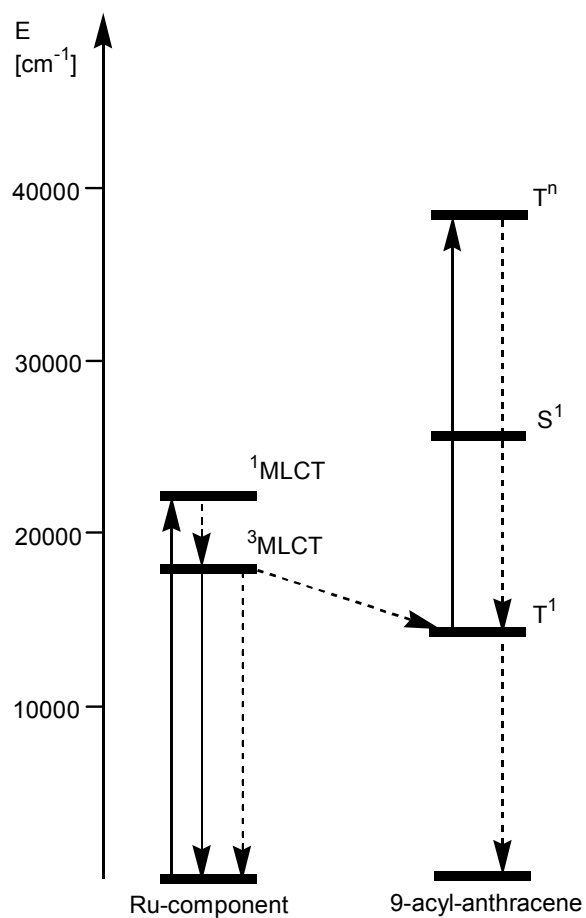
As can be easily seen the spectrum of the adducts (containing 1 or 2 Ru-based moieties and/or 1 or 2 **L-A** units) is essentially the sum of the absorption spectra of **5** and **L-A**. This indicates that no strong ground state electronic interaction between the two chromophores ( $\text{Ru}(\text{bpy})_3^{2+}$  and anthracene) is observed but does not indicate that the assembly is indeed formed when the components are mixed together. In order to have the proof of the formation of the assembly, steady state and time resolved spectroscopy has been employed.

The emission spectra of **5** and of the assembly show the characteristic luminescence of the ruthenium-based component but with different intensities. As one would expect, in the assembly a quenching of the emission is observed. This is in agreement with what was previously reported for covalently linked systems<sup>[49-51]</sup>. However an accurate evaluation of the luminescence quenching in the mixture is not possible only from the emission because of the statistical approach employed to build up the dyad. In fact the presence of free ruthenium complex, **5**, influences the total emission quantum yield, making the correct evaluation of the quenching impossible. It is interesting to notice however that the presence of free anthracene eventually, does not corrupt our measurements since the fluorescence of the anthracene is located in a region (400-500 nm) that does not overlap with the ruthenium emission.

In order to have a quantitative evaluation of the quenching and to understand the process, responsible for the decrease in the emission intensity, time resolved measurements were performed. The excited state lifetime of compound **5**, measured under deaerated conditions, detected at about 620 nm, was 525 ns (see table 1). A monoexponential model describes the observed decay trace. Within the assembly of **5** and **L-A** through the scandium complex (adduct **20** or **21**) the excited state lifetime monitored at 650 nm, shows a biexponential behavior. The long lived component has a lifetime identical to the unquenched complex **5**. The short component of the decay trace is calculated to have a lifetime of 4 ns.

The quenching process can be due in principle to two different mechanisms: photoinduced electron transfer from the anthracene to the ruthenium moiety or energy transfer from the excited ruthenium unit to the lowest excited state of the anthracene. The electron transfer process can be ruled out because of the endoergonicity of the process ( $\Delta G = +0.32\text{V}$ ).<sup>[53]</sup> The occurrence of energy transfer from the Ru-based to the anthracene-based component can be explained on the basis of the schematic energy level diagram (scheme 6) showing that the energy is transferred from the  $^3\text{CT}$  Ru-based excited state to the lowest triplet excited state of anthracene ( $T_1$ ), which then is radiationless deactivated to the ground state. The driving force for this exoergonic process is  $\Delta G = -0.30\text{ eV}$ , as calculated from the involved energy levels.<sup>[53]</sup>

In such a process the lowest triplet excited state of anthracene must be populated, and time resolved transient spectroscopy has indeed shown that a strong absorption band is formed after the laser pulse (2 ns) at about 430 nm which has a lifetime of  $\tau = 125\text{ }\mu\text{s}$  (figure 3). As already shown,<sup>[49]</sup> this band is characteristic of a triplet - triplet absorption and the extremely long lifetime in deaerated solution confirms this assignment.



**Scheme 6.** Energy diagram of Ru-based component and 9-acyl-anthracene. Full arrows indicate radiative processes, whereas dashed arrows represent radiationless pathways.

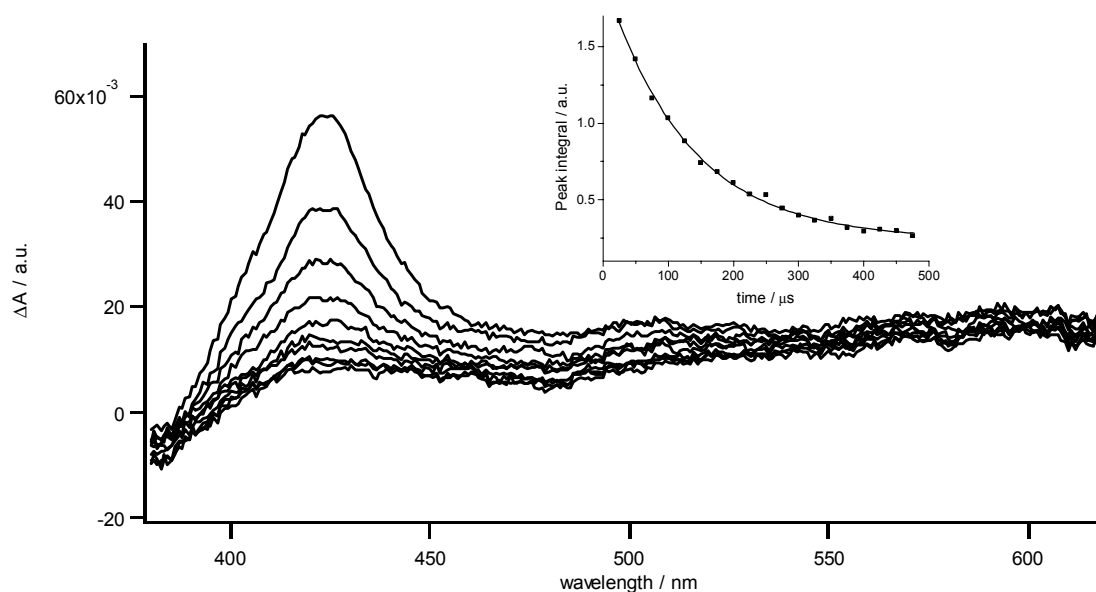


**Figure 3.** Transient absorption spectra of the ruthenium – anthracene assembly in deaerated acetonitrile (timeframe 50  $\mu s$ ). Inset: kinetics of the decay trace measured at 425 nm.

The efficiency of the energy transfer in the experimental conditions used ( $c \approx 10^{-5}$  M) exclude any possible bimolecular process. In order however to gain further proof that the Ru-complex and the anthracene are linked via the Sc unit a photochemical experiment was performed. Upon irradiation in aerated solution with a 250 Watt Xe-lamp, equipped with an interference filter to select the 460 nm band of the  $\text{Ru}(\text{bpy})_3^{2+}$ , the absorption spectrum of the assembly changes dramatically (figure 4). In particular the disappearance of the anthracene bands at 250 and 340-400 nm is observed. On the other hand, the emission intensity of the Ru-based component increases up to 50% over the irradiated period.

The results obtained in aerated solution can be interpreted by sensitization via the Ru-based  $^3\text{CT}$  excited state of the Ru-Sc-anthracene (**Ru-Sc-An**) assembly, with formation of singlet oxygen (eq. 1), followed by attack of singlet oxygen on an anthracene ring to form an endoperoxide derivative (eq. 2), which then may evolve to give other products

(indicated by **Ru-Sc-X**) where the central ring of anthracene has lost its aromatic character (eq. 3).<sup>[52,54]</sup>



The quenching process operated by the anthracene-based moiety in the photoproducts (eq. 3)(where the anthracene aromaticity has been destroyed and, as a consequence, the T<sup>1</sup> level is not any more the lowest excited state, scheme 6) cannot occur. This result indicates that the T<sup>1</sup> excited state of anthracene does indeed play a role in the energy transfer process quenching the Ru based emission observed for **Ru-Sc-An** and more importantly that the two units are connected.

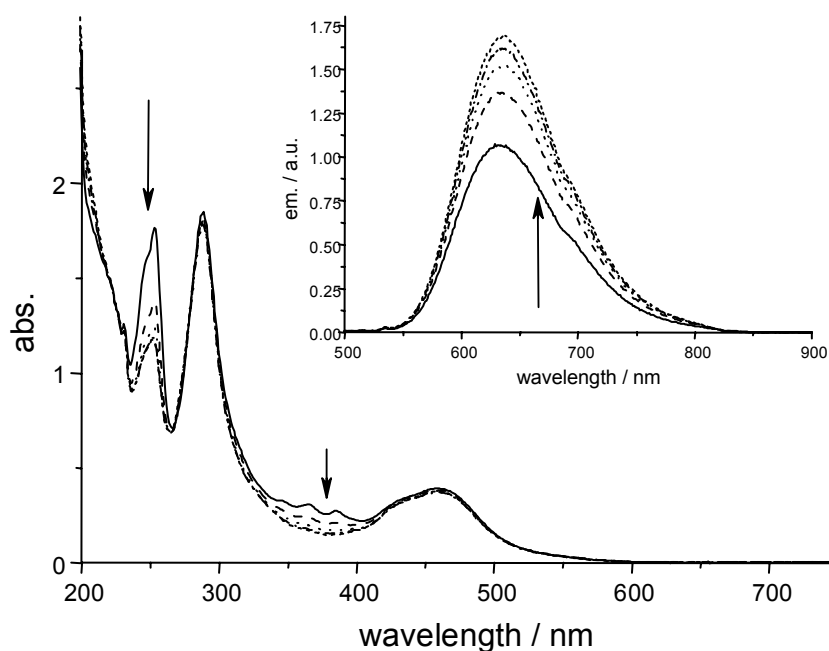


**Figure 4.** Absorption spectra of the ruthenium – anthracene assembly ( $C \approx 3 \times 10^{-5} \text{ M}$ ) at  $t = 0$  (full line) and after 1, 2, 3, and 4 hours (broken lines) of illumination in aerated acetonitrile. Inset: Emission spectra under same conditions.

The same experiment has been performed at identical conditions, but using one equivalent of **5** and two equivalents of **L-A** without addition of any source of scandium ions. The absorption spectra show the same changes for the anthracene bands, over time, as those observed for the assembly. Obviously the ruthenium moiety still generates singlet oxygen upon irradiation, which reacts with anthracene to give endoperoxides in solution, effecting the absorption patterns of **L-A**. However, the ruthenium luminescence remained unchanged in this experiment because of no interaction with the anthracene.

Finally further evidence for the dynamic character of the assembly comes from a ligand competition study. An excess of 2,4-pentadione was added to a solution of the donor-acceptor assembly. Since the average lifetime of the scandium complexes is in the order of ms, a rather fast exchange of ligands was expected. The excess of 2,4-pentadione will lead to a disassembling of some of the dyad and the displacement of **L-A** with unsubstituted acetyl acetonate. The substitution of the 9-acyl-anthracene (quencher)



with the “naked” acac would therefore lead to an increase in the emission intensity since the deactivation pathway (energy transfer) present in the assembly, has been removed. Indeed the integration of the emission spectra before and after the addition of the 2,4-pentadione shows a significant increase of intensity up to 44% upon excitation in the isoabsorptive wavelength of 460 nm. The absorption spectra of the solution remains unchanged above 350 nm upon addition of excess of 2,4-pentadione.

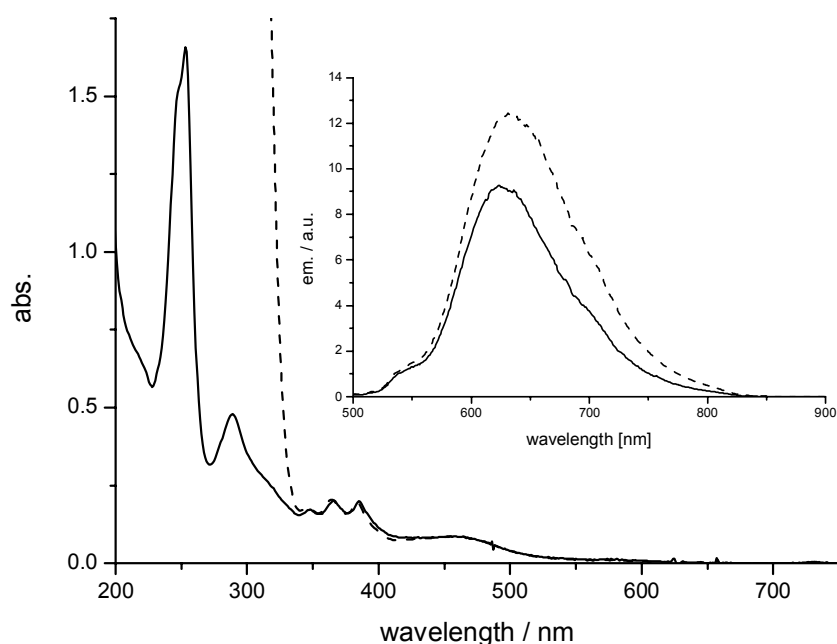


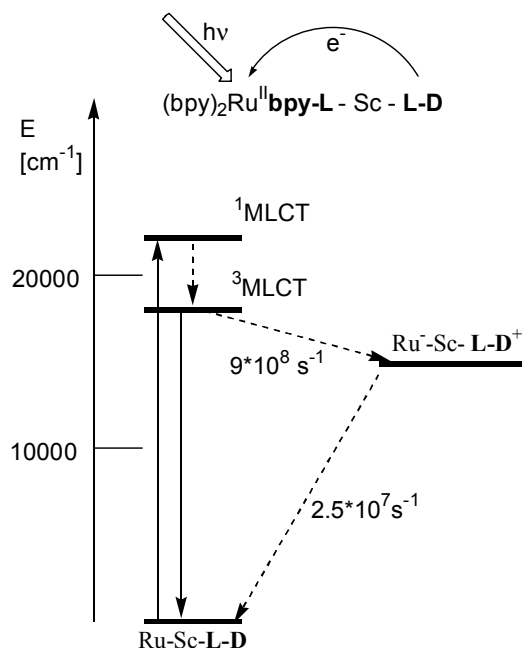
**Figure 5.** Absorption spectra of **Ru-Sc-An** in acetonitrile (straight line) and upon addition of 2,4-pentadione (dashed line). Inset: Emission spectra under same conditions.  $C \approx 10^{-5}$  M

From all these results we conclude that within the donor acceptor scandium complexes **Ru-Sc-An** the emission of the  $\text{Ru}(\text{bpy})_3^{2+}$  moiety is quenched by a fast intramolecular triplet-triplet energy transfer process from the Ru-based component to 9-acyl-anthracene bearing ligands. The rate constant calculated from the quenched and unquenched ruthenium excited state lifetime is  $k_{\text{en}} = 2.5 \cdot 10^8 \text{ s}^{-1}$ .

### 2.3.6 Self-assembly of electron donor-acceptor dyads. Intramolecular Electron Transfer

Substitution of the ‘naked’ acac ligand with a 1,4-*N,N,N',N'*-tetramethyldiaminobenzene derivative, **L-D**, leads to the possibility to build up an assembly containing an electron donor, **L-D** and an electron acceptor complex **5**. In order to have the same statistical complexes as in the previous section, **5** and **L-D** were mixed in a ratio of 1 : 2 in the presence of scandium ions.

To estimate any bimolecular electron transfer contribution, **5** and **L-D** were mixed in a ratio of 1 : 2 in absence of scandium ions. The data showed no evidence for bimolecular processes under the experimental conditions ( $c \approx 10^{-5}$  M, aerated acetonitrile) employed. In fact a monoexponential decay, ( $\tau = 150$  ns) was observed that, as already discussed, corresponds to the value of the free Ru-component **5** (see table 1). In the presence of scandium ions under identical experimental conditions the formation of assemblies (**16** – **19**, see scheme 4) can occur and a dyad is formed. Such assembly formation can be followed spectroscopically since in **16** and **17** a decrease in the emission intensity of the ruthenium based component should be expected on the basis of a thermodynamically allowed photoinduced electron transfer from the donor to the Ru-component (scheme 7). Indeed a quenching of the ruthenium based component has been observed. The emission decay, monitored at 640 nm, becomes biexponential with a long component, due to the unquenched  $\text{Ru}(\text{bpy})_3^{2+}$  - unit, and a short lived component,  $\tau = 10$  ns, due to the quenched luminescence. Upon light excitation an efficient electron transfer from the donor-based component, **L-D**, to the excited ruthenium unit (electron acceptor) is expected on thermodynamical grounds (scheme 7). The process is in fact exoergonic ( $\Delta G = -0.41\text{V}$ )<sup>[55]</sup> and in acetonitrile at room temperature is expected to be fast for the assembly. The rate calculated for the forward electron transfer process is  $k_{\text{et}} = 9 \cdot 10^8 \text{ s}^{-1}$ .



**Scheme 7.** Energy diagram of the assembly Ru-Sc-L-D with a schematic representation of the photoinduced electron transfer process. Full arrows indicate radiative processes, whereas dashed arrows represent radiationless pathways.

Oxidized tetramethyldiaminobenzene has a well known absorption band between 500 and 750 nm. We have therefore used time resolved transient absorption spectroscopy to detect the formation of the tetramethyl-phenylendiamino radical cation. Excited  $\text{Ru}(\text{bpy})_3^{2+}$  exhibits two absorption bands (bipyridinium radical anion), resulting from the transfer of an electron from the ruthenium to the bipyridine (MLCT transition), as can be clearly seen in figure 6a. The absorption at 550 nm unfortunately overlaps with the band, expected for the oxidized radical cation of L-D. Nevertheless, from a comparison between the transient absorption spectra of **5** and the full assembly of **5** with Sc and L-D we are able to proof the formation of the characteristic radical cation of tetramethyl-phenylendiamin (figure 6).

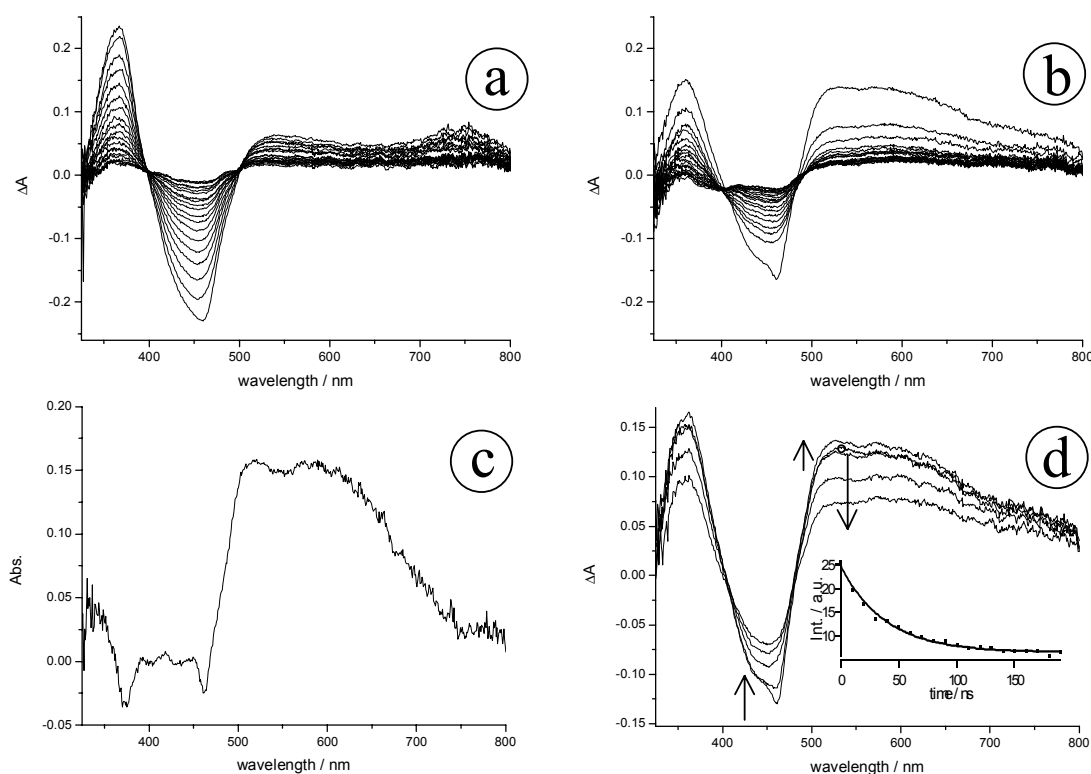


**Figure 6.** Transient absorption spectra of **5** (a) and  $(bpy)_2Ru(bpy-L)-Sc-L-D$  (b), 25 ns timeframe, excitation wavelength is 460nm. (c) shows the difference spectra between (a)- and normalized (b)- frame 1. (d) shows the decay traces of  $(bpy)_2Ru(bpy-L)-Sc-L-D$  after 1 (bold line), 2, 5, 10, and 20 ns, inset: lifetime trace of the radical cation with  $\tau = 40$  ns.

Figure 6a displays the spectra of **5**, recorded in acetonitrile with 25 ns between each frame with minimum instrumental gate time of 5 ns. The first frame was recorded at 1ns after the laser pulse. In the spectrum, the negative band at 460 nm is due to the bleaching of the ground state of  $Ru(bpy)_3^{2+}$ . The strong band at 375 nm and the weak band above 520 nm are due to the formed bipyridinium radical anion since a MLCT state is the lowest excited state. The ratio between these two bands is about 3:1. In figure 6b we show the spectra of the full assembly  $(bpy)_2Ru(bpy-L)-Sc-L-D$ , recorded under identical conditions. The band above 520 nm is much more dominant in this case and the ratio between this one and the 375 nm band rose to almost 1:1. By normalizing the first frame of these two graphs to the same intensity of the bipyridinium radical anion band at 375 nm and subtracting them from each other, we obtained the transient

absorption spectrum, displayed in figure 6c.<sup>[56]</sup> By comparison with the spectra reported in the literature for the radical cation of tetramethyl-phenylendiamin,<sup>[56]</sup> it is clear that the transient in figure 6c is indeed the same species. In order to follow the formation of the transient band at 550 nm (forward electron transfer) and its decay, that from the emission lifetime should occur within 10 ns, we performed the same transient spectra in shorter timescale (figure 6d). As can be seen, the first spectrum does not correspond to the full formation of the radical cation, since the band is still growing after 2 ns. At longer delays (10, 20 ns) the decay of this species can be monitored and a lifetime of  $\tau = 40$  ns was estimated (see inset figure 6d). From the decay of the radical cation absorption, we have calculated the rate for the back electron transfer reaction  $k_{\text{back}} = 2.5 \times 10^7 \text{ s}^{-1}$ .

## 2.4 CONCLUSION

Substituted  $\beta$ -diketones bearing either  $\text{Ru}(\text{bpy})_3^{2+}$  as an energy donor or electron acceptor component, 9-acyl-anthracene as acceptor moiety for energy transfer or 1,4-*N,N,N',N'*-tetramethyldiaminobenzene as electron donating group have been used to form photoactive dyads around a  $\text{Sc}^{\text{III}}$ -ion by self- assembling. Assemblies obtained by coordination with  $\text{Sc}(\text{III})$  ion having  $\text{Ru}(\text{bpy})_3$ - based components and anthracene-substituted ligands show efficient intramolecular energy transfer from the excited ruthenium complex to the lowest excited state of the anthracene-bound component. Within scandium complexes of  $\text{Ru}(\text{bpy})_3$  and 1,4-*N,N,N',N'*-tetramethyldiaminobenzene substituted ligands photoinduced electron transfer processes were detected. It is interesting to notice that even though the energy or electron donor / acceptor systems are not directly linked, the photoinduced processes are rather fast. The Sc ion plays only a structural role and is not directly involved in the process. The use of the dynamic assembly strategy for the generation of photoactive donor acceptor dyads provides access to systems which are not static and react on external stimuli. Such systems are of high complexity and their study is a challenge. However, due to their dynamic nature they may offer advantages for practical applications.

## 2.5 REFERENCES

- [1] V. Balzani, Ed. *Electron Transfer in Chemistry*; Wiley-VCH: Weinheim, **2001**.
- [2] M. N. Paddon-Row, *Stimulating Concepts in Chemistry*; F. Vögtle, J. F. Stoddart, M. Shibasaki, Eds.; Wiley-VCH: Weinheim, **2000**, pp 267 - 291.
- [3] M. R. Wasielewski, *Chem. Rev.* **1992**, 92, 435 – 461.
- [4] T. J. Meyer, *Acc. Chem. Res.* **1989**, 22, 163 – 170.
- [5] M. N. Paddon-Row, *Electron Transfer in Chemistry*; V. Balzani, Ed.; Wiley-VCH: Weinheim, **2001**; Vol. 3, pp 179 – 271.
- [6] D. Gust, T. A. Moore, A. L. Moore, *Electron Transfer in Chemistry*; V. Balzani, Ed.; Wiley-VCH: Weinheim, **2001**; Vol. 3, pp 272 – 336.
- [7] F. Scandola, C. Chiorboli, M. T. Indelli, M. A. Rampi, *Electron Transfer in Chemistry*; V. Balzani, Ed.; Wiley-VCH: Weinheim, **2001**; Vol. 3, pp 337 - 408.
- [8] L. De Cola, P. Belser, *Coord. Chem. Rev.* **1998**, 177, 301 – 346.
- [9] J.-M. Lehn, *Science* **2002**, 295, 2400 – 2403.
- [10] J.-M. Lehn *Supramolecular Chemistry*; Wiley-VCH: Weinheim, **1995**.
- [11] M. Fujita, Ed. *Molecular Self-Assembly. Organic Versus Inorganic Approaches (Structure and Bonding Vol.96)*; Springer Verlag: Berlin, **2001**.
- [12] A. Sautter, D. G. Schmid, G. Jung, F. Würthner, *J. Am. Chem. Soc.* **2001**, 123, 5424 – 5430.
- [13] F. Würthner, A. Sautter, C. Thalacker, *Angew. Chem.* **2000**, 112, 1298 – 1300; *Angew. Chem. Int. Ed. Engl.* **2000**, 39, 1243 – 1245.
- [14] T. H. Ghaddar, E. W. Castner, S. S. Isied, *J. Am. Chem. Soc.* **2000**, 122, 1233 - 1234.

- [15] A. S. Salameh, T. H. Ghaddar, S. S. Isied, *J. Phys. Org. Chem.* **1999**, *12*, 247 – 254.
- [16] T. Chin, Z. Gao, I. Lelouche, Y.-g. Shin, S. Purandare, S. Knapp, S. S. Isied *J. Am. Chem. Soc.* **1997**, *119*, 12849 – 12858.
- [17] M. D. Ward, F. Barigelletti, *Coord. Chem. Rev.* **2001**, *216 – 217*, 127 – 154.
- [18] C. M. White, M. F. Gonzalez, D. A. Bardwell, L. H. Rees, J. C. Jeffery, M. D. Ward, N. Armaroli, G. Calogero, F. Barigelletti, *J. Chem. Soc., Dalton Trans.* **1997**, 727 – 735.
- [19] Nelissen, H. F. M.; Schut, A. F. J.; Venema, F.; Feiters, M. C.; Nolte, R. J. M. *Chem. Commun.* **2000**, 577 - 578.
- [20] H. F. M. Nelissen, M. Kercher, L. De Cola, M. C. Feiters, R. J. M. Nolte, *Chem. Eur. J.* accepted.
- [21] J. M. Haider, M. Chavarot, S. Weidner, I. Sadler, R. M. Williams, L. De Cola, Z. Pikramenou, *Inorg. Chem.* **2001**, *40*, 3912 - 3921.
- [22] A. E. Kaifer, *Acc. Chem. Res.* **1999**, *32*, 62 - 71.
- [23] C. J. Chang, J. D. K. Brown, M. C. Y. Chang, E. A. Baker, D. G. Nocera; in *Electron Transfer in Chemistry*; V. Balzani, Ed.; Wiley-VCH: Weinheim, 2001; Vol. 3, 409 - 461.
- [24] T. Hayashi, H. Ogoshi, *Chem. Soc. Rev.* **1997**, *26*, 355 – 364.
- [25] M. D. Ward, *Chem. Soc. Rev.* **1997**, *26*, 365 - 375.
- [26] R. Billing, D. Rehorek, H. Henning, *Top. Curr. Chem.* **1990**, *158*, 151 - 200.
- [27] C. A. Hunter, J. K. M. Sanders, G. S. Beddard, S. Evans, *J. Chem. Soc., Chem. Commun.* **1989**, 1767 – 1767.
- [28] G. De Santis, L. Fabbriizzi, M. Licchelli, A. Poggi, A. Taglietti, *Angew. Chem.* **1996**, *108*, 224 – 226; *Angew. Chem. Int. Ed. Engl.* **1996**, *35*, 202 – 204.

- [29] M. Di Casa, L. Fabbrizzi, M. Licchelli, A. Poggi, A. Russo, A. Taglietti, *Chem. Commun.* **2001**, 825 – 826.
- [30] C. A. Hunter, R. K. Hyde, *Angew. Chem.* **1996**, *108*, 2064 – 2067; *Angew. Chem. Int. Ed. Engl.* **1996**, *35*, 1936 – 1939.
- [31] H. Imahori, E. Yoshizawa, K. Yamada, K. Hagiwara, T. Okada, Y. Sakata, *J. Chem. Soc., Chem. Commun.* **1995**, 1133 – 1134.
- [32] B. König, M. Pelka, H. Zieg, T. Ritter, H. Bouas-Laurent, R. Bonneau, J.-P. Desvergne, *J. Am. Chem. Soc.* **1999**, *121*, 1681 - 1687.
- [33] W. H. F. Sasse, *Org. Synth. Coll. Vol. V.* **1973**, 102 - 107.
- [34] D. G. McCafferty, B. M. Bishop, C. G. Wall, S. G. Hughes, S. L. Mecklenberg, T. J.; Meyer, B. W. Erickson, *Tetrahedron* **1995**, *51*, 1093 - 1106.
- [35] G. Wang, D. E. Bergstrom, *Synlett* **1992**, 422 - 424.
- [36] B. P. Sullivan, D. J. Salmon, T. J. Meyer, *Inorg. Chem.* **1978**, *17*, 3334 – 3341.
- [37] L. Della Ciana, I. Hamachi, T. J. Meyer, *J. Org. Chem.* **1989**, *54*, 1731 - 1735.
- [38] G. R. Loppnow, D. Melamed, A. D. Hamilton, T. G. Spiro, *J. Phys. Chem.* **1993**, *97*, 8957 - 8968.
- [39] Sc(acac)<sub>3</sub> was prepared by mixing ScCl<sub>3</sub> and an excess of 2,4-pentadione in dry methanol and deprotonation with ammonia gas, upon which the desired product precipitated out of the solution
- [40] *Gmelin Handbook of Inorganic Chemistry*; Springer Verlag: Berlin; **1981** Vol. D3, 76 - 96.
- [41] Y. Hatakeyama, H. Kido, M. Harada, H. Tomiyasu, H. Fukutomi, *Inorg. Chem.* **1988**, *27*, 992 - 996.
- [42] A. Juris, V. Balzani, F. Barigelletti, S. Campagna, P. Belser, A. von Zelewsky, *Coord. Chem. Rev.* **1988**, *84*, 85 - 277.



- [43] J. P. Sauvage, J.-P. Collin, J.-C. Chambron, S. Guillerez, C. Coudret, V. Balzani, F. Barigelletti, L. De Cola, L.; Flamigni, *Chem. Rev.* **1994**, *94*, 993 - 1019.
- [44] V. Balzani, A. Juris, M. Venturi, S. Campagna, S. Serroni, *Chem. Rev.* **1996**, *96*, 759 - 833.
- [45] C. Kaes, A. Katz, M. W. Hosseini, *Chem. Rev.* **2000**, *100*, 3553 - 3590.
- [46] F. Kröhnke, *Synthesis* **1976**, 1 - 24.
- [47] D. F. Evans, *J. Chem. Soc* **1961**, 1987 - 1993.
- [48] Despite several attempts we were not able to detect molecular ions of scandium complexes bearing one or more charged ruthenium acac ligands using EI, ESI, FAB, MALDI mass spectrometry techniques.
- [49] S. Boyde, G. F. Strousse, W. E. Jones, T. J. Meyer, *J. Am. Chem. Soc.* **1989**, *111*, 7448 - 7454.
- [50] P. Belser, R. Dux, M. Baak, L. De Cola, V. Balzani, *Angew. Chem.* **1995**, *107*, 634 – 637; *Angew. Chem. Int. Ed. Engl.* **1995**, *34*, 595 - 598.
- [51] L. De Cola, V. Balzani, P. Belser, R. Dux, M. Baak, *Supramol. Chem.* **1995**, *5*, 297 - 299.
- [52] M. Klessinger, J. Michl, *Excited States and Photochemistry of Organic Molecules*, VCH: Weinheim, **1995**.
- [53] calculated from the  $E^{00}$  of the Ru-based component ( $17170\text{ cm}^{-1}$ ) and the energy of the lowest triplet state of 9-acyl-anthracene ( $14700\text{ cm}^{-1}$ ) (see Murov, S.; Carmichael, I.; Hug, G. L. *Handbook of Photochemistry*; 2<sup>nd</sup> ed.; Marcel Dekker: New York, 1993.).
- [54] R. Schmidt, H.-D. Bauer, *J. Photochem.* **1986**, *34*, 1 - 12.
- [55] calculated from the redox potentials of the single components, determined in 0.1 M TBAPF<sub>6</sub>-CH<sub>3</sub>CN against Fc/Fc<sup>+</sup> (**L-D**<sup>0/+</sup>: -0.07 V; Ru(bpy)<sub>3</sub><sup>2+\*/+</sup>: 0.34 V).

- [<sup>56</sup>] A reference spectrum for the tetramethyl-phenylendiamino radical cation can be found for example at: S. Steenken, A. J. S. C. Vieira, *Angew. Chem.* **2001**, *112*, 578 – 581; *Angew. Chem. Int. Ed. Engl.* **2001**, *40*, 571 – 573.

### 3 Photoinduced Electron Transfer between Metal Coordinated Cyclodextrin Assemblies and Viologens<sup>‡</sup>

#### Abstract

Two novel tris(bipyridine) ruthenium(II) complexes bearing two and six  $\beta$ -cyclodextrin binding sites on their ligands have been synthesised and characterised. Photophysical studies indicate that the appended cyclodextrins protect the luminescent ruthenium core from quenching by oxygen, resulting in longer excited state lifetimes and higher emission quantum yields compared to the reference compound, the unsubstituted ruthenium tris(bipyridine). Inclusion of suitable guests such as dialkyl-viologens leads to a quenching of the luminescence of the central unit. In these supramolecular donor-acceptor dyads an efficient photoinduced electron transfer from the excited ruthenium moiety (the donor) to the viologen unit (the acceptor) is observed. The alkyl chain length of the acceptor plays an important role on the binding properties; when it exceeds a certain limit the binding becomes strong enough for electron transfer to occur. Interestingly, a viologen with only one long alkyl tail instead of two shows no efficient quenching, indicating that cooperative interactions between two cyclodextrins binding one viologen are essential to raise the binding constant of the supramolecular dyad.

---

<sup>‡</sup> The results of this chapter have been accepted for publication:

H. F. M. Nelissen, M. Kercher, L. De Cola, M. C. Feiters, R. J. M. Nolte, *Chem. Eur. J.*

### 3.1 INTRODUCTION

Green plants and photosynthetic bacteria use sunlight as their source of energy. Through photosynthesis they are able to convert the light into chemical energy, which in turn is used to trigger biological processes. The photosynthetic pathway is characterised by a very high quantum efficiency, which is the result of extremely fast electron transfer over large distances, via a complicated cascade of chromophores, and a very slow back transfer of the electron.<sup>[1]</sup> Although much progress has been made in the unravelling of this pivotal process, the explanation of the underlying mechanisms remain one of the biggest challenges for science. Many synthetic models have been made to obtain a better understanding of the photophysical properties of simple systems.<sup>[2]</sup> Most of these are focused on the generation of charge-separated species through photoinduced electron transfer. Covalently linked donor-acceptor (DA) dyads have given us more insight into the processes, which influence the transfer of the electron such as the distance and orientation of both the donor and the acceptor chromophore<sup>[3]</sup> and the nature of the solvent.<sup>[4]</sup> The synthesis of such covalently linked dyad systems requires a great deal of effort and therefore non-covalently linked systems which benefit from the supramolecular principles discovered over the last decades have attracted much interest.<sup>[5]</sup> More recently, the better understanding of the photophysical properties has led to the incorporation of function in these systems as in light driven molecular machines<sup>[6]</sup> and chemical sensors.<sup>[7]</sup> Tris(bipyridine) ruthenium(II) complexes are well known in this field because of their excellent photophysical properties and excited state redox properties.<sup>[8]</sup> Ruthenium(II) is especially interesting since it forms kinetically stable bonds with bipyridines, which makes the synthesis of heteroleptic compounds possible.<sup>[8, 9]</sup> Attaching functional groups to the bipyridine ligands offers a route to bring together several components for a specific function through coordination around the metal.

Recently, the synthesis of bipyridine ligands with two<sup>[10, 11]</sup> appending cyclodextrins has been reported, as well as the use of these compounds to construct cyclodextrin assemblies through the coordination of metal ions.<sup>[12, 13]</sup>

In this paper we report the synthesis of two tris(bipyridine) ruthenium(II) complexes bearing two (**1**), and six (**2**)  $\beta$ -cyclodextrin (CD) moieties from the bipyridine-spaced dimer **3**. In the ligand the cyclodextrins are connected to the 4,4'-position of the bipyridine to avoid problems with steric crowding around the metal centre. The ruthenium complex will function as an electron donor while the cyclodextrins act as a binding site for an electron acceptor, i.e. viologen derivatives such as dinonyl, methyl-nonyl and dipentyl (compounds **4-6**, see Table 1).

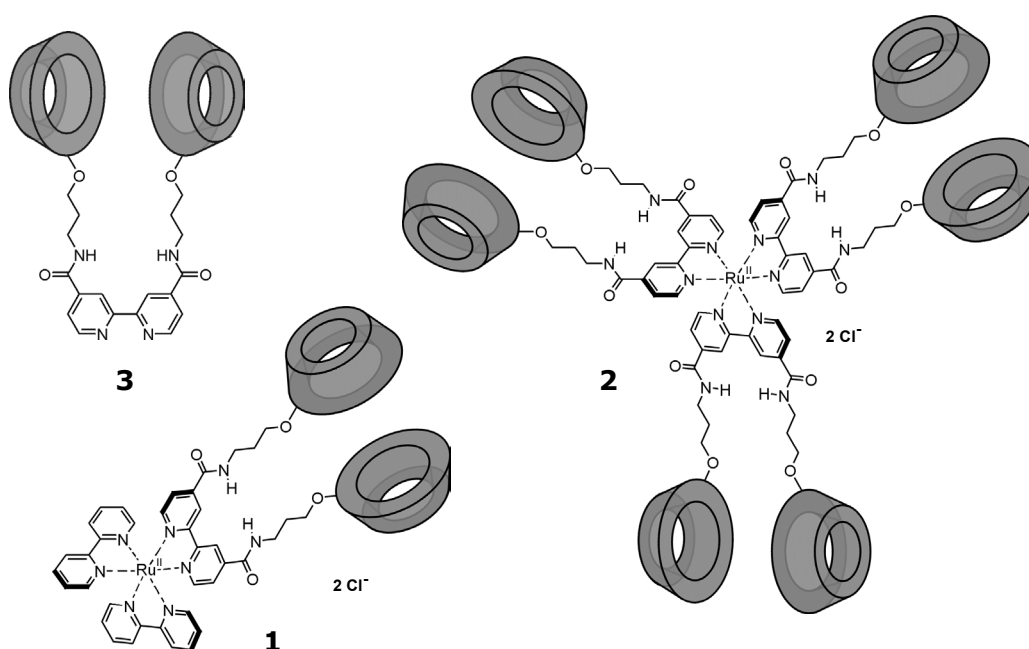
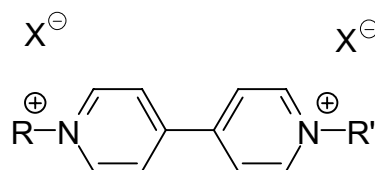


**Table 1.** *N,N'*-dialkyl-4,4'-bipyridines ( $X^-$ , counterion)

	R	R'	$X^-$
<b>4</b>	C <sub>9</sub> H <sub>19</sub>	C <sub>9</sub> H <sub>19</sub>	Br <sup>-</sup> , Br <sup>-</sup>
<b>5</b>	C <sub>5</sub> H <sub>11</sub>	C <sub>5</sub> H <sub>11</sub>	Br <sup>-</sup> , Br <sup>-</sup>
<b>6</b>	C <sub>9</sub> H <sub>19</sub>	CH <sub>3</sub>	Br <sup>-</sup> , I <sup>-</sup>



In ligand **3** two cyclodextrin binding sites are present in one ligand, and they are connected via their secondary sides. For such a compound cooperative binding<sup>[14]</sup> interactions can be expected for the association with ditopic guests, i.e. guests which have two parts each of which can be bound by a cyclodextrin. Similar cooperative effects between the cyclodextrin binding sites in **1** and **2** for ditopic viologens can lead to higher binding constants and hence the possibility to detect photoinduced electron transfer reactions even at very low host concentrations. In this paper we present an investigation of the photophysical properties of compounds **1** and **2**, including electron transfer reactions to a bound viologen acceptor as studied by steady-state and time-resolved fluorescence spectroscopy. In addition, we describe the conformational behaviour of these compounds in water (D<sub>2</sub>O).

## 3.2 RESULTS AND DISCUSSION

### 3.2.1 *Synthesis*

The synthesis of the bipyridine-spaced dimer **3** has been described by us before.<sup>[10, 12]</sup> This ligand was used to construct the two ruthenium(II) complexes **1** and **2**.<sup>[15]</sup> Compound **2** was synthesised by reacting three equivalents of **3** with RuCl<sub>3</sub> in a refluxing ethanol/water mixture (1:1, v/v). The heteroleptic complex **1** was formed by reaction of ligand **3** with Ru(bpy)<sub>2</sub>Cl<sub>2</sub> (1 eq) in the same solvent system. Complexes **1** and **2** were isolated as their chloride salts by pouring the respective reaction mixtures in acetone and collecting the precipitates. Minor impurities were removed by size exclusion chromatography. All compounds were fully characterised by <sup>1</sup>H NMR, mass spectrometry and elemental analysis. For both complexes two diastereoisomers are formed, as a result of the chirality of the octahedral coordination around the ruthenium centre. No efforts were taken to separate these isomers.

The viologens **4-6** (Table 1) were synthesised according to well-established literature procedures<sup>[16]</sup> by reacting 4,4'-bipyridine with an excess of the appropriate alkylhalogenide in acetonitrile.

### 3.2.2 Photophysical Properties

An overview of the spectroscopic data is given in Table 2, which also includes the data measured for the reference compound  $\text{Ru}(\text{bpy})_3^{2+}$ . The UV-VIS spectra of compounds **1** and **2** in aqueous solution show the characteristic metal to ligand charge transfer bands (MLCT) centred at around 450-480 nm and the intense ligand centred (LC) absorptions around 300 nm (Figure 1). The MLCT absorptions of complexes **1** and **2** show a red shift in comparison with  $\text{Ru}(\text{bpy})_3^{2+}$  due to the presence of the electron withdrawing amide groups on the bipyridines. The red shift of compound **2** is less pronounced since it is compensated by a blue shift caused by the reduced  $\sigma$ -donor capacity of the three amide-functionalised bpy ligands.<sup>[17]</sup> The shoulder in the LC band of compound **1** nicely reflects the fact that one of the 2,2'-bipyridine ligands is replaced by a more electron poor bipyridine, resulting in a bathochromic shift of almost 20 nm. Also visible is the reduced oscillator strength of the substituted bipyridine, which is reflected in the lower molar extinction coefficient of the LC band for compound **2**.

**Table 2.** Spectroscopic and photophysical data for the ruthenium complexes in aqueous solution.

	Abs	Em	$\epsilon$	$\tau_{\text{deacrated}}$	$\tau_{\text{acrated}}$	$\Phi_{\text{acrated}}$	$k_q(\text{O}_2)$
	$\lambda_{\text{max}}(\text{nm})$	$\lambda_{\text{max}}(\text{nm})$	$(\text{M}^{-1}\text{cm}^{-1})$	(ns)	(ns)	$\times 10^2$	$(\text{M}^{-1}\text{s}^{-1})$
$\text{Ru}(\text{bpy})_3^{2+}$	451	605	13000	608	390	2.8 <sup>a)</sup>	$3.2 \times 10^9$
<b>1</b>	477	658	14600	480	400	1.8	$1.4 \times 10^9$
<b>2</b>	464	625	17200	960	811	7.2	$0.7 \times 10^9$

<sup>a)</sup> Taken from ref. 8.

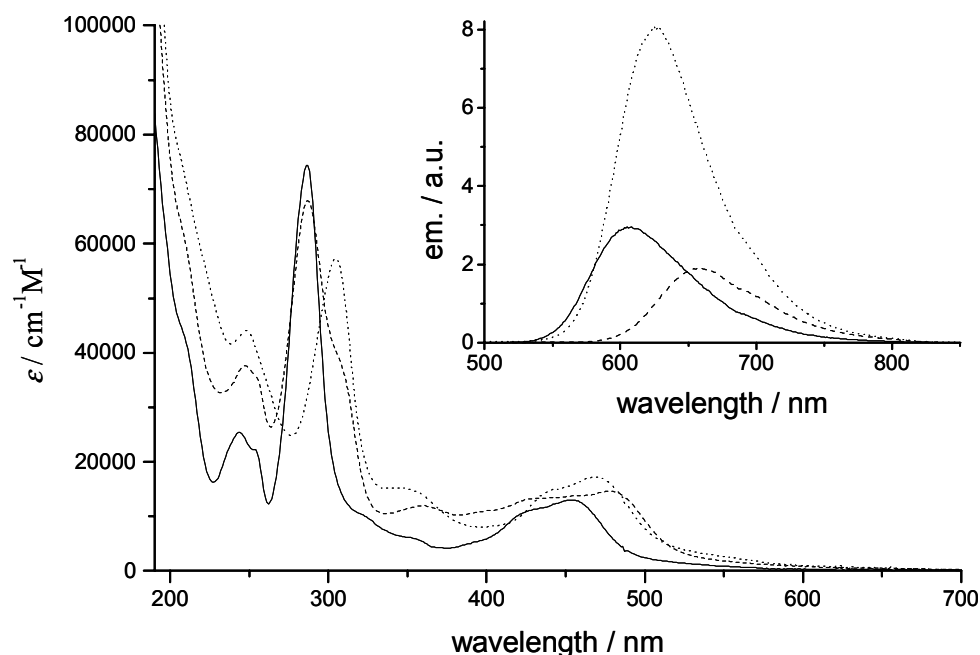


**Figure 1** : Absorption and emission (inset) spectra of  $\text{Ru}(\text{bpy})_3$  (full line), **1** (dashed line), and **2** (dotted line) in aqueous solution at 25 °C.

The emission properties in aqueous solution of compounds **1** and **2** – when excited in their MLCT band – showed the same trends as the absorption spectra (Figure 1, inset). Red-shifts of the emission maxima compared to  $\text{Ru}(\text{bpy})_3^{2+}$  were observed for both complexes. We measured the excited state lifetimes  $\tau$  of compounds **1** and **2**, which were monoexponential for both complexes. The results (Table 2) reveal a remarkably high value for **2**, which is more than twice as high as that of the model compound  $\text{Ru}(\text{bpy})_3^{2+}$ . The same holds for the emission quantum yield  $\Phi$  for compound **2** (almost threefold increase, see Table 2). Such behaviour can be easily explained by the quenching of dioxygen in water solution for the three complexes. From the experimental lifetimes in solution in the presence (aerated) and absence (deaerated) of oxygen (Table 2) it becomes clear that for **2** the quenching is much less effective in comparison with  $\text{Ru}(\text{bpy})_3^{2+}$ . This is due to the structure of complex **2** in which the six cyclodextrins efficiently shield the ruthenium core from the environment. A similar phenomenon has



been observed for ruthenium complexes bearing dendritic wedges on their bipyridine ligands.<sup>[18]</sup> The effect of oxygen quenching can best be quantified by calculating the rate constant ( $k_q$ ) for this process from the Stern-Volmer equation (equation 1):<sup>[8]</sup>

$$\frac{\tau_0}{\tau} = 1 + k_q \tau_0 [O_2] \quad \text{(equation 1)}$$

where  $\tau$  and  $\tau_0$  represent the respective lifetimes in aerated and deaerated solutions and  $[O_2]$  is the saturated concentration of oxygen in water ( $2.9 \times 10^{-4}$  M at 298K).<sup>[19]</sup> The calculated values (Table 2) reveal that the complexes bearing cyclodextrins indeed have a lower quenching rate than the reference compound  $Ru(bpy)_3^{2+}$ .

### 3.2.3 Photoinduced electron transfer processes

Quenching of the emission of ruthenium complexes by *N,N'*-dialkyl-4,4'-bipyridinium ions (viologens) is well documented.<sup>[20]</sup> This process operates via a photoinduced electron transfer mechanism from the excited ruthenium moiety to the viologen (the acceptor). It can occur both inter- and intramolecularly, for example in dyads, where the ruthenium complex and the viologen are covalently linked.<sup>[21]</sup> The present systems are supramolecular analogues of these dyads. The  $\beta$ -cyclodextrin hosts can bind the viologen guest, bringing it close to the luminescent metal centre, thereby promoting electron transfer reactions that would otherwise not occur bimolecularly in the diluted conditions used for the supramolecular assembly.

As the viologen guest, we have investigated *N,N'*-dinonyl-4,4'-bipyridine **4**, *N,N'*-dipentyl-4,4'-bipyridine **5**, and *N*-methyl-*N'*-nonyl-4,4'-bipyridine **6** (Table 1). Long alkyl tails are needed to secure their binding to the cyclodextrins, since the doubly charged bipyridinium unit is too hydrophilic to show a strong interaction with the CD

cavity.<sup>[22]</sup> The binding of the viologen **4** to compounds **1** and **2** was studied by fluorimetric and microcalorimetric titrations and the results are summarised in Table 3.

**Table 3.** Binding constants for the complexes of *N,N'*-dinonylviologen **4** to compound **1** and **2**.

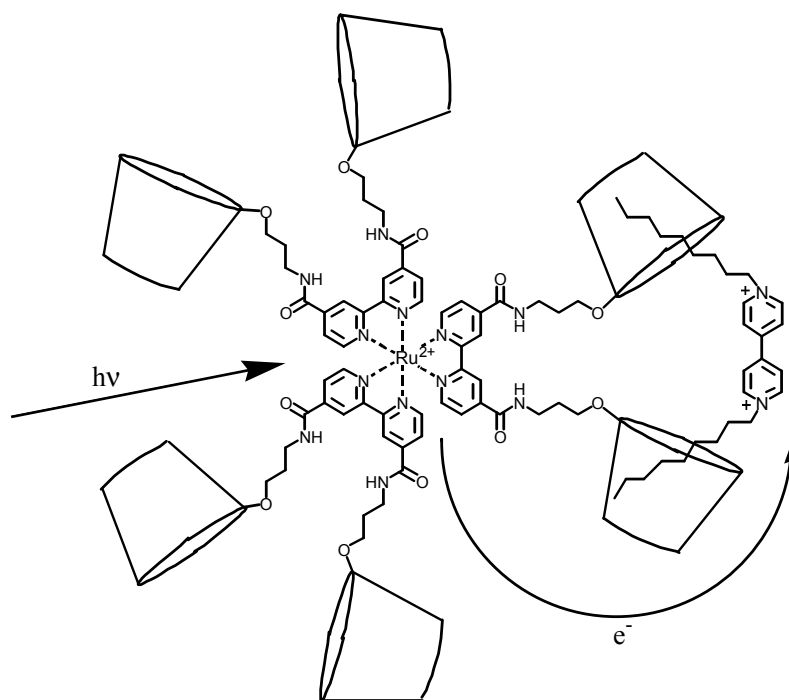
	$K_b$ 1:1	$K_b$ 2:1
	( $M^{-1}$ )	( $M^{-1}$ )
<b>1</b>	$2.4 \times 10^4$ <sup>[a]</sup>	-
<b>2</b>	$2.4 \times 10^5$ <sup>[b]</sup>	$4.0 \times 10^4$ <sup>[b]</sup>

<sup>[a]</sup> Obtained from fluorimetric titrations performed at 25 °C in an aqueous 0.1 M Tris-HCl buffer of pH 7.0. <sup>[b]</sup> Microcalorimetric data taken from ref. 12.

Compound **1** can be considered to be a cyclodextrin dimer, in which the two CD-cavities can cooperate in the binding of ditopic guest molecules. With its two long alkyl tails, the viologen guest **4** is ditopic in nature and the binding constant of its complex with **1** can be expected to be much higher than the value reported for the complex with monomeric  $\beta$ -cyclodextrin ( $K_b=2 \times 10^2 M^{-1}$ ).<sup>[22]</sup> Table 3 shows that they are indeed higher by at least two orders of magnitude. The surprisingly high binding constants for the complexes of viologen **4** with **1** and **2** are clearly the result of cooperative interactions between multiple  $\beta$ -cyclodextrin cavities. This phenomenon was further investigated with photophysical studies.

Intercomponent photoinduced electron transfer was investigated in aqueous solution where the concentration of the complexes was maintained constant ( $\sim 10^{-5}$  M) and increasing amounts of the viologen were added to the solution to up to 5 molar

equivalents. Under these dilute conditions bimolecular processes can be neglected and the observed quenching of the emission of the ruthenium unit can only be ascribed to intercomponent electron transfer between the excited ruthenium moiety (donor) and the bound viologen (electron acceptor), as shown in Scheme 1.



**Scheme 1.** Schematic representation of the photoinduced electron transfer process upon excitation of the ruthenium unit in **2**.

The decrease in emission intensity for complexes **1** and **2** (Figure 4) upon addition of **4** was accompanied by a decrease of the excited state lifetime. Due to the fact that the assembly of the supramolecular dyad is not 100% complete at these dilute conditions, a biexponential decay was observed for both complexes. The decay resolved into a long component - corresponding to the unquenched ruthenium species - and a short component due to the quenching of the excited state because of the electron transfer reaction. The lifetimes of these short components were determined to be 22 ns and 88 ns for complexes **1** and **2**, respectively.

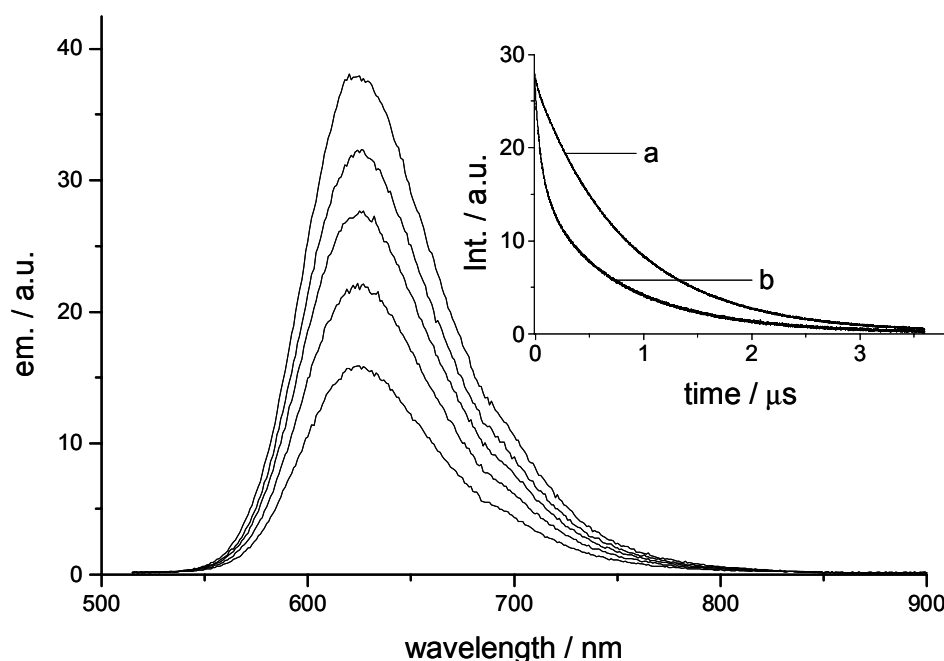


**Figure 4.** Changes in the emission spectra of **2** upon addition of 0, 0.5, 1, 2, and 5 molar equivalents (top to bottom) of **4** in aerated aqueous solution. Inset: Lifetime decay traces of (a) **2** alone and of (b) **2** in the presence of two equivalents of **4**.

Transient absorption spectroscopy did not reveal the formation of the mono-reduced viologen species ( $V^{+•}$ ) which has a characteristic absorption at around 600 nm.<sup>[23]</sup> This is not particularly surprising, since the forward electron transfer is considerably slow (vide supra) and we would expect a fast back electron transfer due to the larger exoergonicity of the process. Values of  $\Delta G = -0.5$  eV for the forward electron transfer and  $\Delta G = -1.6$  eV for the back electron transfer have been estimated from the  $E_{00}$  value and the redox properties of related components.<sup>[24]</sup>

Furthermore, it is known that the reduced viologen ( $V^{+•}$ ), being less hydrophilic than the fully oxidised state viologen ( $V^{2+}$ ), binds more strongly to the cyclodextrin cavity.<sup>[25]</sup> This may lead to a deeper inclusion of the viologen unit into the cavity of the  $\beta$ -cyclodextrin, bringing the viologen and the ruthenium complex even closer. From the

lifetime values, the rate constants of the forward electron transfer ( $k_{et}$ ) can be calculated according to equation 2:

$$k_{et} = \frac{1}{\tau} - \frac{1}{\tau_0} \quad \text{(equation 2)}$$

where  $\tau$  and  $\tau_0$  are the respective lifetimes in the presence and absence of the viologen guest. The calculated values are  $k_{et} = 4.3 \times 10^7 \text{ s}^{-1}$  and  $k_{et} = 1.0 \times 10^7 \text{ s}^{-1}$  for the compounds **1** and **2**, respectively. This difference can be explained by considering the difference in structures between **1** and **2**. Contrary to complex **1**, which contains only one cyclodextrin-appended bipyridine ligand, complex **2** has cyclodextrin substituents on all its bipyridine ligands, leading to a steric hindrance around the ruthenium core and a more extended conformation, resulting in an increase in the distance between the donor-acceptor pair for **2** compared to **1**. For comparison, in a covalently linked dyad where the ruthenium and the viologen are connected via seven methylene groups with the spacer threaded through a cyclodextrin, the rate for electron transfer was determined to be an order of magnitude slower, i.e.  $2.3 \times 10^6 \text{ s}^{-1}$ .<sup>[26]</sup>

A viologen (**5**) with shorter alkyl chains than **4**, viz. pentyl chains, was also studied to investigate the dependence of the binding and the electron transfer rate on the chain length. Experiments carried out under exactly the same conditions as described above for **4** did not lead to a decrease in the emission intensity of the ruthenium complex **2** upon addition of **5**, and no short-lived component was detected in its decay curve. This result is ascribed to the apparent failure of the viologen with pentyl chains **5** to bind sufficiently strongly to complex **2** to give efficient quenching. A similar effect of alkyl chain length has been described in the literature for the binding of alkanoates to  $\beta$ -cyclodextrins in aqueous solution: the binding constants for hexanoate, octanoate, and decanoate increase from  $K_b = 67 \text{ M}^{-1}$ , to  $K_b = 1250 \text{ M}^{-1}$ , and  $K_b = 6600 \text{ M}^{-1}$ , respectively.<sup>[27]</sup> The same trend has been observed for other guests with hydrophilic head groups and hydrophobic alkyl chains of varying length.<sup>[27]</sup>

To investigate a possible cooperative effect in the binding of dinonylviologen **4**, we used the asymmetrically substituted viologen **6**, which has one methyl and one nonyl substituent. The methyl group of **6** is obviously shorter than the critical chain length needed for an efficient binding into the cavity of the cyclodextrin, and this compound, therefore, should be considered as a monotopic guest. The emission experiments show that in order to observe a quenching the concentration of **6** should be increased at least 10 times compared to that of **4**. We also performed a microcalorimetric titration to determine the binding constant of the complex between **2** and **6**. The results are summarised in Table 4. A comparison of the data in Tables 3 and 4 shows that monononylviologen **6** displays a much weaker binding to complex **2** than the dinonylviologen **4** with an association constant lower by an order of magnitude. This is not surprising as **6** was expected to behave as a monotopic guest. These results establish that the strong cooperative binding of viologen **4** to complex **2** is essential to ascertain a sufficiently high concentration of the self-assembled donor-acceptor pair in solution for the electron transfer to be observed by spectroscopic investigations.

**Table 4.** Binding constants for the complex of N-methyl-N'-nonylviologen **6** to ruthenium complex **2**.<sup>[a]</sup>

	$K_b$ ( $M^{-1}$ )	$\Delta H$ ( $kcal\ mol^{-1}$ )	$T\Delta S$ ( $kcal\ mol^{-1}$ )
1:1	$1.2 \times 10^4$	-0.97	4.59
1:2	$3.5 \times 10^3$	-1.29	2.18

<sup>[a]</sup> Obtained from microcalorimetric titrations performed at 25 °C in an aqueous 0.1 M Tris-HCl buffer of pH 7.0.

### 3.3 CONCLUSION

We have prepared and spectroscopically investigated ruthenium complexes bearing  $\beta$ -cyclodextrin hosts and their interaction with viologen derivatives as guests. For the supramolecular host-guest complexes the combination of results of steady-state binding studies of *N,N'*-dinonylviologen to the ruthenium complexes **1** and **2** and time-resolved spectroscopy prove that the presence of multiple cyclodextrin binding sites in one molecule not only enhances the binding of ditopic guest molecules like the viologen but also shields the ruthenium complex from quenching by oxygen. The resulting high quantum yield and emission lifetime in particular of complex **2** make this compound very interesting for the use in sensor devices as we have already briefly communicated.<sup>[12]</sup> Through a comparison of the time resolved luminescence studies of viologen **4** and **6**, together with the determination of the binding constants for these compounds to the complexes **1** and **2** via calorimetric titration, we have established that cooperative effects of two  $\beta$ -cyclodextrins in the binding of the viologen guests are present.

### 3.4 EXPERIMENTAL

#### 3.4.1 General

Acetonitrile was distilled from  $\text{CaH}_2$  prior to use.  $\text{RuCl}_3 \cdot 3\text{H}_2\text{O}$  and  $\text{Ru}(\text{bpy})_2\text{Cl}_2$  were purchased from Aldrich and used as received. NMR spectra were taken on a Bruker AC-300 and a Bruker AMX-500. Chemical shifts are reported relative to the solvent reference ( $[\text{D}_6]\text{DMSO}$ : 2.54 ppm,  $\text{D}_2\text{O}$ : 4.72 ppm). Mass spectra were taken on a VG 7070E (FAB) or a Finnigan MAT 900S (ESI) instrument. Luminescence spectra were measured on a Perkin Elmer LS-50B and a SPEX Fluorolog I instrument. UV-Vis spectra were recorded on a Varian Cary 50 or a diode-array HP8453 instrument. Microcalorimetric titrations were performed on a Microcal VP-ITC titration microcalorimeter.

Size exclusion chromatography was performed on a Sephadex G75 column with a bed volume of 100 mL and an elution speed of 25 mL/hour. Compounds were detected by their UV-Vis absorption at 254 nm.

Fluorimetric titrations were performed at a constant concentration of fluorophore by making a stock solution of the respective ruthenium complex ( $1.0 \times 10^{-5}$  M) and using this solution to make a stock solution of the appropriate *N,N'*-dialkylbipyridinium salt (typically  $2.0 \times 10^{-4}$  M). All measurements were carried out in a 1.00 cm quartz cuvette (4 mL) at 25 °C in an aqueous 0.1 M Tris-HCl buffer of pH 7.0. The excitation wavelength was 458 nm for **1** with excitation slits of 5 nm and emission slits of 10 nm. Small aliquots of the bipyridinium solution were added to a cuvette filled with 2.00 mL of the ruthenium solution. After every addition an emission spectrum was taken and the intensity at a fixed wavelength was determined. These intensities were plotted as a function of the bipyridinium concentration and the data points were analysed assuming a 1:1 equilibrium using a non-linear least-squares curve fitting procedure.

### 3.4.2 Microcalorimetric Titrations

Titration were performed by adding aliquots of a sample solution of the guest to the host solution (cell volume = 1.415 mL). All measurements were carried out at 25 °C in an aqueous 0.1 M Tris-HCl buffer of pH 7.0. Since viologens are known to aggregate in aqueous solution a control experiment was performed by diluting the same guest solution, showing a constant heat flow per injection. This proved that no aggregation occurred at the concentrations used. The final titration curves were corrected for the heat of dilution of the guest and the host in the buffer and analysed using a non-linear least-square minimisation method with an appropriate model (either 1:1 or 1:2, host:guest).



### 3.4.3 Time-resolved photophysics

The electron transfer experiments with the viologens were carried out using freshly prepared solutions of ruthenium complex **2** ( $1 \times 10^{-5} \text{ M}^{-1}$ ) in distilled water. The viologen was added in aliquots from a stock solution. The observed curve was fitted to a biexponential decay assuming a constant value of 811 ns for the unquenched lifetime of **2**. The sample was excited with a Coherent Infinity ND:YAG-XPO laser (1 ns pulses FWHM). For detection a Hamamatsu C5680-21 streak camera with a Hamamatsu M5677 Low-Speed Single-Sweep Unit was used. Where necessary single wavelength emission decay traces were recorded with a Tektronix Oscilloscope (TDS 468) coupled to a photomultiplier. A photodiode was employed for triggering. The emission was observed through an Oriel 77250 monochromator at an angle of 90 degrees with respect to the excitation, with a 500 nm cut-off filter.

The quantum yields were determined by comparison of the emission intensity of isoabsorbing aerated aqueous solutions of **1** and **2** with  $\text{Ru}(\text{bpy})_3$ .<sup>[28]</sup>

### 3.4.4 Synthesis

#### *Ruthenium complex 1*

This compound was synthesised analogous to complex **2** by mixing equimolar quantities of **3** (50.4 mg) and  $\text{Ru}(\text{bpy})_2\text{Cl}_2$  (9.3 mg). Yield 56 mg (94 %);  $^1\text{H}$  NMR (500 MHz,  $[\text{D}_6]\text{DMSO}$ , 298K)  $\delta$  9.37 (s, 2H), 8.87 (d, 4H), 8.22 (dd, 4H), 7.92 (d, 4H), 7.81 (d, 2H), 7.74 (d, 2H), 7.57 (dd, 4H), 5.04 (s, 2H), 4.87 (s, 12H), 3.80-3.38 (m, 84H), 1.86 (br.s, 4H); MS ( $\text{ESI}^+$ ,  $\text{H}_2\text{O}$ ):  $m/z$  1502  $[\text{M}-2\text{Cl}]^{2+}$ ; elemental analysis calcd (%) for  $\text{C}_{122}\text{H}_{174}\text{N}_{82}\text{O}_{72}\text{RuCl}_2 \cdot 24\text{H}_2\text{O}$ : C = 41.73; H = 7.01; N = 3.19. found: C = 41.53; H = 6.88; N = 3.02.

***Ruthenium complex 2***

In a 1:1 (v/v) mixture of ethanol and water 60 mg of cyclodextrin dimer **3** and 2.0 mg of  $\text{RuCl}_3 \cdot 3\text{H}_2\text{O}$  (0.33 eq) were mixed and refluxed for 36 hours. The dark orange solution was poured into acetone and the precipitate was isolated by centrifugation. The crude product was purified by size exclusion chromatography (Sephadex G75, eluent water). After lyophilisation the yield was 55.8 mg (90 %).  $^1\text{H}$  NMR (300 MHz,  $[\text{D}_6]\text{DMSO}$ , 298K)  $\delta$  9.25 (br.s, 6H), 7.94 (br.s, 6H), 7.85 (br.s, 6H), 5.04 (br.s, 6H), 4.86 (br.s, 36H), 3.75-3.08 (m, 252H), 1.84 (br.s, 12H); MS (Maldi-TOF) :  $m/z$  7950.6  $[\text{M}]^+$  calc. 7949.1. elemental analysis calcd (%) for  $\text{C}_{306}\text{H}_{474}\text{N}_{12}\text{O}_{216}\text{RuCl}_2 \cdot 65\text{H}_2\text{O}$ : C = 40.28; H = 6.68; N = 1.84. Found: C = 39.61; H = 6.01; N = 1.83.

***General procedure for symmetrically substituted viologens***

1 equivalent of 4,4'-bipyridine was mixed with an excess of the appropriate 1-alkylbromide in acetonitrile and refluxed for 18 hours. The precipitate was isolated by filtration and washed several times with acetonitrile and diethylether.

***N,N'-dinonyl-4,4'-bipyridinium dibromide (4)***

$^1\text{H}$  NMR (300 MHz,  $\text{D}_2\text{O}$ , 298K)  $\delta$  9.08 (d,  $^3J_{\text{HH}}=6.7$  Hz, 4H), 8.51 (d,  $^3J_{\text{HH}}=6.7$  Hz, 4H), 4.69 (t,  $^3J_{\text{HH}}=7.3$  Hz, 4H), 1.32 (br.s, 4H), 1.22 (br.s, 20H), 0.80 (t,  $^3J_{\text{HH}}=6.9$  Hz, 6H); MS (FAB, glycerol)  $m/z$  : 410  $[\text{M}-2\text{Br}]$ .

***N,N'-dipentyl-4,4'-bipyridinium dibromide (5)***

$^1\text{H}$  NMR (300 MHz,  $\text{D}_2\text{O}$ )  $\delta$  8.96 (d,  $^3J_{\text{HH}}=6.7$  Hz, 4H), 8.38 (d,  $^3J_{\text{HH}}=6.7$  Hz, 4H), 4.56 (t,  $^3J_{\text{HH}}=7.0$  Hz, 4H), 1.93 (t,  $^3J_{\text{HH}}=6.7$  Hz, 4H), 1.20 (m, 8H), 0.73 (m, 6H); MS (FAB, glycerol)  $m/z$  : 148.9  $[\text{M}^{2+}]$ .

***N*-methyl-*N'*-nonyl-4,4'-bipyridinium bromide iodide (6)**

*N*-methyl-4,4'-bipyridinium iodide<sup>[29]</sup> (1.0 g, 3.35 mmol) and 1-nonylbromide (3.5 mL, 15.58 mmol) were refluxed in 100 mL of acetonitrile for 18 hours. The orange precipitate was filtered and washed two times with acetonitrile and three times with 20 mL of diethylether, yielding 890 mg of **6** (52.5 %). <sup>1</sup>H NMR (300 MHz, D<sub>2</sub>O, 298K) δ 8.98 (d, <sup>3</sup>*J*<sub>HH</sub>=6.6 Hz, 2H), 8.91 (d, <sup>3</sup>*J*<sub>HH</sub>=6.6 Hz, 4H), 8.40 (dd, <sup>3</sup>*J*<sub>HH</sub>=6.6 Hz, <sup>3</sup>*J*<sub>HH</sub>=6.6 Hz, 4H), 4.59 (m, 2H), 4.37 (m, 3H), 1.96 (br m, 2H), 1.17 (br m, 12H), 0.69 (t, <sup>3</sup>*J*<sub>HH</sub>=6.7 Hz, 3H); MS (FAB, glycerol) *m/z* : 298.0 [*M*<sup>+</sup>] (100 %), 148.8 [*M*<sup>2+</sup>] (90 %).

### 3.5 REFERENCES

- [1] (a) M.A. Fox, *Photoinduced electron transfer*; Elsevier: New York; **1988**. (b) J. Barber, B. Anderson, *Nature*, **1994**, 370, 31-34.
- [2] H. Kurreck, M. Huber, *Angew. Chem.* **1995**, 107, 929-947; *Angew. Chem. Int. Ed. Engl.* **1995**, 34, 849-866.
- [3] (a) J. M. Warman, M. P. de Haas, M. N. Paddon-Row, E. Cotsaris, N. S. Hush, H. Oevering, J. W. Verhoeven, *Nature*, **1986**, 320, 615-616. (b) E. H. Yonemoto, G. B. Saupe, R. H. Schmehl, S. M. Hubig, R. L. Riley, B. L. Iverson, T. E. Mallouk, *J. Am. Chem. Soc.* **1994**, 116, 4786-4795.
- [4] (a) P. Pasman, G. F. Mes, N. W. Koper, J. W. Verhoeven, *J. Am. Chem. Soc.* **1985**, 107, 5839-5843. (b) J. A. Schmidt, A. Siemiarczuk, A. C. Weedon, J. R. Bolton, *J. Am. Chem. Soc.* **1985**, 107, 6112-6114.
- [5] (a) M. R. Wasielewski, *Chem. Rev.* **1992**, 92, 435-461. (b) M. D. Ward, *Chem. Soc. Rev.* **1997**, 26, 365-375.
- [6] (a) V. Balzani, A. Credi, F. M. Raymo, J. F. Stoddart, *Angew. Chem.* **2000**, 112, 3484-3530; *Angew. Chem. Int. Ed. Engl.* **2000**, 39, 3349-3391. (b) V. Balzani, A. Juris, *Coord. Chem. Rev.* **2001**, 211, 97-115.
- [7] M. H. Keefe, K. D. Benkstein, J. T. Hupp, *Coord. Chem. Rev.* **2000**, 205, 201-228.
- [8] A. Juris, V. Balzani, F. Barigelletti, S. Campagna, P. Belser, A. von Zelewsky, *Coord. Chem. Rev.* **1988**, 84, 85-277.
- [9] D. Husek, Y. Inoue, S. R. L. Everitt, H. Ishida, M. Kunieda, M. G. B. Drew, *Inorg. Chem.* **2000**, 39, 308-316.
- [10] H. F. M. Nelissen, M. C. Feiters, R. J. M. Nolte, *J. Org. Chem.* **2002**, 67, 5901 – 5906.

- [11] (a) Y. Liu, B. Li, T. Wada, Y. Inoue, *Chem. Eur. J.* **2001**, *7*, 2528-2538. (b) Y. Liu, Y. Chen, S. X. Liu, X. D. Guan, T. Wada, Y. Inoue, *Org. Lett.* **2001**, *3*, 1657-1660.
- [12] H. F. M. Nelissen, A. F. J. Schut, F. Venema, M. C. Feiters, R. J. M. Nolte, *Chem. Commun.* **2000**, 577-578.
- [13] For other examples of metal complexes from bipyridine functionalised cyclodextrins see: (a) R. Deschenaux, M. M. Harding, T. Ruch, *J. Chem. Soc., Perkin Trans. 2* **1993**, 1251-1258. (b) R. Deschenaux, A. Greppi, T. Ruch, H. P. Kriemler, F. Raschdorf, R. Ziessel, *Tetrahedron Lett.* **1994**, *35*, 2165-2168. (c) R. Deschenaux, T. Ruch, P. F. Deschenaux, A. Juris, R. Ziessel, *Helv. Chim. Acta* **1995**, *78*, 619-635. (d) S. Weidner, Z. Pikramenou, *Chem. Commun.* **1998**, 1473-1474. (e) F. Charbonnier, T. Humbert, A. Marsura, *Tetrahedron Lett.* **1999**, *40*, 4047-4050. (f) D. Armspach, D. Matt, *Chem. Commun.* **1999**, 1073-1074. (g) D. Armspach, D. Matt, A. Harriman, *Eur. J. Inorg. Chem.* **2000**, 1147-1150. (h) J. M. Haider, Z. Pikramenou, *Eur. J. Inorg. Chem.* **2001**, 189-194. (i) J. M. Haider, M. Chavarot, S. Weidner, I. Sadler, R. M. Williams, L. De Cola, Z. Pikramenou, *Inorg. Chem.* **2001**, *40*, 3912-3921.
- [14] (a) F. Venema, C. M. Baselier, E. van Dienst, B. H. M. Ruël, M. C. Feiters, J. F. J. Engbersen, D. N. Reinhoudt, R. J. M. Nolte, *Tetrahedron Lett.* **1994**, *35*, 1773-1776. (b) F. Venema, C. M. Baselier, M. C. Feiters, R. J. M. Nolte, *Tetrahedron Lett.* **1994**, *35*, 8661-8664. (c) F. Venema, H. F. M. Nelissen, P. Berthault, N. Birlirakis, A. E. Rowan, M. C. Feiters, R. J. M. Nolte, *Chem. Eur. J.* **1998**, *4*, 2237-2250.
- [15] The synthesis of compound **2** has already been briefly reported in ref. 12.
- [16] P. M. S. Monk, *The viologens: physicochemical properties, synthesis and applications of the salts of 4,4'-bipyridine*; Wiley: Chichester; **1998**.
- [17] (a) M. J. Cook, A. P. Lewis, G. S. G. McAuliffe, V. Skarda, A. J. Thomson, *J. Chem. Soc. Perkin Trans. II* **1984**, 1293-1301. (b) M. J. Cook, A. P. Lewis, G. S.

- G. McAuliffe, V. Skarda, A. J. Thomson, J. L. Glasper, D. J. Robbins, *J. Chem. Soc. Perkin Trans. II* **1984**, 1303-1311.
- [18] (a) J. Issberger, F. Vögtle, L. De Cola, V. Balzani, *Chem. Eur. J.* **1997**, *3*, 706-712. (b) F. Vögtle, M. Plevoets, M. Nieger, G. C. Azzellini, A. Credi, L. De Cola, V. De Marchis, M. Venturi, V. Balzani, *J. Am. Chem. Soc.* **1999**, *121*, 6290-6298.
- [19] S. L. Murov, I. Carmichael, G. L. Hug, *Handbook of Photochemistry*; Dekker: New York; **1993**.
- [20] M. Z. Hoffman, F. Bolleta, L. Moggi, G. L. Hug, *J. Phys. Chem. Ref. Data* **1989**, *18*, 219.
- [21] (a) E. H. Yonemoto, R. L. Riley, Y. I. Kim, S. J. Atherton, R. H. Schmehl, T. E. Mallouk, *J. Am. Chem. Soc.* **1992**, *114*, 8081-8087. (b) P. D. Beer, N. C. Fletcher, T. Wear, *Inorg. Chim. Act.* **1996**, *251*, 335-340. (c) P. R. Ashton, R. Ballardini, V. Balzani, E. C. Constable, A. Credi, O. Kocian, S. J. Langford, J. A. Preece, L. Prodi, E. R. Schofield, N. Spencer, J. F. Stoddart S. Wenger, *Chem. Eur. J.* **1998**, *4*, 2413-2422.
- [22] A. Diaz, P. A. Quintela, J. M. Schuette, A. E. Kaifer, *J. Phys. Chem.* **1988**, *92*, 3537-3542.
- [23] D. R. Prasad, K. Mandal, M. Z. Hoffman, *Coord. Chem. Rev.* **1985**, *64*, 175-190.
- [24] Electrochemical experiments on **1** and **2** faced severe problems, probably due to the high molecular weight, low diffusion coefficient, adsorption on the electrode surface, and irreversible processes. Redox properties from related compounds were taken from: (a) C. R. Bock, J. A. Conner, A. D. Gutierrez, T. J. Meyer, D. G. Whitten, B. P. Sullivan, J. K. Nagle, *J. Am. Chem. Soc.* **1979**, *101*, 4815-4824. (b) C. M. Elliott, E. J. Hershenhart, *J. Am. Chem. Soc.* **1982**, *104*, 7519-7526.
- [25] A. Mirzoian, A. E. Kaifer, *Chem. Eur. J.* **1997**, *3*, 1052-1058.

- [26] E. H. Yonemoto, G. B. Saupe, R. H. Schmehl, S. M. Hubig, R. L. Riley, B. L. Iverson, T. E. Mallouk, *J. Am. Chem. Soc.* **1994**, *116*, 4786-4795.
- [27] M. V. Rekharsky, Y. Inoue, *Chem. Rev.* **1998**, *98*, 1875-1917.
- [28] J. V. Houten, R. J. Watts, *J. Am. Chem. Soc.* **1976**, *98*, 4853-4858.
- [29] Prepared from 4,4'-bipyridine and methyl iodide according to L. A. Kelly, M. A. J. Rogers, *J. Phys. Chem.* **1994**, *98*, 6386-9391. Spectroscopic data were in agreement with those reported in the literature.





## **4 Energy transfer between $\text{Ru}(\text{bpy})_3^{2+}$ and DO3A complexed lanthanides**

### **Abstract**

The synthesis of a novel transition metal sensitizer for lanthanide luminescence is presented.  $\text{Ru}(\text{bpy})_3^{2+}$  was substituted with 1,4,7,10-tetraaza-cyclododecane-1,4,7-triacetate (DO3A) in the 4 position of one of the 2,2'-bipyridines. Complexation with Yb and Nd, lanthanides with accessible energy levels, to allow energy transfer from the excited transition metal complex, was achieved. Upon excitation in the visible bands of the Ru- component an energy transfer from the excited  $\text{Ru}(\text{bpy})_3^{2+}$ - moiety to the lanthanide can be observed by a decrease of the Ru- based emission, as well as the sensitization of the near IR emission of the lanthanide.

## 4.1 INTRODUCTION

Lanthanides have attracted a lot of attention in various fields of material science. Recent progress has been made in development of new phosphors for lighting,<sup>[1]</sup> high-efficiency luminescent devices for LED's,<sup>[2]</sup> magnetic resonance imaging (MRI),<sup>[3]</sup> luminescent probes for analytes,<sup>[4]</sup> protein- and amino-acid labels,<sup>[5]</sup> tags for time-resolved luminescence microscopy,<sup>[6]</sup> chiral sensing,<sup>[7]</sup> and many more.<sup>[8-10]</sup>

Lanthanides possess very unique physical properties. Their optical transitions involve the f-orbitals, which are not involved in the coordination to ligands. The f-orbitals are situated deep inside the closed Xe-shell.<sup>[11,12]</sup> Because of the interconfigurational transitions sharp and line-like emission spectra are observed. Unfortunately the intrinsic absorbencies of lanthanide ions are very low ( $\epsilon < 10 \text{ M}^{-1}\text{cm}^{-1}$ ) because the  $4f \rightarrow 4f$  transitions are parity forbidden and sometimes also forbidden by the spin selection rule.<sup>[8]</sup> The ligands must contain suitable chromophores, in order to absorb light with good efficiency, and possess accessible energy levels in order to populate the excited state of the lanthanides via a photoinduced energy transfer from the excited ligand to the metal. Another disadvantage of these metals is that vibrations of O-H, as contained in solvents like water and alcohols, are able to quench the excited state of  $\text{Ln}^{3+}$ .<sup>[13]</sup> Weak vibronic coupling of lanthanide(III) ions with OH-oscillators, present often in molecules in the first coordination sphere of the metal provides a route for radiationless deactivation of the lanthanide ion.<sup>[14]</sup> In figure 1 a schematic representation of the vibronic quenching is depicted. The intensity of the vibronic transition decreases with the Franck-Condon factor, which decreases with  $\nu$  (see figure 1). The use of deuterated solvents is an effective way to retain the luminescence and repress the vibronic deactivation.

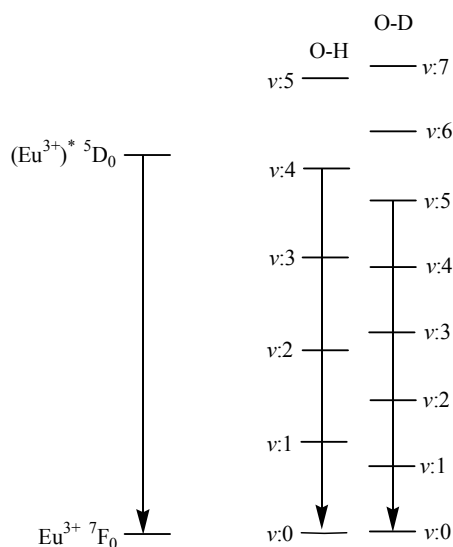


**Figure 1.** Schematic representation of the vibronic quenching of  $(\text{Eu}^{3+})^*$  by the 4<sup>th</sup> overtone of the O-H vibration, or the 5<sup>th</sup> overtone of the O-D vibration.

Finally lanthanide complexes are rather unstable and hydrolysis is often a cause for decomposition. In order to overcome these problems, cage type structures have been developed.<sup>[15]</sup> By complexation with polydentate ligands, and eventually full saturation of the coordination sphere of the f-metal, the presence of solvent molecules can be excluded. In case of uncomplete saturation, vacant sites will still be occupied by coordinating solvent molecules.

Most studies on sensitized lanthanide emission are based on UV-absorbing ligands. The UV- region is traditionally the domain of absorption of most of the organic molecules. Very few examples have been published on excitation in the visible.<sup>[16-24]</sup> Only very recently attempts to use transition metal complexes, such as ruthenium trisbipyridine and ferrocene, as sensitizers for lanthanides have been reported.<sup>[24,25]</sup> Since the most used emitters in the lanthanide family are  $\text{Eu}(\text{III})$  and  $\text{Tb}(\text{III})$  complexes, the use of visible light to sensitize their emission is precluded. Their emission is in fact in the red and green part, respectively, of the spectrum, therefore requiring an energy donor with suitable excited state in order to promote energy transfer from the absorbing chromophore to the excited states of  $\text{Eu}(\text{III})$  or  $\text{Tb}(\text{III})$ . The gap between such donor and acceptor moieties must fulfill the thermodynamic requirements but must fall in a few

thousand wavenumber difference. The rate of the process is critical since it has to compete with the rate of deactivation of the sensitizer.

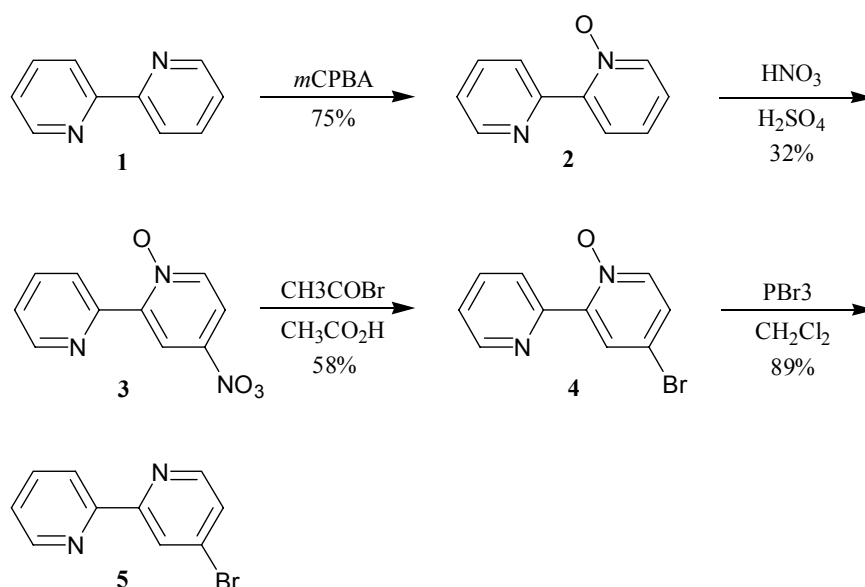
With sensitizers such as  $\text{Ru}(\text{bpy})_3^{2+}$ , only lanthanide ions, possessing lower excited states, such as Nd, Yb, and Er, which emit in the near IR region, fulfill this criteria. Van Veggel et al. have shown that the energy transfer is not highly efficient in a *m*-terphenyl based system, with appended  $\text{Ru}(\text{bpy})_3^{2+}$ - moiety.<sup>[24]</sup> The energy transfer rate was determined to be  $\sim 10^6 \text{ s}^{-1}$  for neodymium and  $\leq 10^5 \text{ s}^{-1}$  for ytterbium. Such rates are far too slow to compete efficiently with the radiative deactivation (emission) of the  $\text{Ru}(\text{bpy})_3^{2+}$  unit. One of the reasons for such low efficiency lies in the design of the system, since the sensitizer and the lanthanide complex are far away and the Dexter- or exchange mechanism, which is the most accepted mechanism for energy transfer in lanthanide chemistry, requires close contact.

The goal of this project is to synthesize a polydentate ligand, suitable for lanthanide binding, with appended ruthenium trisbipyridine. As polydentate ligand, a derivative of the well known 1,4,7,10-tetraaza-cyclododecane-1,4,7,10-tetraacetate (DOTA) was selected, in which only three acetates are connected to the azamacrocycle (DO3A). The binding constants for lanthanide ions of this ligand are extremely high. The stability constant of the  $\text{Gd-DOTA}^-$  was reported to be between  $10^{22}$  and  $10^{28} \text{ l} \cdot \text{mol}^{-1}$ .<sup>[26]</sup> Complexes of DO3A with other lanthanides have association constants in the same order of magnitude. The advantage of this system over the one of van Veggel et al.<sup>[24]</sup> will be the high stability of the lanthanide complex and the close proximity between  $\text{Ru}(\text{bpy})_3^{2+}$  unit and the lanthanide ion, which should result in a higher efficiency for the energy transfer process and therefore higher quantum yield of the lanthanide emission.

The obtained multicomponent system was investigated towards photoinduced energy transfer which resulted in excitation of the Ru-based component and consecutive emission of the lanthanide(III) ion. Most suitable for this purpose were ytterbium and neodymium, which have the right energy levels, to be sensitized by ruthenium trisbipyridine.

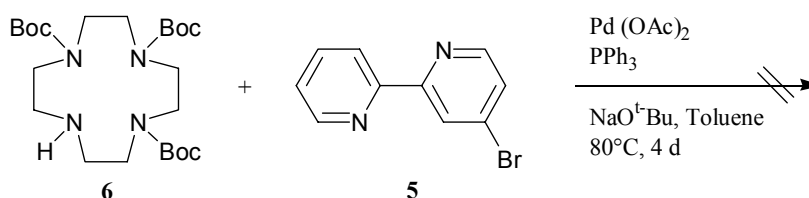
## 4.2 SYNTHESIS

The synthesis for the starting material, 4-bromo-2,2'-bipyridine (**5**) is depicted in scheme 1. Commercially available 2,2'-bipyridine (**1**) is mildly oxidized with *meta*-chloroperbenzoic acid, to give the corresponding N-oxide (**2**).<sup>[27]</sup> Reaction with a mixture of nitric- and sulfuric- acid, nitrates the 4 position of the N-oxide activated pyridine ring.<sup>[28]</sup> Treatment with acetyl bromide in acetic acid exchanges the nitrate for bromide and reaction with phosphorus tribromide removes the N-oxide, leading to **5** (scheme 1).<sup>[28]</sup>



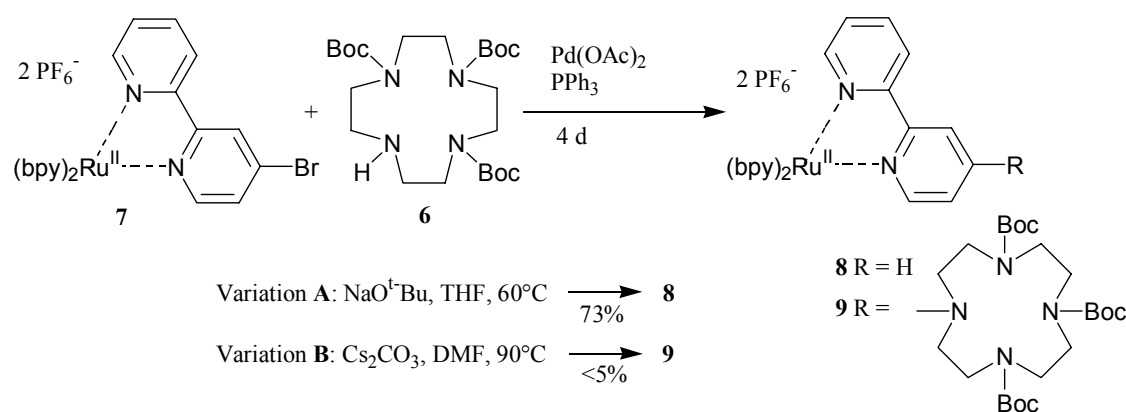
**Scheme 1.** Synthesis of 4-bromo-2,2'-bipyridine.

The bromobipyridine **5** was employed as arylhalogenide in a palladium catalyzed coupling reaction with amines.<sup>[29,30]</sup> Best to my knowledge, a direct linkage of a bipyridine in 4- position and a cyclen derivative has not been reported yet.



**Scheme 2.** Attempted reaction of 4-bromo-2,2'-bipyridine with tris-Boc-cyclen.

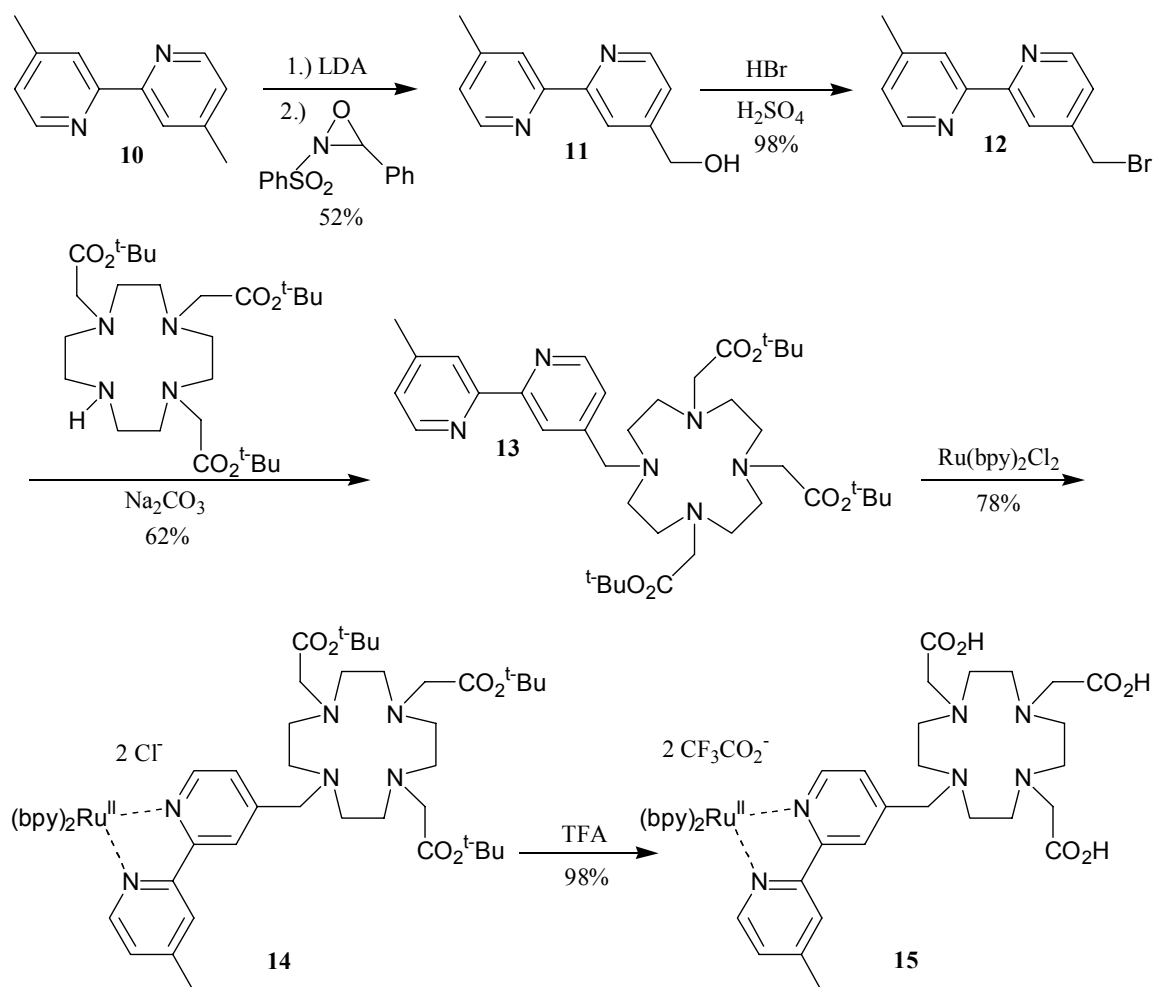
A palladium catalyzed coupling under standard conditions was not successful (see scheme 2). A possible explanation is that the bipyridine, as a good bidentate ligand, is complexing the palladium and deactivating it.<sup>[31]</sup> However, addition of copper acetate, to complex the bipyridine with copper ions and inhibit the complexation of the catalytic palladium, did not improve conversion. After formation of the ruthenium trisbipyridine complex as its hexafluorophosphate salt (**7**), toluene was not a suitable solvent any longer. However, complex **7** was soluble in tetrahydrofuran. The coupling attempt yielded dehalogenated ruthenium trisbipyridine **8** (scheme 3, Variation A). Altering the reaction condition, applying DMF as a solvent and temperatures of 80 – 90 °C led to the same product.



**Scheme 3.** Reaction of 4-bromo-2,2'-bipyridine  $\text{Ru}(\text{bpy})_2$  with tris-Boc-cyclen.

Application of a weak base such as cesium carbonate finally led to the desired coupling product **9** (scheme 3, Variation B). The compound was identified by mass spectra. To our misfortune, the obtained yields are below 5%. The reaction is proceeding, according to the application of a weak base, very slow. Longer reaction times and higher temperature result in elimination of Boc-groups. Since the direct coupling lead to such low yields, we decided to abandon this synthetic strategy.

Instead of building up the target molecule via a catalyzed N - C aromatic coupling reaction it should be possible to connect both moieties by an aliphatic substitution reaction, by introducing a  $\text{CH}_2$ - spacer.



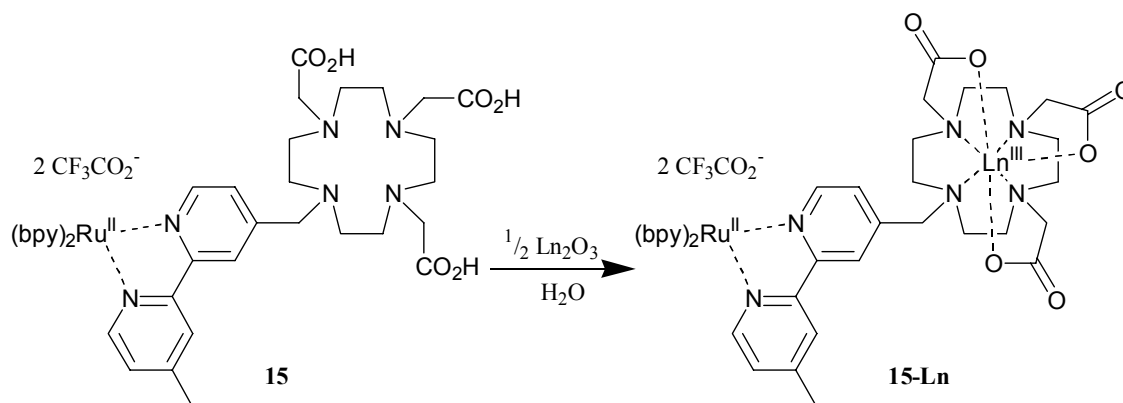
**Scheme 4.** Synthetic route to methylene spaced  $\text{Ru}(\text{bpy})_3$ -DO3A.

4,4'-Dimethyl-2,2'-bipyridine (**10**) was synthesized from commercially available 4-picoline according to a procedure by Sasse.<sup>[32]</sup> Deprotonation with LDA and reaction with 2-phenylsulfonyl-3-phenyloxaziridine<sup>[33]</sup> led to 4-hydroxymethylen-4'-methyl-2,2'-bipyridine (**11**) in 52% yield.<sup>[34]</sup> The alcohol was transformed into the bromide (**12**) by the method of Berg et al.<sup>[35]</sup> quantitatively (scheme 4).

A substitution reaction with tris-Boc-cyclen (**6**) produced only poor yields of the corresponding product. Even though the NMR spectra looked promising, the mass spectra revealed a mixture of starting material and product, which could not be separated by repeated column chromatography.

We received a donation of [4,7-bis-*tert*-butoxycarbonylmethyl-1,4,7,10-tetraazacyclododec-1-yl]acetic acid *tert*-butyl ester from Bracco S.p.A. Milano, Italy, as a DO3A precursor. This compound was used as nucleophile in the substitution reaction. The bromo- derivative **12** was refluxed in acetonitrile with tris *tert*-buthyl protected DO3A in the presence of sodium carbonate.<sup>[36]</sup> Chromatography on silica yielded the substitution product **13** in 68% yield (scheme4). In a mixture of alcohol and water, **13** could be complexed with ruthenium-bis-bipyridine-bis-chloride to form an orange red complex **14**. Extraction with methylene chloride, to remove unreacted starting material, failed because of the good solubility of the ruthenium complex **14**. Separation of bis- and tris-bipyridine was accomplished in 78% by size exclusion chromatography on a cross-linked polystyrene stationary phase and methylene chloride. The deprotection of the DO3A- ligand was realized by treatment with 80% trifluoroacetic acid in  $\text{CH}_2\text{Cl}_2$  in 98% yield.<sup>[37]</sup> The free heptadentate DO3A (**15**) was dissolved in water and freeze dried. For the complexation of lanthanides, 0.5 equivalent of the corresponding lanthanide oxide  $\text{Ln}_2\text{O}_3$  was added to one equivalent of the DO3A substituted ruthenium tris-bipyridine complex **15** in a small amount of water and stirred at 90 °C for 48h (see scheme 5). The product was again lyophilized.

A shift of the carbonyl vibration in the infrared spectrum from  $1695\text{ cm}^{-1}$  for the free acid, to  $1680\text{ cm}^{-1}$  for the lanthanide containing DO3A, indicated the complete complexation of the ytterbium and neodymium ion, respectively. The ESI mass spectra also showed the complexation of lanthanides. The free compound **15** was not detected any longer.



**Scheme 5.** Complexation of lanthanides into the DO3A- moiety of **15**.



### 4.3 PHOTOPHYSICS

The photophysical properties of **15** were compared with the reference compound  $\text{Ru}(\text{bpy})_3^{2+}$  (figure 2).

The substitution on one of the bipyridine ligands is not altering the photophysical properties of the complex significantly. Only a small shift towards lower energies is observed in the absorption and more clearly in the emission spectra. This was already anticipated, since the DO3A- moiety is linked to one of the bipyridines via a  $\text{CH}_2$ -spacer. The carbon bridge is acting as an ‘insulator’ for the electronic interaction between the ruthenium complex and the cyclen unit.

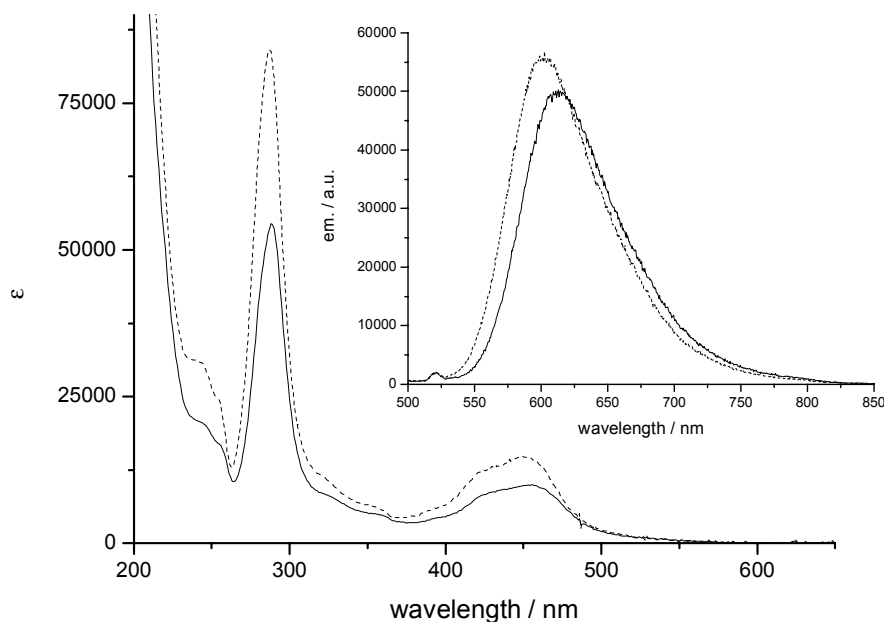


**Figure 2.** Absorption and emission spectra (inset) of **15** (full line) and  $\text{Ru}(\text{bpy})_3^{2+}$  (dashed line) in methanol.

**Table 1.** Photophysical data for Ru(bpy)<sub>3</sub><sup>2+</sup>, **15**, and protonated **15** (**15-H**<sup>+</sup>) in aerated methanol. Ru(bpy)<sub>3</sub><sup>2+</sup>- data taken from the literature.<sup>[38]</sup>

	Abs. $\lambda_{\text{max}}$ / nm	$\epsilon$ / M <sup>-1</sup> cm <sup>-1</sup>	Em. $\lambda_{\text{max}}$ / nm	$\Phi$	$\tau$ / ns
Ru(bpy) <sub>3</sub> <sup>2+</sup>	453	14650	609	0.017	210
<b>15</b>	455	10000	614	0.015	200
<b>15-H</b> <sup>+</sup>	455		614	0.021	240

The observed emission in the visible region derives from the MLCT transition of the ruthenium trisbipyridine (see figure 3). As a reference system the lanthanide free **15** (figure 3A), as well as the protonated **15-H**<sup>+</sup> (figure 3C) is displayed. The spectra of **15-H**<sup>+</sup> was obtained from a solutions of 1% trifluoroacetic acid (TFA) in methanol.

A striking feature of the emission of free **15** is that it is quenched by about 20% compared with **15-H**<sup>+</sup>. A possible explanation could be that the free electron pairs of the tertiary amines of the cyclene backbone act as electron donors towards the ruthenium metal center and quench its emission. Protonation of these amines results in higher quantum yields, because this pathway of deactivation of excited Ru(bpy)<sub>3</sub><sup>2+</sup> is eliminated, since the free electron pairs are occupied in bonds.

Upon complexation of neodymium (figure 3D), the intensity of the ruthenium luminescence decreases significantly. This is expected and can easily be explained by an energy transfer from the transition metal complex to the lanthanide. However, the energy transfer is not complete, since the decrease of the emission intensity can be calculated to about 50% of the intensity of **15-H**<sup>+</sup>.

The ytterbium (figure 3B) shows only a small decrease of Ru-based emission, compared with **15-H**<sup>+</sup>. The energy transfer is even less efficient than in the neodymium case.

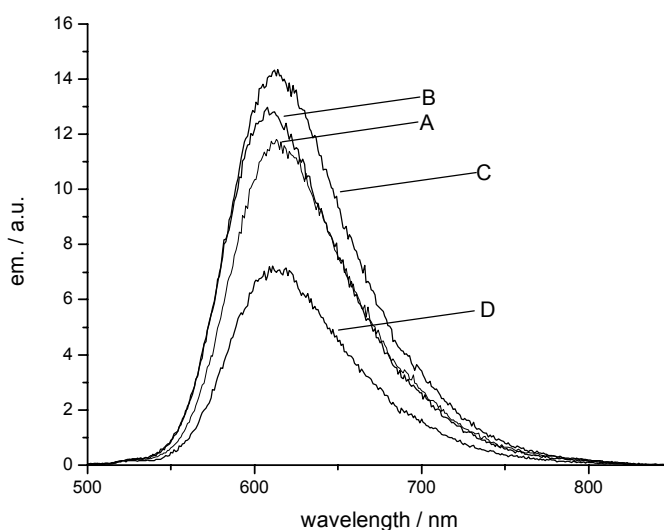
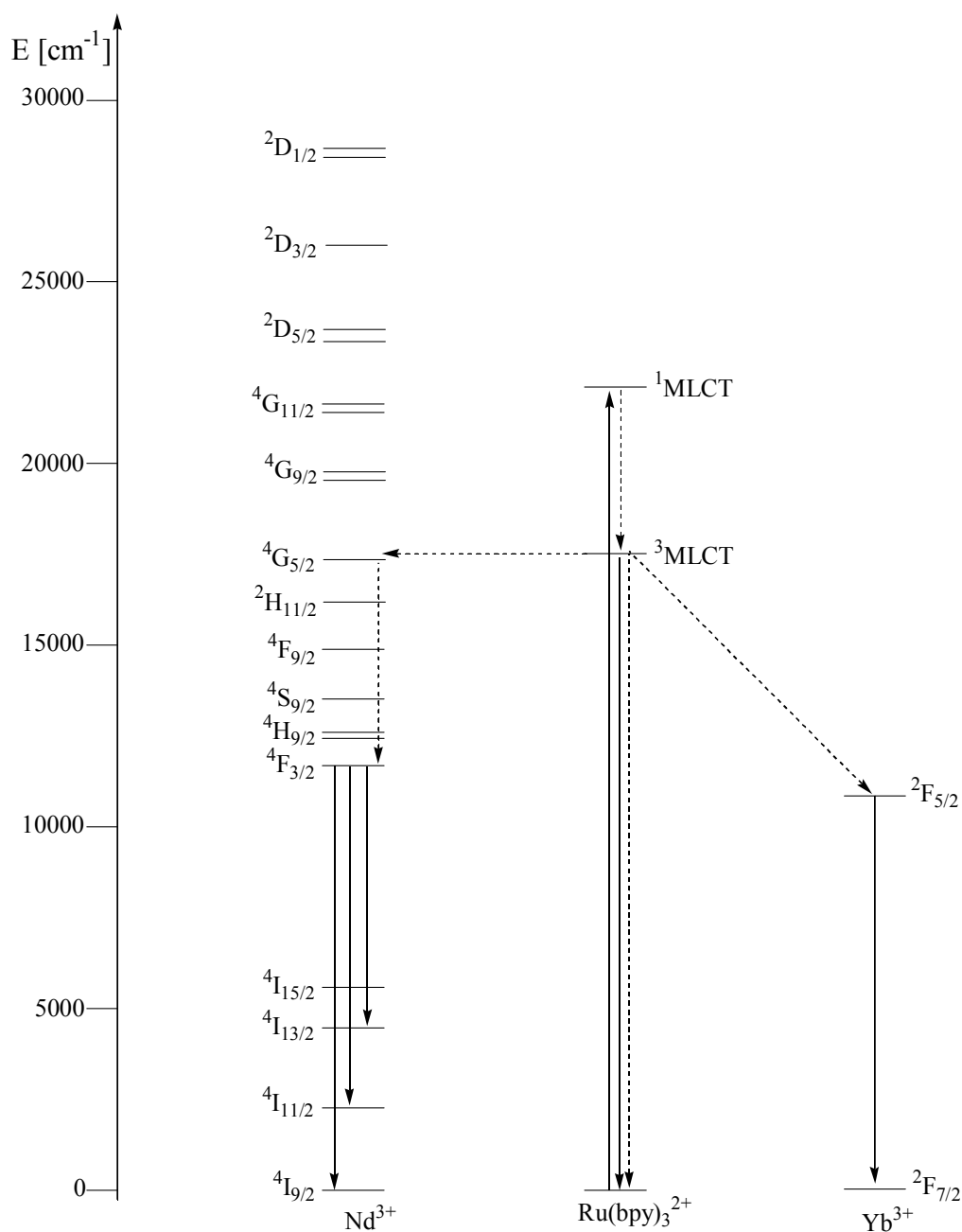


**Figure 3.** Emission spectra of **15** (A), **15-Yb** (B), **15-Nd** (D), **15-H<sup>+</sup>** (C) in  $\text{CH}_3\text{OH}$ . Excitation at 455 nm.

The difference in Ru- based emission between Nd- and Yb-containing **15** can be explained with the difference of energy of accessible acceptor levels (see scheme 6). The donating energy level of the  $\text{Ru}(\text{bpy})_3^{2+}$ -moiety is the  $^3\text{MLCT}$  at about  $17200\text{ cm}^{-1}$ . It is in close proximity of the  $^4\text{G}_{5/2}$  state of  $\text{Nd}^{3+}$  to which the energy transfer probably takes place.<sup>[39]</sup> Nevertheless, the lanthanide will deactivate to the  $^4\text{F}_{3/2}$  state, which is the lowest emissive state in neodymium. The transitions  $^4\text{F}_{3/2} \rightarrow ^4\text{I}_{13/2}$ ,  $^4\text{F}_{3/2} \rightarrow ^4\text{I}_{11/2}$ , and  $^4\text{F}_{3/2} \rightarrow ^4\text{I}_{9/2}$  can be observed at 880, 1060 and 1330 nm, respectively. Our equipment only allows us to monitor the latter two transitions.

The  $\text{Yb}^{3+}$  only possesses a  $^2\text{F}_{5/2}$  state below the donating  $^3\text{MLCT}$  of the ruthenium (scheme 6). The  $\Delta E$  of the gap is about  $7000\text{ cm}^{-1}$ , resulting in a small spectral overlap, necessary for the Dexter- mechanism.



**Scheme 6.** Energy diagram of  $\text{Nd}^{3+}$ ,  $\text{Yb}^{3+}$ , and  $\text{Ru}(\text{bpy})_3^{2+}$ . Full arrows represent radiative processes and dashed arrows radiationless processes.<sup>[13]</sup>

Time resolved measurements in aerated solutions also show a significant difference between the two investigated lanthanides. The lifetime of the Ru-based emission of **15** was determined to 200 ns aerated methanol (see table 1). Nevertheless, the lifetime of metal containing **15** must be compared with the protonated species (**15-H**<sup>+</sup>) since we

already saw that the cyclen-amines quench the ruthenium emission (figure 3). The lifetime of **15-H**<sup>+</sup> was measured to 240 ns.

The metal containing species **15-Yb**, and **15-Nd** could be fitted monoexponentially with a  $\tau = 200$  ns and  $\tau = 130$  ns, respectively. From these numbers, the energy transfer rate  $k_{ET}$  can be calculated according to:

$$k_{ET} = \frac{1}{\tau_{15-Ln}} - \frac{1}{\tau_{15-H^+}} \quad (\text{equation 1})$$

and results in  $8.3 \cdot 10^5 \text{ s}^{-1}$  and to  $3.5 \cdot 10^6 \text{ s}^{-1}$  in aerated solution for ytterbium and neodymium, respectively.

The emission of Yb<sup>3+</sup> in the NIR region could be observed under aerated and deaerated conditions. In the region of 900 – 1100 nm a significant background is observed, slowly tailing to zero (figure 4). This can be attributed to the luminescence of the ruthenium trisbipyridine, based on comparison with Ru(bpy)<sub>3</sub><sup>2+</sup> as a reference compound (spectra not shown here) which exhibits the very similar behavior.

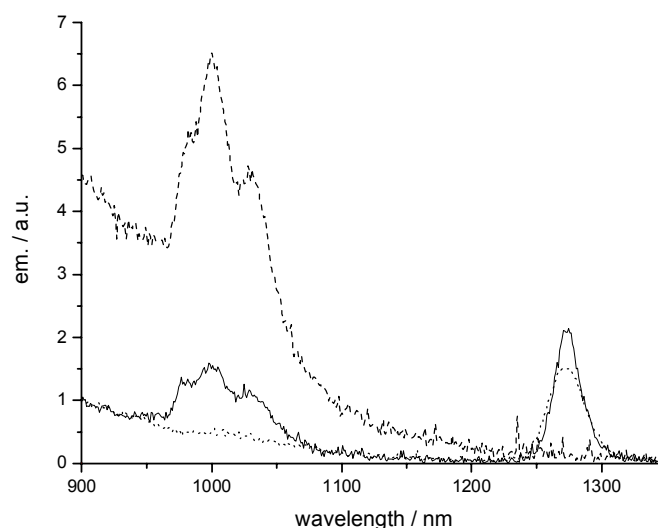


**Figure 4.** NIR emission of aerated **15-Yb** (full line), deaerated **15-Yb** (dashed line) and aerated **15** (dotted line) in CD<sub>3</sub>OD. Excitation at 455 nm

The band at about 1270 nm in figure 3 can be assigned to  $(^1\Delta)\text{O}_2$ .  $\text{Ru}(\text{bpy})_3^{2+}$  is a well known sensitizer for singlet oxygen, <sup>[40]</sup> as already mentioned in chapter 2. Deaeration is eliminating the band from the spectrum.

Deaeration of the sample in principle should not change the intensity of the lanthanide luminescence, since it is independent of quenching by oxygen. The significantly stronger emission (see figure 4), can be explained by the fact that the sensitizing unit,  $\text{Ru}(\text{bpy})_3^{2+}$ , is not quenched since no oxygen is present, and therefore exhibits a stronger luminescence. This can be seen in the stronger tailing of the baseline in figure 4. The more intense luminescence is equivalent to a higher population of the triplet state, from which the energy transfer to the lanthanide can occur. Stronger luminescence from the lanthanide ion therefore is a result from a higher population and longer lifetime of the triplet state of the ruthenium- unit.

The same spectra have been recorded with **15-Nd** (Figure 5). With **15-Nd** we again observe an increase of the lanthanide based emission upon deaeration, due to the aforementioned mechanism. Also the band at around 1270 nm vanishes, when no oxygen is present.

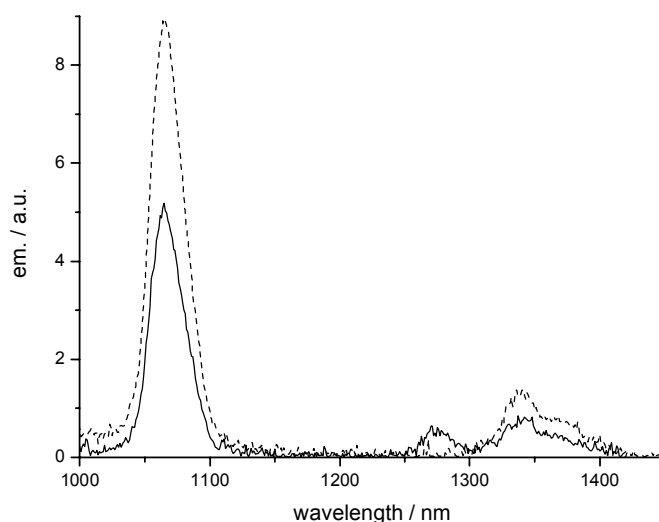


**Figure 5.** NIR emission of aerated **15-Nd** (full line), deaerated **15-Nd** (dashed line) in  $\text{CD}_3\text{OD}$ . Excitation at 455 nm.

In identical conditions, the compound **15-Nd** exhibits clearly a stronger luminescence in the near infra red region than **15-Yb**. The near IR emission of Nd is about 4 times stronger in intensity compared with Yb. A likely rational for this observation could be that the energy transfer between the ruthenium complex and the lanthanides is more efficient for Nd. This explanation is in good agreement with the observed intensity and lifetimes of the Ru- based emission, which also indicate a stronger quenching of the Ru moiety. The energy level scheme (see scheme 6) shows infact that the matching between the donor excited state (Ru- moiety) and the acceptor (Nd- or Yb- ions) is extremely good for **15-Nd** since slightly exoergonic for neodymium while too exoergonic for ytterbium.

An attempt was made to determine the lifetime of the lanthanide near infra red – emission (figure 6).

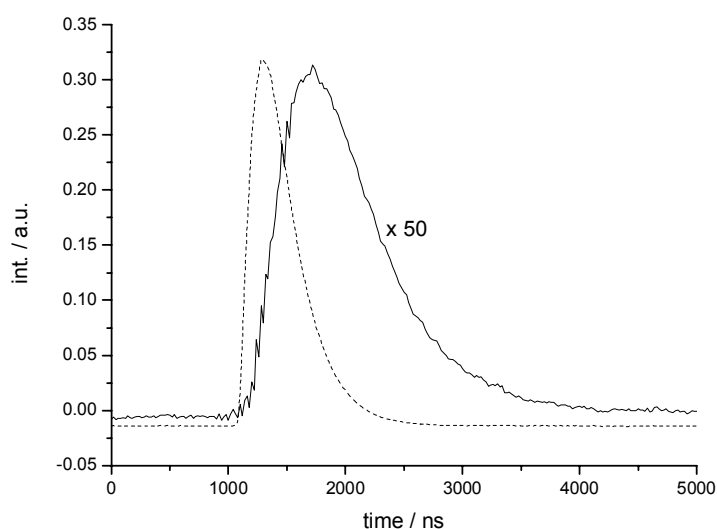


**Figure 6.** Decay traces of IR140 (dashed line) and **15-Nd** (full line).

The luminescent dye IR140 is showing the detector response time, which is about 400 ns. The excited  $\text{Nd}^{3+}$  in **15-Nd** is decaying with a lifetime  $\tau$  of about 600 ns in deuterated methanol. The obtained value is within the typical range of lifetimes of  $\text{Nd}^{3+}$ , complexed in polyaza-polydentate ligands in deuterated methanol.<sup>[41]</sup>

The same measurements have been performed with **15-Yb**. The recorded decay times however were much shorter than the system response and therefore not reliable. This could be also due to the weak intrinsic luminescence of Yb<sup>3+</sup> in this system.

The number of solvent molecules, bound in the first coordination sphere of the lanthanide can be determined by equation 2.<sup>[42]</sup>

$$n = q * \left( \frac{1}{\tau_{H_2O}} - \frac{1}{\tau_{D_2O}} \right) \quad (\text{equation 2})$$

The factor q is depending on the lanthanide ion and the lifetimes  $\tau$  are the respective lifetimes in water and deuteriumoxide. In our case we were unable to accurately determine the number of solvent molecules in the first coordination sphere. Nevertheless, from a solvent dependence study we yield evidence that solvent molecules are bound to the lanthanide ion.

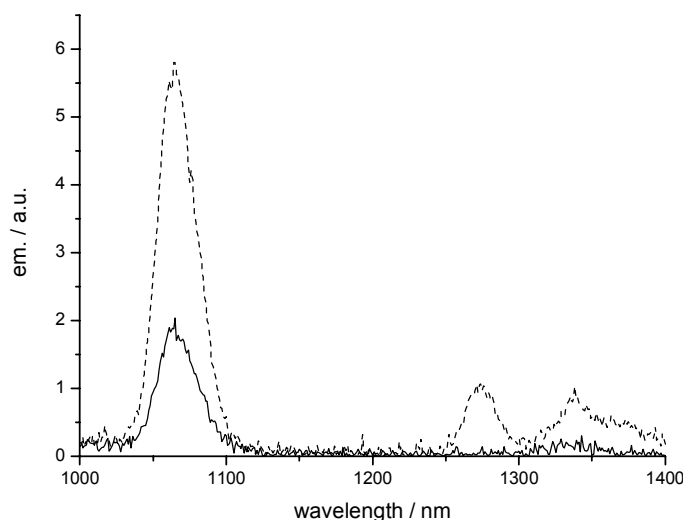


**Figure 7.** Near infra red emission spectra of **15-Nd** in CH<sub>3</sub>OH (full line) and CD<sub>3</sub>OD. Excitation at 455 nm.

Upon use of deuterated solvent, the neodymium based emission triples its intensity (figure 7). This indicates a less efficient quenching of solvent, due to the matching of a higher vibrational overtone of the O-D vibration, in comparison to O-H. An



improvement of the system will be the replacement of coordinated solvent with a chelating ligand.

In the paper by van Veggel et al., an octadentate ligand was used for the study. This may already offer advantages in the emission intensity of the lanthanide-based transitions. Even higher coordination numbers have been realized very recently by Quici et al. for a phenanthroline appended DO3A,<sup>[43]</sup> and by Parker et al. with a DO3A- derivative, bearing a tetraazatriphenylen.<sup>[44]</sup> Both groups nevertheless are only able to use UV excitation to pump the lanthanide.

#### 4.4 CONCLUSION

A novel system containing a  $\text{Ru}(\text{bpy})_3^{2+}$ - unit as sensitizer, and DO3A as polydentate ligand for lanthanide ions has been developed and successfully applied in the study of photoinduced energy transfer towards  $\text{Yb}^{3+}$  and  $\text{Nd}^{3+}$ . The expectations of increased efficiency, compared with the system of van Veggel et al.,<sup>[24]</sup> were not fulfilled. The closer spacial proximity between the lanthanide ion and the Ru- complex did not resolve in fast energy transfer perhaps because of the presence of an insulation  $\text{CH}_2$ -spacer. In the continuation of this project, the exchange of ruthenium for osmium will be investigated.  $\text{Os}(\text{bpy})_3^{2+}$  possesses a  $^3\text{MLCT}$  state at about  $14300\text{ cm}^{-1}$  and is therefore much closer to the emitting energy levels of ytterbium and neodymium.

#### 4.5 EXPERIMENTAL

##### 4.5.1 Photophysical measurements

Measurements on the lanthanides were all performed in deuterated solvents.

The NIR-fluorescence spectra were recorded on a PTI Alphascan fluorimeter, in which a 75W quartz-tungsten-halogen lamp is focussed through a SPEX 1680 double monochromator onto the sample. The excitation light was modulated by a mechanic chopper at 35-70 Hz. The emission was detected under a right angle with a 830 nm cutoff filter. Through a PTI single monochromator, the beam focussed onto a liquid

nitrogen cooled germanium detector (North Coast EO-817L), which was connected to a Stanford Research SRS530 lock-in amplifier, detecting the modulated signal.

The lifetime of lanthanides was determined using a setup consisting of a 337 nm nitrogen laser (Laser Technik Berlin MSG405-TD, pulses nominally 20 μJ, 0.5 ns FWHM), an Edinburgh Instruments single monochromator and a North Coast EO-817P liquid nitrogen cooled germanium detector. The response time of the system was measured from the luminescence of IR140 in to about 400 ns FWHM. The system response is determined by the Ge-detector response. The signal was recorded by Tektronix digitizing oscilloscope, which is triggered by the laser clock, and transferred to a microcomputer for analysis. For the different lanthanide luminescence lifetime determinations, the detector was tuned to 980 nm for Yb<sup>3+</sup> and 1060 nm for Nd<sup>3+</sup>.

#### 4.5.2 Synthesis

##### 4-Hydroxymethylene-4'-methyl-2,2'-bipyridine (11):<sup>[34]</sup>

To a solution of 370 mg (2 mmol) of 4,4'-dimethyl-2,2'-bipyridene in dry THF at -78°C 2.05 mmol (1.02 eq.) of freshly prepared lithiumdiisopropylamine in 20 ml THF were added, to form the deeply red anion. After stirring for 30 minutes one equivalent of 2-phenylsulfonyl-3-phenyloxaziridine in THF was slowly added whereby the solution turned yellow. The mixture was allowed to warm up to room temperature, quenched with aqueous sat. NH<sub>4</sub>Cl, washed with brine and the organic phase was evaporated to dryness. Column chromatography of the crude product on silica (CH<sub>2</sub>Cl<sub>2</sub>:CH<sub>3</sub>OH:aq. NH<sub>3</sub>-solution; 200:10:1; *R<sub>F</sub>* = 0.1) yielded 207 mg (52 %) of **9**. <sup>1</sup>H-NMR (CDCl<sub>3</sub>, 300 MHz) δ = 2.34 (s, 3H), 4.66 (s, 2H), 5.25 (br, 1H), 7.05-7.18 (m, 2H), 8.07-8.19 (m, 2H), 8.39-8.46 (m, 2H). <sup>13</sup>C-NMR (CDCl<sub>3</sub>, 75 MHz, APT) δ = 21.4 (-), 63.1 (+), 119.0 (-), 121.4 (-), 122.6 (-), 125.0 (-), 148.7 (+), 148.9 (-), 152.2 (+), 155.9 (+), 156.0 (+). IR (KBr) ν = 3200, 1596, 1456, 819 cm<sup>-1</sup>.

**[4,7-Bis-*tert*-butoxycarbonylmethyl-10-(4'-methyl[2,2']bipyridine-4-ylmethyl)-1,4,7,10-tetraaza-cyclododec-1-yl]acetic acid *tert*-butyl ester (14):**

To a solution of 400 mg (0.77 mmol) of [4,7-bis-*tert*-butoxycarbonylmethyl-1,4,7,10-tetraaza-cyclododec-1-yl]acetic acid *tert*-butyl ester (**8**) and 660 mg (8 equivalents, 6.3 mmol) Na<sub>2</sub>CO<sub>3</sub> in 60 ml acetonitrile, 300 mg (1.15 mmol) of 4-bromomethylen-4'-methyl-2,2'-bipyridine (**9**) in 40 ml acetonitrile was slowly added. Upon addition the mixture turned red. After stirring at 75 – 80 °C for 36 hours, the inorganic salts were filtered off and the solvent was evaporated in vacuum. Chromatography on silica with CH<sub>2</sub>Cl<sub>2</sub>:CH<sub>3</sub>OH:25% aq. NH<sub>3</sub>-solution (140:10:1; *R*<sub>F</sub> = 0.05) yielded 332 mg (0.48 mmol, 62 %) of slightly yellow **10** (Mp. 84 °C). <sup>1</sup>H-NMR (CDCl<sub>3</sub>, 300 MHz) δ = 1.2–1.4 (m, br, 29H) 2.0–2.5 (m, br, 4H) 2.30 (s, 3H), 2.6–3.1 (m, br, 12H), 6.95 (d, *J* = 5.1 Hz, 1H), 7.27 (d, *J* = 4.8 Hz, 1H), 8.03 (s, 1H), 8.31 (m, 2H), 8.42 (d, *J* = 4.8 Hz, 1H). <sup>13</sup>C-NMR (CDCl<sub>3</sub>, 75 MHz, APT) δ = 21.3 (-), 28.0 (-), 50.3 (+), 55.7 (+) 56.2 (+), 59.1 (+), 82.6 (+), 83.0 (+), 122.0 (-), 122.8 (-), 124.7 (-), 125.0 (-), 147.4 (+), 148.1 (+), 149.1 (-), 149.4 (-), 155.4 (+), 157.0 (+), 172.7 (+), 173.6 (+). IR (KBr) ν = 2977, 2931, 2834, 1723, 1672, 1596, 1456, 1369, 1311, 1230, 1160, 1111, 847, 757 cm<sup>-1</sup>. MS (EI, 70 eV): *m/z* (%) = 696.5 (9) [M<sup>+</sup>], 595.5 (31) [M<sup>+</sup>-C<sub>5</sub>H<sub>9</sub>O<sub>2</sub>], 513.5 (7) [M<sup>+</sup>-C<sub>12</sub>H<sub>11</sub>N<sub>2</sub>], 313.4 (31) [C<sub>16</sub>H<sub>29</sub>N<sub>2</sub>O<sub>4</sub><sup>+</sup>], 257.4 (28) [C<sub>12</sub>H<sub>21</sub>N<sub>2</sub>O<sub>4</sub><sup>+</sup>], 201.3 (33) [C<sub>8</sub>H<sub>13</sub>N<sub>2</sub>O<sub>4</sub><sup>+</sup>], 184.3 (100) [C<sub>12</sub>H<sub>12</sub>N<sub>2</sub><sup>+</sup> (dmbpy)], 157.3 (32) [C<sub>8</sub>H<sub>15</sub>O<sub>2</sub>N], 102.2 (17) [C<sub>5</sub>H<sub>10</sub>O<sub>2</sub><sup>+</sup> (CO<sub>2</sub>-*t*-Bu)], 56.2 (26) [C<sub>4</sub>H<sub>8</sub><sup>+</sup> (*t*-Bu)], 41.1 (31) [C<sub>2</sub>H<sub>3</sub>N<sup>+</sup>]. HRMS (C<sub>38</sub>H<sub>60</sub>N<sub>6</sub>O<sub>6</sub>): calc. 696.4574, found 696.4567

***tert*-Butyl-bis(2,2'-bipyridin){[4,7-bis-*tert*-butoxycarbonylmethyl-10-(4'-methyl [2,2']-bipyridine-4-ylmethyl)-1,4,7,10-tetraaza-cyclododec-1-yl]ethanoate} ruthenium(II)-bis(chloride) (14):**

A mixture of 91.4 mg (130 μmol) of **10** and 72.3 mg (138 μmol) of bis(2,2'-bipyridine)-dichloro-ruthenium(II) dihydrate was refluxed in 50 ml of ethanol and 2 ml of water for 16 h. The solvent was evaporated under vacuum. Gel permeation chromatography on Bio-Beads<sup>®</sup> S-X1 with methylene chloride as eluent yielded 124 mg (102 μmol, 78%) reddish brown **11**. The product was dissolved in water and lyophilized. <sup>1</sup>H-NMR (CDCl<sub>3</sub>, 300 MHz) δ = 0.6–1.5 (m, br), 2.0–3.3 (m, br, 24H), 7.14 (s, 2H), 7.3–7.6 (m, br, 12H), 7.9–8.1 (m, 4H), 8.9–9.1 (m, 4H). <sup>13</sup>C-NMR (CDCl<sub>3</sub>, 75 MHz, APT) δ = 14.2 (-), 21.5 (-), 28.0 (-), 28.1 (-), 28.2 (-), 29.5 (+), 29.8 (+), 54.4 (+), 55.7 (+), 57.1 (+), 82.6 (+), 82.8 (+), 125.9 (-), 127.6 (-), 128.1 (-), 129.0 (-), 130.3 (-), 138.7 (-), 146.3 (+), 149.6 (-), 150.3 (-), 150.7 (-), 151.0 (-), 151.5 (-), 156.4 (+), 156.7 (+), 156.9 (+), 157.2 (+), 172.6 (+), 174.0 (+). IR (KBr) ν = 2975, 2925, 2852, 1724, 1667, 1619, 1463, 1422, 1368, 1311, 1230, 1157, 843, 773 cm<sup>-1</sup>. MS (ESI): *m/z* (%) = 1189.4 (6), 566.2 (32), 555.2 (100) [M<sup>2+</sup>], 527.22(29) [M<sup>2+</sup> - *t*-Bu], 499.2 (27) [M<sup>2+</sup> - 2 *t*-Bu], 471.2 (67) [M<sup>2+</sup> - 3 *t*-Bu]. HRMS (C<sub>58</sub>H<sub>76</sub>N<sub>10</sub>O<sub>6</sub>Ru<sup>2+</sup>): calc. 555.2491, found 555.2489.

**Bis(2,2'-bipyridin){[4,7-bis-carbonylmethyl-10-(4'-methyl[2,2']bipyridine-4-yl-methyl)-1,4,7,10-tetraaza-cyclododec-1-yl]acetic acid}ruthenium(II)-bis(trifluoroacetate)(15):**

Compound **11**(100 mg, 84.6 μmol) was stirred for 16 h in 3ml of 80% trifluoroacetic acid / methylene chloride. The volatile components were evaporated in vacuo. The residue was dissolved 3 times in 5 ml methylene chloride and 3 times in 5 ml

diethylether and taken to dryness. The residue was dissolved in 3 ml of water and lyophilized to yield 84 mg (83  $\mu$ mol, 98%) of the free acid **12**. <sup>1</sup>H-NMR (D<sub>2</sub>O, 500 MHz)  $\delta$  = 2.38 (s, 3H) 2.8–3.9 (m, br, 22H), 4.67 (br, solvent peak), 7.09 (d, 1H), 7.20 – 7.25 (m, 5H), 7.35 (s, br, 1H), 7.45 (dd, 1H), 7.59 (s, 2H), 7.65 (d, 4H), 7.85 – 7.91 (m, 5H), 8.19 (s, 1H), 8.37 (d, 5H). <sup>13</sup>C-NMR (D<sub>2</sub>O, 125 MHz, APT)  $\delta$  = 20.7 (+), 49.1 (-), 50.2 (-), 54.1 (-), 55.4 (-), 57.1 (-), 113.0 (-), 115.3 (-), 117.6 (-), 120.0 (-), 124.1 (+), 124.2 (+), 125.0 (+), 125.6 (+), 127.2 (+), 127.4 (+), 127.5 (+), 128.0 (+), 128.7 (+), 137.6 (+), 137.6 (+), 137.7 (+), 150.6 (-), 151.3 (+), 151.4 (+), 151.6 (+), 152.3 (+), 156.1 (-), 157.1 (-), 157.2 (-), 157.2 (-), 158.1 (-), 162.5 (-), 162.8 (-), 163.1 (-), 163.3 (-). IR (KBr)  $\nu$  = 1695, 1465, 1424, 1355, 1203, 1182, 1132, 834, 802, 770, 721 cm<sup>-1</sup>. MS (ESI):  $m/z$  (%) = 1056.3 (10) [M<sup>2+</sup>+CF<sub>3</sub>COO<sup>-</sup>], 471.2 (100) [M<sup>2+</sup>]. HRMS (C<sub>46</sub>H<sub>52</sub>N<sub>10</sub>O<sub>6</sub>Ru<sup>2+</sup>): calc. 471.1552, found 471.1550.

### General method for the complexation of lanthanides:

Up to 10 mg of **12** were reacted with 0.5 eq. of Ln<sub>2</sub>O<sub>3</sub> in 10 ml of water for 48h at 90°C. The samples were lyophilized and readily used. The NMR data were not indicative. TSQ- and HRMS, as well as IR- spectroscopy confirmed the formation of the lanthanide species.

### 15-Yb:

IR (KBr)  $\nu$  = 1680, 1464, 1446, 1423, 1203, 1133, 837, 801, 768, 720 cm<sup>-1</sup>. MS (ESI):  $m/z$  (%) = 1226.4 (2) [M<sup>2+</sup>+CF<sub>3</sub>COO<sup>-</sup>], 556.3 (100) [M<sup>2+</sup>].

**15-Nd:**

IR (KBr)  $\nu$  = 1683, 1464, 1446, 1423, 1203, 1132, 836, 800, 768, 720 cm<sup>-1</sup>. MS (ESI):

$m/z$  (%) = 1196.3 (2) [M<sup>2+</sup>+CF<sub>3</sub>COO<sup>-</sup>], 541.4 (100) [M<sup>2+</sup>].

#### 4.6 REFERENCES

- [1] T. Jüstel, H. Nikol, C. Ronda, *Angew. Chem.* **1998**, *110*, 3250 – 3271; *Angew. Chem. Int. Ed. Engl.* **1998**, *37*, 3084 – 3103.
- [2] S. Capecchi, O. Renault, D.-G. Moon, M. Halim, M. Etchells, P. J. Dobson, O. V. Salata, V. Christou, *Adv. Mater.* **2000**, *12*, 1591 – 1594.
- [3] P. Caravan, J. J. Ellison, T. J. McMurry, R. B. Lauffer, *Chem. Rev.* **1999**, *99*, 2293 – 2352.
- [4] D. Parker, *Coord. Chem. Rev.* **2000**, *205*, 109 – 130.
- [5] V. W. W. Yam, K. K. W. Lo, *Coord. Chem. Rev.* **1999**, *184*, 157 – 240.
- [6] L. J. Charbonnière, R. Ziessel, M. Guardigli, A. Roda, N. Sabatini, M. Cesario, *J. Am. Chem. Soc.* **2001**, *123*, 2436 – 2437.
- [7] H. Tsukube, S. Shinoda, *Chem. Rev.* **2002**, *102*, 2389 - 2404.
- [8] J.-C. G. Bünzli, C. Piguet, *Chem. Rev.* **2002**, *102*, 1897 - 1928.
- [9] K. Kuriki, Y. Koike, Y. Okamoto, *Chem. Rev.* **2002**, *102*, 2347 - 2356.
- [10] J. Kido, Y. Okamoto, *Chem. Rev.* **2002**, *102*, 2357 - 2368.
- [11] H. G. Friedman, G. R. Choppin, D. G. Feuerbacher, *J. Chem. Educ.* **1964**, *41*, 354 – 359.
- [12] A. J. Freeman, R. E. Watson, *Phys. Rev. B* **1962**, *127*, 2058 – 20xx.
- [13] G. Stein, E. Würzberg, *J. Phys. Chem.* **1975**, *62*, 208 – 213.
- [14] W. DeW. Horrocks Jr., D. R. Sudnick, *J. Am. Chem. Soc.* **1979**, *101*, 334 – 340.
- [15] B. Alpha, j.-M. Lehn, G. Mathis, *Angew. Chem.* **1987**, *99*, 259 – 261; *Angew. Chem. Int. Ed. Engl.* **1987**, *26*, 266 – 267

- [16] M. H. V. Werts, J. W. Hofstraat, F. A. J. Geurts, J. W. Verhoeven, *Chem. Phys. Lett.* **1997**, 276, 196 – 201.
- [17] M. H. V. Werts, J. W. Verhoeven, J. W. Hofstraat, *J. Chem. Soc., Perkin Trans. 2* **2000**, 433 – 439.
- [18] M. H. V. Werts, R. H. Woudenberg, P. G. Emmerink, R. van Gassel, J. W. Hofstraat, J. W. Verhoeven, *Angew. Chem.* **2000**, 112, 4716 – 4718; *Angew. Chem. Int. Ed. Engl.* **2000**, 39, 4542 – 4544.
- [19] W.-K. Wong, A. Hou, J. Guo, H. He, L. Zhang, W.-Y. Wong, K.-F. Li, K.-W. Cheah, F. Xue, T. C. W. Mak, *J. Chem. Soc., Dalton Trans.* **2001**, 3092 – 3098.
- [20] R. J. Curry, W. P. Gillin, A. P. Knights, R. Gwilliam, *Appl. Phys. Lett.* **2000**, 77, 2271 – 2273.
- [21] M. I. Gaiduk, V. V. Grigoryants, A. F. Mironov, V. D. Rmyantseva, V. I. Chissov, G. M. J. Sukhin, *Photochem. Photobiol. B* **1990**, 7, 15 – 20.
- [22] M. P. Oude Wolbers, F. C. J. M. van Veggel, F. G. A. Peters, E. S. E. van Beelen, J. W. Hofstraat, F. A. J. Geurts, D. N. Reinhoudt, *Chem. Eur. J.* **1998**, 4, 772 – 780.
- [23] S. I. Klink, P. Oude Alink, L. Grave, F. G. A. Peters, J. W. Hofstraat, F. Geurts, F. C. J. M. van Veggel, *J. Chem. Soc. Perkin Trans. 2* **2001**, 363 – 372.
- [24] S. I. Klink, H. Keizer, F. C. J. M. van Veggel, *Angew. Chem.* **2000**, 112, 4489 – 4491; *Angew. Chem. Int. Ed. Engl.* **2000**, 39, 4319 – 4321.
- [25] S. I. Klink, H. Keizer, H. W. Hofstraat, F. C. J. M. van Veggel, *Synth. Met.* **2002**, 127, 213 – 216.
- [26] V. Comblin, D. Gilsoul, M. Hermann, V. Humblet, V. Jaques, M. Mesbashi, C. Sauvage, J. F. Desreux, *Coord. Chem. Rev.* **1999**, 185 – 186, 451 – 470.
- [27] L. Della Ciana, I. Hamachi, T. J. Meyer, *J. Org. Chem.* **1989**, 54, 1731 – 1735.



- [28] J. B. R. d. Vains, A. L. Papet, A. Marsura, *J. Heterocyclic Chem.* **1994**, *31*, 1069 - 1077.
- [29] J. Louise, J. F. Hartwig, *Tetrahedron Lett.* **1995**, *36*, 3609 – 3612.
- [30] A. S. Guram, R. A. Rennels, S. L. Buchwald, *Angew. Chem.* **1995**, *107*, 1456 – 1458; *Angew. Chem. Int. Ed. Engl.* **1995**, *34*, 1348 – 1350.
- [31] Personal communication M. Subat.
- [32] W. H. F. Sasse, *Org. Synth. Coll. Vol. V.* **1973**, 102 – 107.
- [33] Synthesized from commercially available *N*-benzylidenebenzenesulfonamide, according to a procedure by: F. A. Davis, S. Chattopadhyay, J. C. Towson, S. Lal, T. Reddy, *J. Org. Chem.* **1988**, *53*, 2087 - 2089.
- [34] M. Kercher, B. König, *Molecules* **2001**, *6*, M205.
- [35] K. E. Berg, A. Tran, M. K. Raymond, M. Abrahamsson, J. Wolny, S. Redon, M. Andersson, L. Sun, S. Styring, L. Hammarström, H. Toftlund, B. Akermark, *Eur. J. Inorg. Chem.* **2001**, 1019 - 1029.
- [36] A. K. Mishra, K. Draillard, A. Faivre-Chauvet, J.-F. Gestin, C. Curtet, J.-F. Chatal, *Tetrahedron Lett.* **1996**, *37*, 7515 – 7518.
- [37] O. Reany, T. Gunnlaugsson, D. Parker, *J. Chem. Soc., Perkin Trans 2* **2000**, 1819 – 1831.
- [38] A. Juris, V. Balzani, F. Barigelletti, S. Campagna, P. Belser, A. von Zelewsky, *Coord. Chem. Rev.* **1988**, *84*, 85 - 277.
- [39] S. I. Klink, PhD-Thesis, Twente, **2000**
- [40] M. Klessinger, J. Michl, *Excited States and Photochemistry of Organic Molecules*, VCH: Weinheim, **1995**.
- [41] A. Beeby, B. P. Burton-Pye, S. Faulkner, G. R. Motson, J. C. Jeffery, J. A. McCleverty, M. D. Ward, *J. Chem. Soc., Dalton Trans.* **2002**, 1923 – 1928.

- [42] W. DeW. Horrocks Jr., D. R. Sudnick, *Acc. Chem. Res.* **1981**, *14*, 384 – 392.
- [43] S. Quici, G. Marzanni, P. L. Anelli, M. Botta, E. Gianolio, G. Accorsi, N. Armaroli, F. Barigilletti, *Inorg. Chem.* **2002**, *10*, 2777 – 2784.
- [44] G. Bobba, J. C. Frias, D. Parker, *Chem. Commun.* **2002**, 890 – 891.

## 5 Zusammenfassung

Im Rahmen der vorliegenden Arbeit wurden supramolekulare Systeme zur Untersuchung von photoinduziertem Energie- und Elektronentransfer aufgebaut und untersucht.

Im Kapitel 2 wurden verschiedene Molekülbausteine synthetisiert, die sich über eine einfache Austauschreaktion um ein zentrales Metallion mittels koordinativer Bindungen selbst anordnen. Dabei entstehen virtuelle Bibliotheken von verschiedenen Donor-Akzeptor Diaden. Die koordinative Bindung zwischen den Acetylacetonatliganden und Scandium(III) ist stabil auf der Zeitskala für Energie- und Elektronentransfer, hier ca.  $10^{-7}$  s. Mit Hilfe spektroskopischer Methoden konnte die Bildung von Donor-Akzeptor Diaden zweifelsfrei nachgewiesen werden. Sowohl für den Fall des Energietransfers [Ru(bpy)<sub>3</sub>-Sc-Anthracen] als auch für Elektronentransfer [Ru(bpy)<sub>3</sub>-Sc-Tetramethylphenylendiamin] konnten als Zwischenprodukte Triplett-Anthracen bzw. das radikalische Kation von Tetramethylphenylendiamin durch Transientenspektroskopie identifiziert werden. Die Transferrate wurde zu  $2.5 \cdot 10^8 \text{ s}^{-1}$  und  $9 \cdot 10^8 \text{ s}^{-1}$  für Energie-, respektive Elektronentransfer bestimmt.

Kapitel 3 befasst sich mit Ruthenium-trisbipyridin Komplexen, die mit 2, bzw. 6 Cyclodextrinen in der Peripherie substituiert sind. Der vollständig, sechsfach substituierte Komplex besitzt eine ungewöhnlich lange Lebenszeit, die durch die gute Abschirmung der sterisch anspruchsvollen zyklischen Oligozucker zu erklären ist, die Sauerstoff, als Hauptursache für kurze Lumineszenzlebenszeiten, vom Metallkern fernhalten. Genügend lange alkylsubstituierte Viologene binden mit hohen Komplexbildungskonstanten ( $2.4 \cdot 10^5 \text{ M}^{-1}$ ) in die Kavitäten der Cyclodextrine, wobei sie einen kooperativen Bindungseffekt zeigen. Dies konnte durch den Vergleich mit unsymmetrisch substituierten Viologen gezeigt werden. Elektronen Transfer zwischen dem Metallkomplex und Dinonylviologen konnte in der Größenordnung von  $10^7 \text{ s}^{-1}$ , beobachtet werden.

Kapitel 4 zeigt die erfolgreiche Entwicklung von binuclearen Ruthenium- Lanthanid-Komplexen und das Studium ihrer photophysikalischen Eigenschaften. Als

mehrzähliger Ligand für Lanthanidionen wurde DO3A an ein Bipyridin gekoppelt. Das Bipyridin seinerseits stellt einen Baustein des Ruthenium- trisbipyridin dar. Durch Anregung in den  $^3\text{MLCT}$  Zustand des Übergangsmetallkomplexes wurde ein Energietransfer zum Lanthanid festgestellt. Dieser manifestiert sich zum einen in einer reduzierten Lumineszenz des Rutheniums, und zum anderen in der Emission des entsprechenden Lanthanidions im nahen Infrarot. Die Rate des Energietransfers zwischen dem Ruthenium Zentrum und dem Lanthanid wurde zu  $8.3 \cdot 10^5 \text{ s}^{-1}$  für Ytterbium und  $3.5 \cdot 10^6 \text{ s}^{-1}$  für Neodymium bestimmt.

## 6 Summery

Within this thesis, supramolecular system for the investigation of photoinduced energy- and electron transfer were synthesized and studied.

In chapter 2, several building block molecules have been synthesized. All components could be self assembled via a simple ligand exchange reaction around a central metal ion. This produced virtual libraries of donor-acceptor-dyads. The coordinative bond between the acetylacetonate as ligand and Sc(III) ions is stable on the timescale of energy- and electron transfer reactions, here  $10^{-7}$  s. Spectroscopic techniques revealed the formation of donor-acceptor-dyads. For the case of energy transfer [Ru(bpy)<sub>3</sub>-Sc-anthracene] as well as electron transfer [Ru(bpy)<sub>3</sub>-Sc-tetramethylphenylendiamine], the transition products triplet-anthracene, respective the radical cation of tetramethylphenylendiamine were identified by transient absorption spectroscopy. The transferrate for energy- and electron transfer rate was determined to be  $2.5 \cdot 10^8 \text{ s}^{-1}$  and  $9 \cdot 10^8 \text{ s}^{-1}$ , respectively.

Chapter 3 deals with ruthenium trisbipyridine complexes, substituted with 2, or 6 cyclodextrins in the periphery. The sixfold substituted complex has suprisingly long lifetime. The complex is very well shielded by the bulky cyclic sugars, so that oxygen, which is the main cause for short luminescence lifetimes, can not penetrate the metal core. Alkylviologens with sufficiently long aliphatic tails bind into the cavities of the cyclodextrins with high association constants ( $2.4 \cdot 10^5 \text{ M}^{-1}$ ). They exhibit a cooperative binding into two cavities simultaneously, which was shown by a comparison with unsymmetrically substituted viologens. Electron transfer between the metal complexes and bisnonyl-viologen was observed with a rate of about  $10^7 \text{ s}^{-1}$ .

Chapter 4 presents the successful development of binuclear ruthenium- lanthanide complexes and the study of their photophysical properties. DO3A, as a polydentate ligand, was linked to a bipyridine. The bipyridine itself is a building block of ruthenium trisbipyridine. Upon excitation in the <sup>3</sup>MLCT band of the transition metal complex, an energy transfer to the lanthanide was observed through (i) a reduced lifetime of the

ruthenium-based luminescence, and (ii) through the emission of the lanthanide in the near infrared.

## 7 Danksagung / Acknowledgement

Die vorliegende Arbeit wurde von Mai 1999 bis September 1999 am Institut für Organische Chemie der Technischen Universität „Carolo-Wilhelmina“ zu Braunschweig, von Oktober 1999 bis September 2000 am Institut für Organische Chemie der Universität Regensburg und von Oktober 2000 bis Juli 2002 am Instituut voor Moleculaire Chemie der Universiteit van Amsterdam unter der Leitung von Prof. Dr. Burkhard König und Prof. Dr. Luisa De Cola angefertigt.

Mein Dank gilt Prof. Dr. Burkhard König für die Möglichkeit zur Anfertigung einer Promotion, die Betreuung vor Ort in Braunschweig und Regensburg, sowie die Fernbetreuung in Amsterdam, die zahlreichen Anregungen und die vielen gewährten Freiheiten.

I am gratefull to Prof. Dr. Luisa De Cola for being my host and co-supervisor throughout my time in Amsterdam, and for getting me involved into the collaborations with Nijmegen and Birmingham.

Special thanks to Vincenzo Adamo, Peter Belser, Loes Boomsma, Christa Braig, Werner Braig, Christoph Bonauer, Anouk Dirksen, Martin Feiters, Daniela Fischer, Tom Fricke, Hans-Christoph Gallmeier, Peter Glover, Uwe Hahn, Hanna Haider, Frantisek Hartl, Gerald Hebbink, Maria Hechavarria Fonseca, Anna Johnson, Ron Jukes, Basak Kaletas, Michael Klein, Cees Kleverlaan, Michael Kruppa, Bernhard Lerche, Stéphanie Leroy, Lisa Liebl, Taasje Maharbiersing, Christian Mandl, Bart Nelissen, Roeland Nolte, Mario Pelka, Zoe Pikramenou, Wolfgang Pitsch, Edward Plummer, Fausto Puntoriero, John van Ramesdonk, Roland Reichenbach-Klinke, Martin Rödel, Miriam Sax, Theo Snoek, Mara Staffilani, Michael Subat, Florian Thieme, Rudi Vasold, Frank Vergeer, Steve Welter, René Williams, and Juriaan Zwier, for their inspiration and collaboration.